การสังเคราะห์ไดเมทิลอีเทอร์และไอโซพาราฟินจากแก๊สสังเคราะห์บนตัวเร่งปฏิกิริยา
ชนิดแคปซูล

นายมนตรี ทองคำ
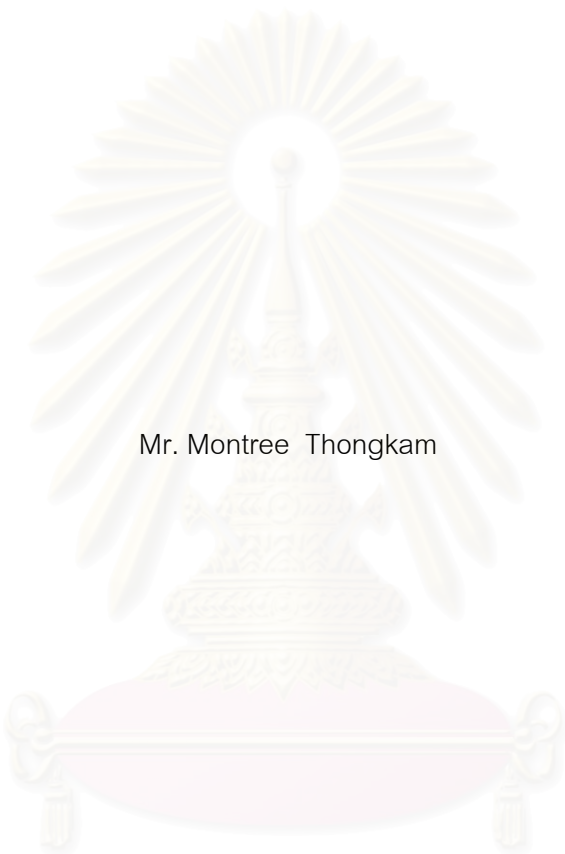
SYNTHESIS OF DIMETHYL ETHER AND ISOPARAFFINS FROM SYNGAS OVER

CAPSULE CATALYSTS

Mr. Montree Thongkam

A Dissertation Submitted in Partial Fulfillment of the Requirements

for the Degree of Doctor of Philosophy Program in Chemical Technology

Department of Chemical Technology

Faculty of Science

Chulalongkorn University

Academic year 2008

Thesis Title   SYNTHESIS OF DIMETHYL ETHER AND ISOPARAFFINS
                    FROM SYN GAS OVER CAPSULE CATALYSTS

By   Mr. Montree Thongkam

Field of Study   Chemical Technology

Advisor   Associate Professor Tharapong Vitidsant, Ph.D.

Co-Advisor   Professor Noritatsu Tsubaki, Ph.D.

Accepted by the Faculty of Science, Chulalongkorn University in Partial
Fulfillment of the Requirements for the Doctoral Degree

.... Dean of the Faculty of Science
(Professor Supot Hannongbua, Dr.rer.nat.)

THESIS COMMITTEE

.... Chairman
(Professor Pattarapan Prasassarakich, Ph.D.)

.... Advisor
(Associate Professor Tharapong Vitidsant, Ph.D.)

.... Co-Advisor
(Professor Noritatsu Tsubaki, Ph.D.)

.... Examiner
(Assistant Professor Chawalit Ngamcharussrivichai, Ph.D.)

.... Examiner
(Assistant Professor Prasert Reubroycharoen, Ph.D.)

.... External Examiner
(Associate Professor Somsak Woramongkolchai, D.Eng.)

มนตรี ทองคำ : การสังเคราะห์ไดเมทิลอีเทอร์และไอโซพาราฟินจากแก๊สสังเคราะห์บน
ตัวเร่งปฏิกิริยาชนิดแคปซูล. (SYNTHESIS OF DIMETHYL ETHER AND
ISOPARAFFINS FROM SYNGAS OVER CAPSULE CATALYSTS) อ.ที่ปรึกษาวิทยา
นิพนธ์หลัก : รศ.ดร.ธราพงษ์ วิทิตศานต์, อ.ที่ปรึกษาวิทยานิพนธ์ร่วม : Prof. Noritatsu
Tsubaki, Ph.D., 124 หน้า.

งานวิจัยนี้ได้แบ่งการทดลองออกเป็น 2 ส่วน การทดลองส่วนแรกศึกษาการสังเคราะห์ได
เมทิลอีเทอร์บนตัวเร่งปฏิกิริยาโครเมียม/ซิงค์ออกไซด์ชนิดแคปซูลจากแก๊สสังเคราะห์ โดยมีการ
เตรียมตัวเร่งปฏิกิริยาชนิดแคปซูลด้วยวิธีการสังเคราะห์แบบไฮโดรเทอร์มอล (Hydrothermal
Synthesis) ซึ่งทำให้สามารถเคลือบเอชซีเอสเอ็มไฟว์ซีโอไลต์(HZSM-5) ลงบนผิวของเม็ดตัวเร่งป
ฏิกิริยาของโครเมียม/ซิงค์ออกไซด์ได้อย่างสมบูรณ์ และทำการวิเคราะห์โครงสร้างตัวเร่งปฏิกิริยา
ด้วยวิธีสแกนนิงอิเลกตรอนไมโครสโคปี(SEM), เอนเนอจีดิฟฟิวซีพเอกซ์เรย์สเปคโตรสโคปี(EDS)
และ เอกเรย์ดิฟแฟรกโตมิเตอร์(XRD) โดยทำการทดลองกับตัวเร่งปฏิกิริยาที่อุณหภูมิ 573, 598
และ 623 เคลวิน ความดัน 5 เมกะปาสคาล ที่อัตราส่วนของน้ำหนักตัวเร่งปฏิกิริยาต่ออัตราการ
ป้อนของแก๊สเท่ากับ 13.6 กรัม.ชั่วโมงต่อโมล ในเครื่องปฏิกรณ์เบดนิ่ง จากการศึกษาทดลองการ
สังเคราะห์ไดเมทิลอีเทอร์ พบว่าตัวเร่งปฏิกิริยาโครเมียม/ซิงค์ออกไซด์ชนิดแคปซูลให้ผลของการ
เลือกเกิด (selectivity) ไดเมทิลอีเทอร์สูงกว่า เมื่อเทียบกับการทดลองที่ใช้ตัวเร่งปฏิกิริยาผสม
ระหว่างโครเมียมซิงค์ออกไซด์กับซีโอไลต์ HZSM-5 โดยได้ผลของการเลือกเกิดไดเมทิลอีเทอร์
45.33 % ที่อุณหภูมิ 598 เคลวิน นอกจากนี้ยังได้ศึกษาการสังเคราะห์ไดเมทิลอีเทอร์ในเครื่อง
ปฏิกรณ์แขวนลอย ที่อุณหภูมิ 573 เคลวิน ความดัน 4 เมกะปาสคาล บนตัวเร่งปฏิกิริยาชนิดเดียว
กัน การทดลองส่วนที่สองศึกษาการสังเคราะห์ไอโซพาราฟินบนตัวเร่งปฏิกิริยาโคบอลต์/อลูมินา
ชนิดแคปซูลจากแก๊สสังเคราะห์ โดยทำการเคลือบเอชบีต้าซีโอไลต์(H-beta zeolite)ลงบนผิวของ
เม็ดตัวเร่งปฏิกิริยาโคบอลต์/อลูมินา ด้วยวิธีการสังเคราะห์แบบไฮโดรเทอร์มอล

ภาควิชา	เคมีเทคนิค	ลายมือชื่อนิสิต	
สาขาวิชา	เคมีเทคนิค	ลายมือชื่ออ.ที่ปรึกษาวิทยานิพนธ์หลัก	
ปีการศึกษา	2551	ลายมือชื่ออ.ที่ปรึกษาวิทยานิพนธ์ร่วม	

4873839123   : MAJOR CHEMICAL TECHNOLOGY

KEYWORDS : DIMETHYL ETHER / METHANOL SYNTHESIS / SYNGAS / CAPSULE

CATALYST / METHANOL DEHYDRATION

MONTREE THONGKAM : SYNTHESIS OF DIMETHYL ETHER AND
ISOPARAFFINS FROM SYNGAS OVER CAPSULE CATALYSTS. ADVISOR :
ASSOC. PROF. THARAPONG VITIDSANT, Ph.D., CO-ADVISOR : PROF.
NORITATSU TSUBAKI, Ph.D., 124 pp.

In this thesis, the experiment is divided into two parts. The first part studied
was dimethyl ether synthesis and was prepared the new capsule catalysts by a
direct hydrothermal synthesis method which directly synthesized H-ZSM-5
membrane was coated completely onto Cr/ZnO catalyst pellets. The dehydration of
methanol to dimethyl ether over Cr/ZnO capsule catalysts was also investigated in
this study. All catalysts have been characterized and were identified by SEM, EDS
and XRD. The experiment was carried out at 573, 598 and 623 K, 5 MPa, W/F = 13.6
g.h/mol, in a fixed bed reactor. It was found that the capsule catalysts have shown
better performance compared to the physical mixing catalysts. Particularly, capsule
catalysts were indicated higher dimethyl ether selectivity, and showed selectivity of
dimethyl ether with 45.33 % at 598 K. In addition, the performance of catalyst was
operated at 573 K, 4 MPa with a slurry phase reactor and was compared with the
conventional FTS catalyst(Cr/ZnO) and physically mixed catalysts. The second part
studied the synthesis of isoparaffins and synthesized H-beta zeolite membrane
coated Co/Al_2O_3 core/shell catalyst by hydrothermal method.

Department :   Chemical Technology   Student's Signature   M. Thongkam

Field of Study :   Chemical Technology   Advisor's Signature   T. Vitidsant

Academic Year :   2008   Co-Advisor's Signature Noritatsu Tsubaki

ACKNOWLEDGEMENTS

CONTENTS

LIST OF TABLES

LIST OF FIGURES

PAGE

CHAPTER I

INTRODUCTION

The long-term energy demand in the Asian region is forecasted to be so large that energy supply and environmental problems would be substantial obstacles to realize sustainable development in this region. Reserves of oil and natural gas resources in Asian region are only 5 %, 7 %, respectively of the world ones and there are few large-scale natural gas fields adequate to LNG. The region is relatively richly endowed with coal reserves, 31% of the world ones, however, around half of them are low rank coal such as sub-bituminous coal or lignite, which contains moisture at high contents. Due to fast increase in the population of the world with increasing necessities, alternative sources for fuel requirement have been searched. Global warming is another important problem that affects human life, animals and plants. Emissions during the combustion of fossil (oil and natural gas) fuels, such as CO_2, NO_x, SO_x etc. are reported to contribute to this problem greatly. Presently, Dimethylether (DME) is one of the most promising alternates of such synthetic fuels. DME is a clean energy source of low environmental load and can be used as a sulfur free fuel for diesel engines without particulates formation and lower NO_x emission in comparison with gas oil. So it is a high performance alternative fuel for diesel engine. DME has properties similar to those of propane and butane, permitting its use as a LPG. DME is also being used as an aerosol propellant to replace chlorofluoro carbons, which were found to destroy the ozone layer of the atmosphere. Owing to the non-toxicity and easy liquefaction properties.[1,3]. With the increasing public concern about the environment, more and more stringent legislations have been and will be implemented on transportation fuels such as gasoline. Presently, an aromatic is used as one of the main components for boosting the octane properties of gasoline. However, the aromatic has been identified as one of the carcinogens. Therefore, its content in gasoline must be decreased accordingly. To date, it seems that isoparaffins are more environmentally acceptable to boost the octane number of gasoline. Indeed, the branched paraffins have a high octane rating without the drawbacks arising from the presently used additives such as tetraethyllead, an aromatic, and an oxygenated compound of MTBE. However, within the limits of the

existing technologies in isomerization and alkylation units, branched paraffins cannot be made through isomerization and alkylation in sufficient amounts to replace the aromatic below 30%. Thus, it is more attractive if branched paraffins can be directly produced from resources rather than petroleum. As a matter of fact, the Fischer-Tropsch (FT) synthesis is an effective route to convert coal, natural gas, or biamass-derived synthesis gas (syngas, $CO + H_2$) to liquid fuels and high-value-added fine chemicals. However, as a result of the Anderson-Schulz-Flory (ASF) polymerization kinetics, the FT products which are composed mainly of normal paraffins are nonselective to any specific product. To selectively synthesize desired products such as diesel or high-octane gasoline, it is essential to circumvent the ASF distribution such that high selectivity to the desired product can be achieved. Several groups have practiced for this purpose by utilizing FT-active components supported on acidic zeolites. However, acidic zeolite is not a stable support under FT reaction conditions, and typical results showed low activity and high methane selectivity. In our previous investigations, a fundamental concept by using a physical mixture of an FT catalyst to synthesize long-chain hydrocarbons and a Pd-supported solid acid catalyst to hydroconvert the FT products into isoparaffins was developed and experimentally evaluated both in one reactor and in a consecutive dual reactor system. Results showed that high selectivity to isoparaffins can be conveniently achieved in a dual reactor system by using Pd/β catalyst in the second reactor. Although the synthesis of zeolite β was reported in 1967, studies for the potential applications in petroleum chemistry, refining, and fine chemical production began only in recent years partly because of the late revelation of its framework structure. Zeolite β has a three dimensional, interconnected channel system with 12-membered elliptical openings having mean diameters of 0.64 - 0.76 nm, which could be of great industrial interest. As a matter of fact, zeolite β has been reported to be a good catalyst for several reactions such as cracking, hydrotreating, and benzene alkylation with light olefins.

Previously in the thesis work, Montree Thongkam carried out during October, 2007 to September, 2008 at University of Toyama and subsequently at Chulalongkorn University, describes a method of catalyst preparation, the fabrication and leak-test of high-pressure through flow tubular reactor (maximum design pressure and temperature:

5 MPa and 350 $^{\circ}$C), dimethyl ether synthesis experiments under various temperatures, analysis and discussion of experimental results. At University of Toyama, a catalyst of Cr/ZnO, with atomic ratios of Cr : Zn = 1 : 2, was prepared and tested in Prof. Tsubaki's Laboratory.

In this research work, the experiment is divided into two parts. The first part studied dimethyl ether synthesis and designed the new capsule catalysts by a direct hydrothermal synthesis method, Zeolite membrane was coated on the Fischer-Tropsch synthesis (FTS) catalyst pellet, Cr/ZnO, and we which were called "capsule catalysts". The experiment was carried out at 573, 598 and 623 K, 5 MPa, W/F = 13.6 g.h/mol, In the reaction, feed gas, CO + H$_2$, diffused through zeolite membrane and arrived at the FTS catalyst. Then the methanol formed there and desorbed. When the methanol diffused into the zeolite membrane, all of them, in the form of methanol, could enter zeolite channels and must be dehydrated, cracked and isomerized by acidic sites inside zeolite channels. For long-chain hydrocarbons, their low diffusion rate in zeolite membrane makes them stay in the membrane layer longer, having a higher possibility of isomerization and cracking reaction inside the membrane. Furthermore, compared to conventional membrane reactors, the catalyst designed above has larger membrane area per unit reactor volume. This kind of capsule catalyst is of great advantage in practical application, because membranes with large area and without pinholes or cracks are very difficult to prepare in most cases. Later, to studied the performance of catalyst a similar catalysts at 573 K, 4 MPa with a slurry phase reactor and compared with the conventional FTS catalyst(Cr/ZnO) and physical mixing catalysts at Chulalongkorn University.

The second part, we studied the synthesis of an H-beta zeolite membrane coated Co/Al$_2$O$_3$ core/shell catalyst by hydrothermal synthesis method and its performance in the direct synthesis of isoparaffins from syngas. This core/shell catalyst promotes the formation of isoparaffins and improves the product distribution. Acidic zeolite, the excellent catalysts for heavy hydrocarbons isomerization and cracking, was selected for the design of new FTS catalyst. In some reports, the mixed catalysts prepared by mixing the conventional FTS catalyst with acidic zeolite exhibited the excellent performance of iso-paraffin synthesis, but many heavy hydrocarbons still

existed in the final products. In FTS reaction on these mixed catalysts, linear FTS hydrocarbons formed on FTS catalyst and then they might be hydrocracked and isomerized on the zeolite acidic sites only at random. As a result, the long-chain hydrocarbons could not be decomposed completely, even though the formation of short-chain iso-paraffins was enhanced. Recently, the present authors introduced a novel multiple-functional H-Beta/ Co/Al$_2$O$_3$ zeolite capsule catalyst into the FTS reaction . In the iso-paraffin direct synthesis via FTS on these zeolite capsule catalysts, syngas (CO + H$_2$) entered the capsule catalyst through zeolite shell to arrive at the catalyst core, and then the formed FTS hydrocarbons on the catalyst core with linear structure could enter the zeolite pores easily, being isomerized and cracked by zeolite acidic sites when they escaped through the zeolite capsule. As a result, middle iso-paraffin synthesis was realized by one step only using this multifunctional zeolite capsule catalyst, deleting the appearance of all heavy hydrocarbons. It was found that the capsule catalyst with maller support size showed higher activity as well as remarkably enhanced iso-paraffin selectivity.

The aim of this work is consideration of the conversion of methanol to DME by dehydrating process and selective synthesis of isoparaffins (C$_4$–C$_6$) from synthesis gas. This process is moderately exothermic and usually is conducted in an adiabatic fixed bed reactor. Methanol dehydration to DME have been studied in a laboratory-scale system at various operating temperatures. A temperature dependent model has been developed to predict the dehydration of methanol to DME at various temperatures. In this study, a new capsule catalyst system of Cr/ZnO and Co/Al$_2$O$_3$ were prepared by the hydrothermal method and evaluated in methanol dehydration reaction to dimethyl ether and isoparrafins synthesis. The fundamental concept is the synthesis of hydrocarbon mixtures rich in C$_4$–C$_6$ (isoparaffins) by hydrocracking and isomerization of the primary hydrocarbons produced by FTS. The catalysts were also characterized by X-ray diffraction (XRD), scanning electron microscopy (SEM) and an energy-diffusive X-ray spectroscopy (EDS).

CHAPTER II

THEORY AND LITERATURE REVIEWS

The driving force for developing alternative fuels is no longer solely to reduce oil dependence on select oil exporting countries. Noxious exhaust emissions generated by combustion of fossil fuels as well as increasing levels of carbon dioxide, a major contributor toward global warming, have necessitated the need to develop alternative fuels that address clean-burning as an important criterion. Dimethyl ether (DME) is identified as a multisource, multipurpose fuel that can effectively both of these concerns by establishing stable indigenous fuel supply and alleviating environmental concerns. Dimethyl Ether can be readily produced from natural gas and coal, renewable resources such as biomass and wood, as well as waste matter. Fischer–Tropsch synthesis (FTS) has recently attracted increasing attention, since high quality diesel fuels without any sulfur or aromatic compounds can be produced directly from syngas derived from natural gas, coal or biomass. It is well known that FTS involves a polymerization reaction beginning with a methylene intermediate to produce a wide distribution of hydrocarbons ranging from methane to wax (C_1–C_{60+}). The FTS product is mostly n-paraffin or n-olefin [1].

2.1. Fischer-Tropsch synthesis and Isoparaffins

Fischer-Tropsch synthesis is the process that converts synthesis gas, i.e. a mixture of carbon monoxide and hydrogen, into a wide range of long chain hydrocarbons and oxygenates. As such, the Fischer-Tropsch synthesis constitutes a practical way for the chemical liquefaction of solid (coal) or gaseous (natural gas) carbon resources. In relation to the classic refining of crude oil, the liquefaction of these carbon sources via the Fischer-Tropsch synthesis provides alternative routes for the production of transportation fuels and petrochemical feedstock.

The Fischer-Tropsch reaction is the chemical heart in the gas-to-liquid technology. The highly exothermic Fischer-Tropsch reaction converts synthesis gas into a large range of linear hydrocarbons, schematically represented as:

$$nCO + 2nH_2 \longrightarrow -(CH_2)_n - + nH_2O \qquad \Delta H = -165 \; kJ. \, mole^{-1}$$
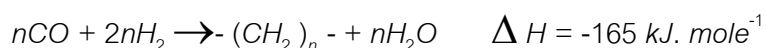
The industrial reaction conditions are 473-573 K and 25-40 bar.

The Fischer-Tropsch process has a lively history of more than 70 years [2,3,4]. The CO hydrogenation capacity of nickel and cobalt was first reported by Sabatier and Senderens in 1902. However, it was only after the pioneering work of Franz Fischer and Hans Tropsch in the 1920.s and 1930.s that the commercial interest in the production of hydrocarbons and oxygenates started to grow. Although all group VIII metals display some activity in the C-C coupling reaction during the hydrogenation of CO, the most active metals for the Fischer-Tropsch synthesis are ruthenium, iron, cobalt, and nickel [5,6]. This is related to the capacity of the metals to dissociate CO. Going to the left and up in the group VIII metals, the CO dissociation intensifies and excessive carbonization of the metal is risked. Going to the right and down, CO dissociation becomes more difficult and the hydrogenation towards alcohols dominates. Iron, cobalt, nickel, and ruthenium display intermediate behavior and are excellent Fischer-Tropsch catalysts. The major disadvantage of nickel is that it readily forms volatile metal-carbonyls, limiting the reaction pressure and thus the Fischer-Tropsch productivity. At industrial conditions, nickel mainly produces methane.

Iron catalysts for the Fischer-Tropsch synthesis generally consist of precipitated iron, which is promoted with potassium and copper to obtain a high activity and selectivity, and with Al_2O_3 and SiO_2 added as structural stabilizers. Typically for these relatively cheap Fe-based catalysts is that the active phase for Fischer-Tropsch appears to be a Fe-carbide. Also, Fe-oxides are formed, which are active for the water-gas shift reaction. This high water-gas shift activity causes these catalysts to be flexible towards the H_2/CO feed ratio of the synthesis gas. This allows the utilization of a large variety of feedstocks, while every syngas manufacturing technology can be applied. Because coal results in a syngas with a low H_2/CO ratio, this feedstock can only be used in combination with a Fe-based catalyst. However, the water-gas-shift activity of the catalyst also results in a low carbon efficiency of the gas-to-liquid process. At high temperature (613 K), Fe-based catalysts are selective for light olefins with a low selectivity towards methane. This only seems possible with Fe-based catalysts, making them unique in this respect. The application of Fe-based catalysts in the production of

heavy wax is limited. This is mainly due to its tendency to form elemental carbon, causing deactivation of the catalyst. Moreover, water, which is produced in large quantities as side product, has an inhibiting effect on the activity, resulting in low conversions per pass. The latter effect results in large recycle streams after water removal.

Cobalt catalysts are usually supported on metal oxides due to the higher cobalt price and better catalyst stability. The active phase is metallic cobalt; the tendency of cobalt to form carbides at 473-573 K and 25-40 bar is low. The water-gas shift activity of Co-based catalysts is low and water is the main oxygen containing reaction product. The cobalt is generally poorly dispersed on metal oxide supports and Ru, Re, or Pt promoters are applied to prevent catalyst deactivation by carbon formation or oxidation. Compared to Fe-based catalysts, olefins tend to reenter the chain growth process by readsorption on Co-based catalysts, increasing the selectivity towards heavy hydrocarbons. Co-based catalysts are very suitable for wax formation in slurry bubble columns and can operate at high conversions per pass.

Ruthenium catalysts are the most active Fischer-Tropsch catalysts. A high molecular weight wax is obtained at reaction temperatures as low as 423 K. The catalyst is active in its metallic form and no promoters are required to stabilize its activity. However, the high price of ruthenium excludes its application on industrial scale and the use of Ru-based catalysts for the Fischer-Tropsch synthesis is limited to academic studies.

An overview of the existing Fischer-Tropsch technologies is given in table 2.1. With Sasol.s fluidized bed processes (CFBR and FBR) as exceptions, all processes are aimed at high wax selectivities. For detailed descriptions of the individual processes the reader is referred to recent literature reviews by Van der Laan and Beenackers [4] and Schulz [6] and to the references given in table 2.1.

Table 2.1 Overview of the current technologies used in the Fischer-Tropsch technology [4,12,13,14,15,16].

Licencor	Status	Syngas production	F-T reactor	Catalyst	reference
Sasol	commercial	PO SR	CFBR FBR TFBR SBCR	Fe Fe Fe Fe, Co	Dry [1996], Espinoza et al. [1999], Steynberg et al. [1999]
Shell	commercial	PO	TFBR	Co	Eilers et al. [1990], Geerlings et al. [1999]
Exxon	pilot plant	CPO	SBCR	Co	Eisenberg et al. [1998]
Syntroleum	laboratory	ATR	TFBR	?	reference in Van der Laan and Beenackers [1999]
Energy International	?	PO	SBCR	Co	Wilson and Carr [1999]
Rentech	pilot plant	PO, SR, ATR	SBCR	Fe	Benham and Bohn [1999]

(Syngas manufacturing: PO=partial oxidation, CPO=catalytic partial oxidation; SR=steam reforming, ATR=autothermal reforming , Fischer-Tropsch reactor: CFBR=circulating fluidized bed reactor; FBR=fluidized bed reactor; TFBR=tubular fixed bed reactor; SBCR=slurry bubble column reactor)

The pioneering work by Fischer and Tropsch in the 1920.s already led to the realization that hydrocarbon chain formation proceeds via the stepwise addition of one C-atom at the time. Detailed product analysis studies [*e.g.* Pinchler *et al.*] indicate that the reaction produces a vast array of hydrocarbons and oxygenates over a large boiling range. The major reaction products at highpressure operation are linear paraffins, linear 1-olefins, and linear 1-alcohols. At lower pressures, the selectivity for mono-methyl branched hydrocarbons and internal-olefins increases. The formation of aromatics is only observed at higher temperatures on Fe-based catalysts and is not observed on Coand Ru-based catalysts. Anderson shows that a polymerization-like process effectively describes the product distribution of the Fischer-Tropsch synthesis. This results in the so-called Anderson-Schulz-Flory (ASF) product distribution:

$$Fn = n \cdot (1-\alpha)^2 \cdot \alpha^{n-1} \tag{2.1}$$

where *Fn* is the fraction of the C-atoms within a chain containing *n* C-atoms. Similar molecular weight distributions were already observed during polycondensation by Schulz [6] and free-radical polymerization by Flory [7].

The entire product spectrum is characterized by a single parameter, i.e. the chain growth probability (α), defined as:

$$\alpha = \frac{\sum\limits_{i=n+1}^{\infty} \phi_i}{\sum\limits_{i=n}^{\infty} \phi_i} = \frac{r_p}{r_p + r_t} \qquad (2.2)$$

where r_p and r_t are the rates of chain propagation and termination, respectively, and ϕ_i is the mole fraction of the product spectrum containing i carbon atoms. Often, the product distribution is described by the termination probability β instead of the chain growth probability. In 1946, Herington defined the termination probability β as:

$$\beta = \frac{\phi_i}{\sum\limits_{i=n+1}^{\infty} \phi_i} = \frac{r_t}{r_p} = \frac{1-\alpha}{\alpha} \qquad (2.3)$$

Equation (2.1) implies that the Fischer-Tropsch reaction is not selective towards a single reaction product or a specific carbon range, with methane as only exception. Methane can be produced with 100 % selectivity. This is schematically represented in figure 2.1, where the product selectivity is plotted against the chain growth probability α. The Fischer-Tropsch synthesis, however, can selectively produce one type of reaction product, *i.e.* the selectivity towards 1-olefins or paraffins can be optimized. The influence of the reaction conditions on the product distribution is indicated in table 2.2. Wax formation is favored at low temperature, high pressure, low H_2/CO feed ratios, and large residence times. Accordingly, Sasol.s tubular fixed bed process, which aims at wax formation, is operated at 492-523 K and 25-40 bar [8]. Sasol.s circulating fluidized bed process, however, aims at gasoline and light olefins and is operated at 603-623 K and 25 bar.

Table 2.2 Influence of the process conditions on the Fischer-Tropsch product distribution. O/P=olefin to paraffin ratio; S_{C1}=methane selectivity; X_{syngas}=syngas conversion; +: increases with increasing parameter value; -: decreases with increasing parameter value; /: situation dependent [9].

	α	O/P	S_{C_1}	X_{syngas}	linearity
Temperature	-	+	+	+	-
Pressure	+	+	-	+	+
H$_2$/CO	-	-	+	+	/
Residence time	+	-	/	/	-

The restraints of the product distribution led to the development of low temperature operation of multi-tubular reactors and slurry column reactors, see table 2.2. At these conditions, chain growth probabilities in excess of 0.9 are obtained, at which the fuel-gas selectivity is low. The Fischer-Tropsch reaction is not a polymerization reaction in the true meaning of the word. Firstly, the monomer has to be formed in-situ on the catalyst surface from the reactants CO and H$_2$. Secondly, the rates of surface reactions are chain length dependent for the formation of the C_1-C_4 hydrocarbons. Thirdly, primary products can undergo secondary reactions that influence the product distribution. These three deviations from ideal polymerization kinetics cause the Fischer-Tropsch product distribution to deviate from the ideal ASF distribution. As shown in Fig. 2.1,2.2, the observed differences between the experimental product distributions and the ideal ASF distribution are:

• a higher than expected C_1 selectivity;

• a lower than expected C_2 selectivity;

• a chain length dependent chain growth probability, leading to a curved distribution and a higher than expected selectivity of heavy hydrocarbons.

It should be noted that erroneous product analyses introduce systematic deviations in the product distribution, which are easily ascribed to mechanistic causes. A well-known problem is the condensation of hydrocarbons prior to product analysis. Because the condensation is chain length dependent, the resulting deviations in the product spectrum can easily be mistaken for mechanistic phenomena. Erroneous

mechanistic explanations may also occur in short non-steady state operation of the reaction where stabilization of the product spectrum is not yet completed [9].
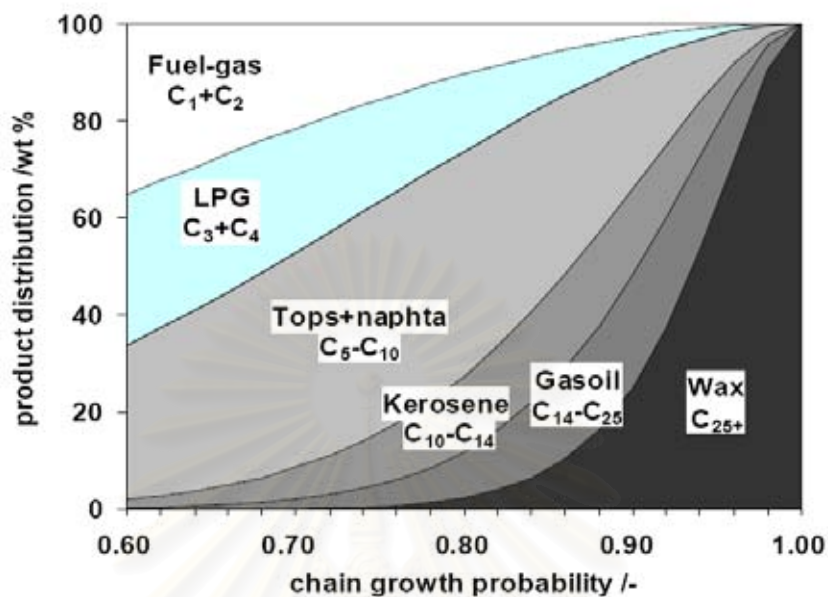
Figure 2.1 Theoretical product distribution as a function of the chain growth probability

(α) according to the ASF distribution [9].
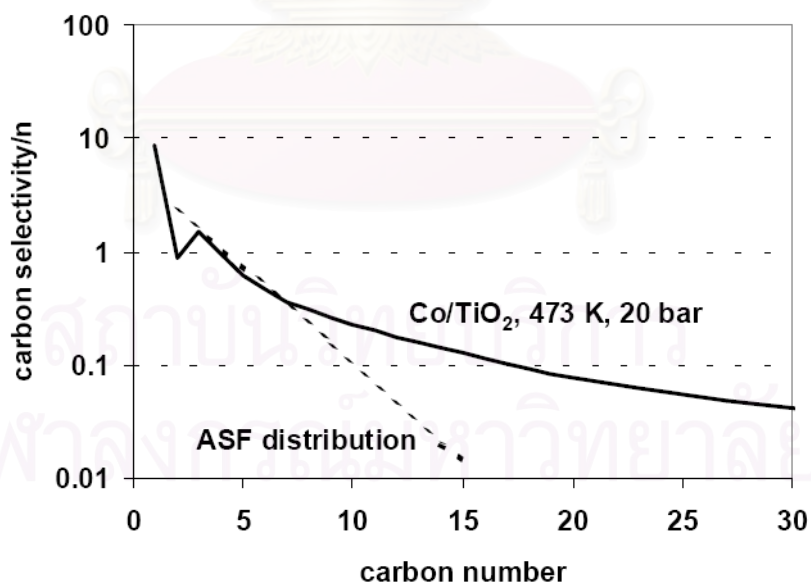
Figure 2.2 Experimental product distribution of a Co/TiO$_2$ catalyst at 473 K and 20 bar in

comparison to the ASF distribution [10].

Although the product distribution demonstrates the polymerization character of the Fischer-Tropsch synthesis, a great deal of controversy still exists on the chemical identity of the monomeric building block and, in relation to this, of the growing hydrocarbon chain. This results from the vast product spectrum of alkanes, alkenes, alcohols, and acids, observed during the Fischer-Tropsch synthesis. From literature, the three major reaction mechanisms for the Fischer-Tropsch synthesis are:

      1. the carbene mechanism

      2. the hydroxy-carbene mechanism

      3. the CO-insertion mechanism

For each mechanism, several variants are reported. Because extensive reviews can be found in literature [2,3,11], only the most important aspects of the reaction mechanisms are reported here.
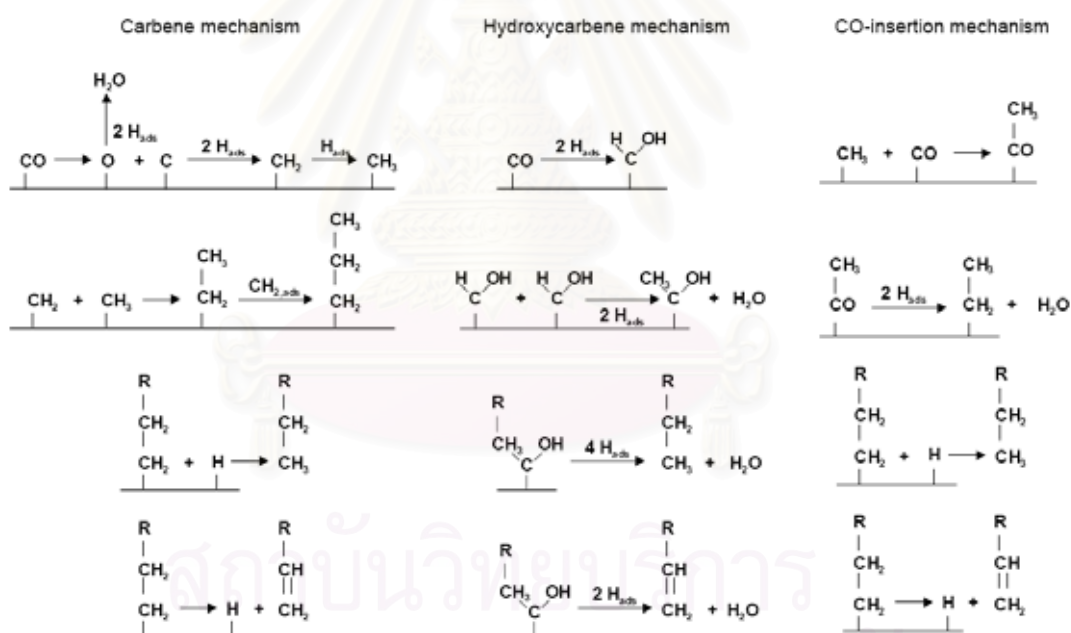
Figure 2.3 Schematic representations of the three basic Fischer-Tropsch reaction

          mechanisms, *i.e.* the carbine mechanism, the hydroxycarbene mechanism,

          and the CO-insertion mechanism [2].

Paraffins have the general formula C_nH_{2n+2}, where "n" is the number of carbon atoms (carbon number) in the molecule. There are two subclasses of paraffins: normal paraffins and isoparaffins.

Normal paraffins have carbon atoms linked to form chain-like molecules, with each carbon – except those at the ends – bonded to two others, one on either side.

n-Paraffin

$$CH_3-CH_2-CH_2-CH_2-CH_2-CH_2-CH_2-CH_2-CH_2-CH_3$$
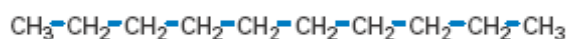
n-Decane $C_{10}H_{22}$

Isoparaffins have a similar carbon backbone, but they also have one or more carbons branching off from the backbone. Normal decane and 2,4-dimethyloctane have the same chemical formula, $C_{10}H_{22}$, but different chemical and physical properties. Compounds like this, with the same chemical formula but a different arrangement of atoms, are called structural isomers.

Isoparaffin

$$CH_3-\underset{\underset{CH_3}{|}}{CH}-CH_2-\underset{\underset{CH_3}{|}}{CH}-CH_2-CH_2-CH_2-CH_3$$
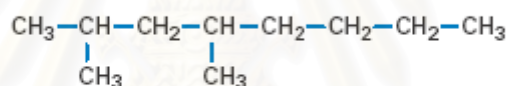
2,4-Dimethyloctane $C_{10}H_{22}$

2.2. Dimethyl ether

Dimethyl ether (DME) is gaining worldwide recognition as a multisource, multipurpose clean fuel and chemical feedstock for the 21st century. It is a technically mature, environmentally friendly, and market acceptable alternative fuel. As shown in Fig. 2.4, DME can be produced from a variety of sources, and its end use includes a number of important applications. Dimethyl ether can be manufactured in large quantities from coal, natural gas, biomass and municipal solid waste. Current technologies for producing DME on a large scale include those of NKK Corporation, Haldor Topsoe, Air Products and Toyo Engineering Corporation (TEC).
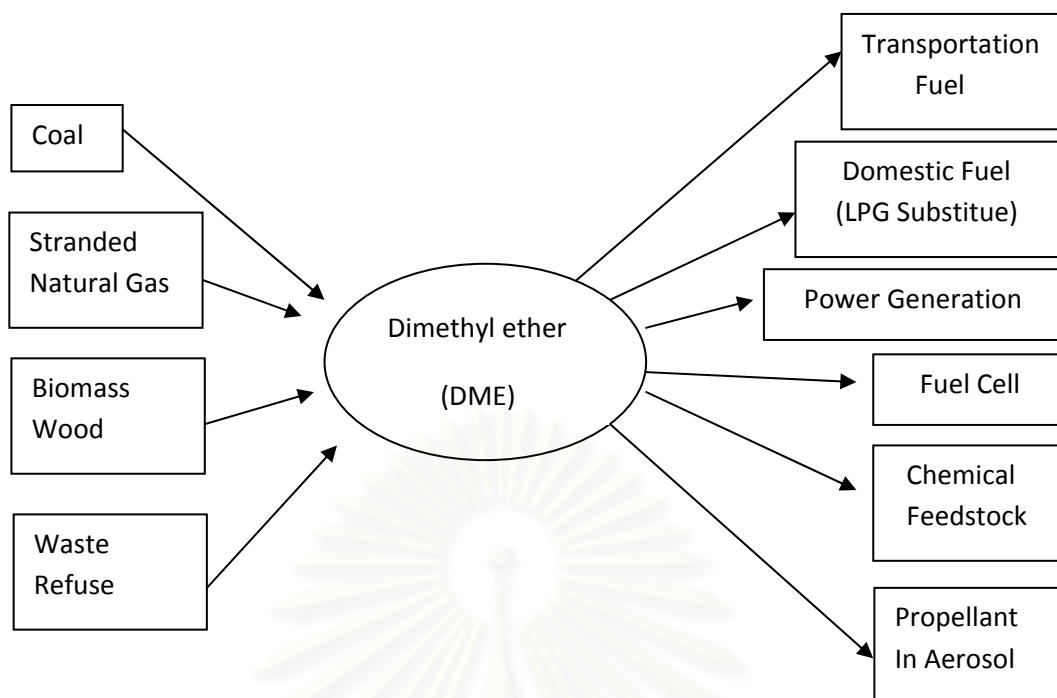
Figure 2.4 Dimethyl ether as a multisource and multipurpose chemical [17]

The simplest ether compound, DME has been shown to be both nontoxic and environmentally benign. Dimethyl ether has a variety of uses in the fuel and the chemical industries. Currently, the major use of DME is an propellant in the aerosols industry, Its cetane number (a quantitative indicator of the ignition quality of diesel engines) is high, ranging from 55 to 60, so that it can be used in diesel engines. Its frame is visible blue frame similar to that of natural gas, and it can be used just as it is in an LPG cooking stove, and it does not produce any aldehydes. The toxicity of DME is low, about the same as that of LPG and even lower than that of methanol [17]. Because of DME 's restrictive use, current world capacity is only 150,000 metrictons/yr [18]. Future mega-plant technology providers include NKK, Haldor Topsoe, Lurgi, Toyo Engineering, Mitsubishi Gas Chemical, Kvaerner, Synetix, etc.

2.3. Properties of Dimethyl ether

Dimethyl ether (DME) is the simplest ether having the chemical formula: CH_3OCH_3. Table 2.3 shows physical properties and combustion characteristics of DME and relating fuels. DME is a colorless gas at ambient temperature, chemically stable,

with a boiling point of -24.9 $^{\circ}$C and as its vapor pressure is about 0.6 MPa at 25 $^{\circ}$C, DME is easily liquefied. Liquid DME is colorless. It is non-carcinogenic, virtually non-toxic, and also non-corrosive in nature. DME is a liquid at the moderate pressure of approximately 496 kPa. Its handling characteristics are very similar to LPG. It is stored in conventional atmospheric pressure tanks as a refrigerated liquid (-25 $^{\circ}$C) or in pressurized tanks (5 bar) at 20 $^{\circ}$C. Dimethyl ether can be ocean transported in LPG tankers. While its net calorific value of 28.88 kJ/kg is lower than of propane, butane and methane, it is higher than that of methanol. With regard to the combustion properties, its explosion limit is wider than that of propane and butane, but almost identical to that of methane and narrower than that of methanol.

Table 2.3 Physical properties and combustion characteristics of DME and other fuels [18].

	Methane	Methanol	Dimethyl ether	Ethanol	Gasoline	Diesel
Formula	CH_4	CH_3OH	CH_3OCH_3	CH_3CH_2OH	C_7H_{16}	$C_{14}H_{30}$
Molecular weight (g mol^{-1})	16.04	32.04	46.07	46.07	100.2	198.4
Density (g cm^{-3})	0.00072[a]	0.792	0.661[b]	0.785	0.737	0.856
Normal boiling point[c] ($^{\circ}$C)	−162	64	−24.9	78	38–204	125–400
LHV[d] (kJ cm^{-3})	0.0346[a]	15.82	18.92	21.09	32.05	35.66
LHV (kJ g^{-1})	47.79	19.99	28.62	26.87	43.47	41.66
Exergy[e] (MJ L^{-1})	0.037	17.8	20.63	23.1	32.84	33.32
Exergy[e] (MJ kg^{-1})	51.76	22.36	30.75	29.4	47.46	46.94
Carbon Content[d] (wt.%)	74	37.5	52.2	52.2	85.5	87
Sulfur content[d] (ppm[f])	∼7–25	0	0	0	∼200	∼250

2.4. Application of Dimethyl ether

High purity DME is currently used as an aerosol propellant owing to its environmentally benign characteristics. It can be widely used as an ultraclean fuel for compression ignition and diesel engines (Buses, Taxies, trucks and off-road vehicles such as construction equipment), a household fuel for heating and cooking, a power generation fuel in gas turbines, a hydrogen source in fuel cell cars, and a chemical feedstock for fuel addition and chemicals.

2.4.1. Dimethyl ether as a transportation fuel

The need to develop alternative fuels is motivated by two important issues. Self-reliance in meeting fuel demands is the first factor, as fossil fuel supply is controlled by a small number of oil exporting countries. Second, the deleterious effect of fossil fuel combustion on the environment has prompted urgent use of clean-burning alternative fuels. Harmful exhaust emission of internal combustion engines, such as nitrogen oxides (NO_x), carbon monoxides(CO), volatile organic compounds and carbon particulates, as well as high levels of carbon dioxides, a greenhouse gas contributing toward global warming, are causing irreparable harm to the environment. Use of DME, a cleaner burning oxygenate, has a very positive impact on these problems. Properties of DME are compared with those of diesel in Table 2.4.

Table 2.4 Comparison of DME properties with diesel [19]

Property	DME	Diesel
Normal boiling point (^{o}C)	-25.1	180-370
Liquid density (g/cm^{3})	0.67	0.84
Ignition temperature (^{o}C)	235	250
Explosion limit (%)	3.4 – 17	0.60 – 0.65
Cetane number	55 – 60	40 – 55
Net heating value (kcal/kg)	6,900	10,000

Dimethyl ether has attractive advantage as an ultraclean transportation fuel alternative, most notably as follows:

- Dimethyl ether molecules have no carbon-to-carbon bonds, which diminish the tendency to form solid carbon particulates during combustion.

- Dimethyl ether has a low autoignition temperature.

- Dimethyl ether has a high cetane number of 55 – 60 , compared to about 45 for diesel. Molecular bonds of DME break up to form radicals at reasonable activation energy, which leads to high cetane number.

- The normal boiling point of DME is -25 $^{\circ}$C. This provides fast fuel/air mixture formation, reduces ignition delay, and imparts excellent cold start properties.

- Oxygen content of DME is 35 wt%, which suppress the formation of soot and facilitates smokeless combustion.

- Dimethyl ether qualifies as a renewable fuel, as it can be produced from biomass and wood.

Dimethyl ether economics are comparable to those of diesel fuel, especially at low NO_x regulation, in term of thermal efficiency. This is possible without major engines modifications, and as such end-user economics could be quite favorable for DME as compared to the cost of converting diesel engines to run on spark-ignited alternative fuels[3] Major potential markets for DME are LPG market, industrial fuel oil market and auto-gas market especially for diesel cars. DME can be mixed with LPG. It is reported that DME can be mixed with LPG up to 25% for use as LPG without any modification of appliances such as cooking heater. LPG market has an advantage of using existing LPG handling facilities such as LPG carrier, storage tanks and distribution system for DME if small modifications are made. As long as the current high price of LPG continues, DME can be price competitive over LPG. However, it may take somewhat longer time to establish distribution infrastructures and modification of engine parts. Therefore, DME may be used first for heavy duty fleets such as public bus and tracks,

followed by gradual penetration into passenger diesel cars under more and more stringent emission control. Big diesel car manufacturers like Nissan Diesel, Hino Motors, Isuzu, Mitsubishi Motors in Japan and Volvo in Sweden are actively developing DME-fueled heavy duty fleet cars.

2.4.2. Dimethyl ether as a household fuel

Dimethyl ether has the capability to substitute LPG as a household fuel for heating and cooking purposes, especially in Asian countries such as Japan, China, and India where the demand for LPG is growing. Utilization of DME as a household fuel can also reduce the burden on developing countries that use solid fuels like coal and firewood, which in turn have harmful effects on the environment. Dimethyl ether can be produced indigenously in developing countries by taking advantage of stranded natural gas fields in their vicinity. Dimethyl ether is a clean fuel and the total investment cost would be small because existing LPG infrastructures could be used with minor modification [20].

Dimethyl ether flame is a visible blue flame similar to that of natural gas, and it can be used in an LPG cooking stove without producing any aldehydes. Its lower explosion limit is higher than that of propane, indicating higher safety than propane in case of leakage. Combustion tests on DME have been conducted with mass-produced household cooking stoves in Japan, and have passed the Japan Industrial Standard combustion test. This study showed that stoves designed to burn city gas (85% methane, 15 % propane) could burn DME well with only an adjustment of the variable air dampers.

The prospect of DME as an alternative fuel to LPG in consumer applications stimulated experiments to investigate DME combustion in existing mass-produced combustion equipment in order to gain an understanding of its combustion characteristics.DME has a WI (Wobbe Index, which is the higher calorific value/(specific gravity)1/2 and is used as a basic measure of heat input for gas appliances) of 51.91

MJ/Nm^3 and an MCP (an index of the rate of gas combustion) of 48 to 50. The WI for DME is close to that of 13A and 12A municipal gases, but its MCP is outside the corresponding range. DME is equivalent to a gas classification of 12C, a type not currently used. Combustion tests of DME were conducted using standard domestic cooking stoves designed for LPG or municipal gas 13A. Combustion of DME using the LPG stove shown in Figure 2.5(a) is clearly unsatisfactory. No significant improvement in combustion was observed, even when the air adjustment damper, which is normally fixed, was closed down to approximately 80%. This lack of improvement is due to the fact that the diameter of the main nozzle on the LPG stove is very small (0.9 mm), thus preventing a sufficient supply of DME and resulting in insufficient heat of combustion. Combustion of DME with the municipal gas 13A stove is shown in Figure 2.5(b). Combustion was relatively satisfactory, but the flame tended to be shorter than is the case when 13A is burned. Changing the opening of the variable air adjustment damper from 8/10 to 5/10 reduced the primary air supply and resulted in good combustion, as shown in Figure 2.5(c). Changing the gas pressure from 1 to 3.3 KPa did not result in any significant difference in combustion. JIS combustion testing (JIS S 2093) to determine the suitability of the gas combustion equipment for DME resulted in passes in all items on the test schedule, from tests in no-wind conditions to tests with large pots, and certification was granted. JIS thermal efficiency testing (JIS S 2093) to determine the performance of gas combustion equipment in use showed a thermal efficiency of 47.9% with DME, approximately 2% less than with municipal gas 13A. DME is well within the JIS standards, which require a thermal efficiency of at least 40%.

(a) LPG specification, damper opening : fixed

(b) 13A specification, damper opening : 8/10

(c) 13A specification, damper opening : 5/10

Figure 2.5 Combustibility of Dimethyl ether [20]

2.4.3. Dimethyl ether for power generation

Dimethyl ether is a promising new gas turbine fuel. Roughly speaking, 1 bcf/day of gas, converted into about 20,000 TPD of DME, can generate about 10,000 MW of power. Utilization of DME for power generation offers tremendous environmental benefits, in term of CO_x, SO_x and NO_x emission [21]. It burns in conventional gas turbines without modifications to the turbine or the combustors. Emissions produced by combustion of conventional fuels in gas turbine include nitrogen oxides, carbon monoxide, unburned hydrocarbons and sulfur oxides. Dimethyl ether produces no sulfur oxide emission, as the fuel is sulfur free. It generates the least amount of NO_x, CO and unburned hydrocarbon as compared with natural gas and distillate and lower CO_2 emissions than the distillates.

BP has introduced a turbine-grade DME fuel that contains 88.0-89.0 wt% DME, 2.9-3.5 % water, 7.0-8.0 wt% methanol and 0.3-0.5 wt% of other oxygenates(with no metals or nitrogen and with only a trace of sulfur). BP and GE power systems are currently implementing a project in India to use DME as a fuel for power generation [22]. Test results of the BP-introduced fuel at General Electric show that its emission properties and other key combustor operating parameters, including dynamic pressures and metal temperatures, are comparable to those of natural gas. The power generation efficiency (D) is expressed in term of a heat rate number that corresponds to the amount of thermal energy needed to generate one unit of electrical energy. A lower heat rate number reflects higher power generation efficiency. The estimated performance of a nominal 700 MW combined cycle power plant base on the GE 9E machine indicates that the heat rate using refrigerated DME would be about 1.6 % lower than that using natural gas and about 6.3 % lower than that using liquid naptha. GE is prepared to pursue commercial offers, including standard commercial terms and guarantees, of DME-fired B/E class (diffusion and DLN burners) and F class (diffusion burners) heavy-duty gas turbines.

NKK Corporation has developed a process for DME production, which will greatly enhance the use of DME in power plants in Asia, especially in Japan, which typically use liquefied natural gas (LNG), LPG, fuel oil and coal. Fuel oil and coal are subject to environmental concerns, most notably the emission of carbon dioxide and treatment or disposal of ash. A possible solution to circumvent this problem would be to generate DME at the mine, which can be shipped and used in more energy-efficient and environmentally conscious manner. Liquefied natural gas and LPG are cleaner burning fuels, albeit at a much higher investment cost. Japan imports LNG, as fuel for electric power generation. Again, it would be economical to import DME produced from natural gas at medium and small-scale gas fields considered too small for LNG development for thermal power generation. The supply source for LPG is limited mainly to the Middle East for countries in Southeast Asia and the Far East. Dimethyl ether can substitute LPG in power generation applications, just like in household applications.

2.4.4. Dimethyl ether for fuel cells

Fuel cells can be powered by DME. Daimler Chrysler A.G. has studied the feasibility of using DME as a fuel in a polymer electrolyte membrane (PEM) fuel cell, in collaboration with Ballard Power Systems and University of Technology RWTH Aachen, Germany. Direct oxidation fuel cells, including the ones using methanol as fuel, are hindered by efficiency losses. The effect of methanol fuel crossover oxidation reaction at the cathode is the most significant efficiency loss, the others being use of parasitic fluid pumps and mild toxicity of methanol vapor. An advantageous finding of the study is that DME is typically not oxidized at the cathode of the fuel cell. This minimizes the unwanted effects of fuel crossover, leading to improved fuel cell efficiencies when compared to direct methanol fuel cells, especially at low to medium current densities.

Researchers at the Electrochemical Engine Center at the Pennsylvania State University have identified additional advantages of using DME as a fuel in PEM fuel cells. It must be noted that DME molecules do not have a carbon-carbon double bond,

enabling nearly complete oxidation in low-temperature PEM fuel cells. Also, DME can be stored in high-density liquid phase at modest pressures of around 5 atm, and delivered as a gas-phase fuel in a pumpless operation. Therefore, use of DME can potencially combine the advantage of easy fuel delivery of pressurized hydrogen and the high energy density storage of liquid fuel [23].

Hydrolyzing DME with steam can produce hydrogen, carbon oxides being the by products. This method utilizes an essentially alkali-metal free catalytic composition of copper or nickel in elemental form, which catalyzes the hydrolysis reaction. A water – gas shift reaction converts carbon monoxide, which is usually present in the hydrolysis product, to relatively inert carbon dioxides. The hydrolysis and shift reactions take place in a single reaction zone, or alternatively, in separate reaction zones where reaction conditions can be individually optimized. When separate zones are provided, the heat is essentially transferred from the water-gas shift reaction zone to the hydrolysis reaction zone. The hydro-shifted product stream can be utilized as fuel to power a turbine, and an integrated heat transfer scheme can be used to recover heat from the turbine exhaust stream. The reaction are carried out at temperature between 150 $^{\circ}$C and 800 $^{\circ}$C, with better results obtained when operating in the range of 350-400 $^{\circ}$C. Dimethyl ether conversion of 88.5 % and hydrogen to carbon monoxides ratio of 2.44 in the product stream were obtained by operating at 350 $^{\circ}$C and 2 $^{\circ}$C/hr [24,25].

2.4.5. Dimethyl ether as a propellant

Dimethyl ether has been increasingly used as a propellant in aerosol formulations to replace chlorofluorocarbons, which are found to destroy the ozone layer of the atmosphere. Dimethyl ether is nontoxic and easily degrades in the troposphere. Although about 90 % of the major current U.S. aerosol industry uses hydrocarbon-based propellants (mostly isobutene and propane), DME could become a more widely used propellant in the coming years. Several aerosol-based household products include

colognes, hair sprays, dyes, personal care mousses, antiperspirants and room air fresheners.

Current suppliers for the DME propellant market include DuPont, Akzo Nobel and Mitsubishi Gas Chemicals. Demeon D, a DME-based product from Akzo Nobel, is used as a propellant in cosmetic formulations, foam blowing and paint or other aerosol .

Dymel[®] A, a product based on DME manufactured by DuPont, is a medium- to high-pressure propellant for general aerosol use, including personal products. It has extremely low toxicity, its lower explosive limit in air is higher than that of propane and isobutene, and it is a chemically stable compound. In aqueous solutions, the propellant is hydrolytically stable over a wide pH range. Dymel A is unique among aerosol propellants in that it has high solubility in both polar and nonpolar solvents. It is completely miscible with most organic solvents and is by itself a very good solvent for many types of polymers, e.g. hair splay and paint resins. Dymel A has 35 wt% solubility in water, which facilitates formulation of single phase products with large amounts of water and is the only liquefied gas aerosol propellant to do so.

2.4.6. Dimethyl ether as a chemical building block

Dimethyl ether is an essential intermediate in the synthesis of hydrocarbon from coal or natural gas derived syngas. Dimethyl ether is a building block for the preparation of many important chemicals, including methyl sulfate [26]. Dimethyl sulfate is an important commercial commodity as a solvent and also as an electrolyte in high-energy-density batteries. Lower olefins like ethylene and propylene or downstream products such as gasoline and range boiling hydrocarbons, are produced from syngas using DME as an intermediate [27,28]. A variety of specialty industrial chemicals such as oxygenates, acetaldehyde, acetic acids, ethylene glycol precursor like 1,2-dimethoxyethane etc. can be formed using DME as a feedstock. Air Products has programs under way to use DME as a chemical building block for higher-molecular-

weight oxygenated hydrocarbons [29]. Some of the chemicals that can be synthesized using DME as a building block are shown in Fig. 2.6.
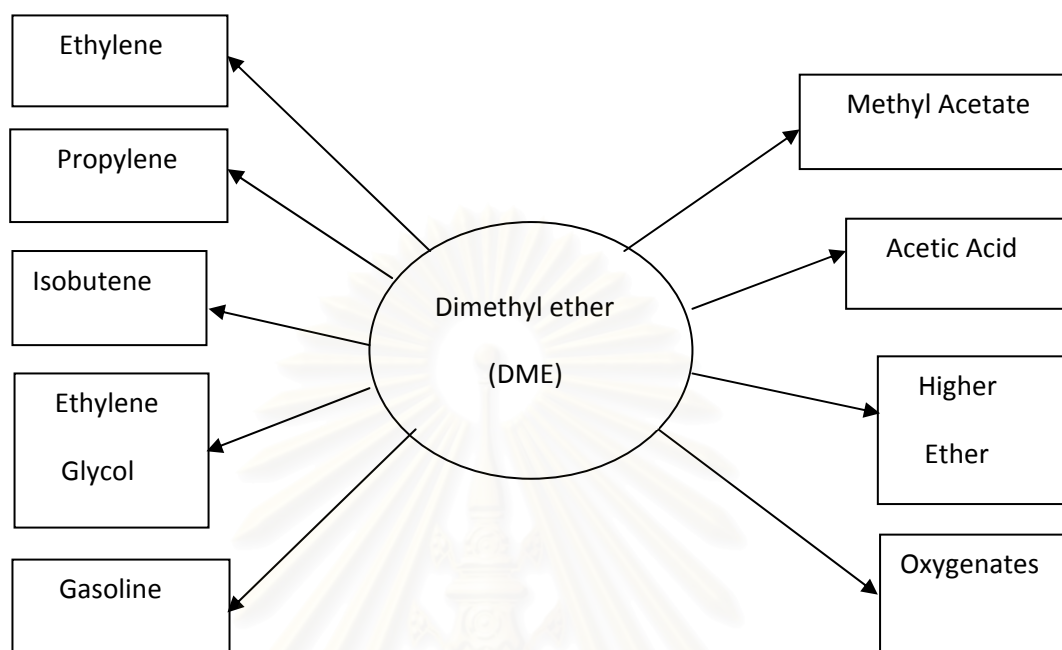
Figure 2.6 Dimethyl ether as a building block for chemical and oxygenates [29]

2.5. Dimethyl ether synthesis process

Dimethyl ether can be produced from natural gas, biomass or other carbon containing materials. Using existing supplies of natural gas combined with current technology, DME can be economically produced on a large scale via synthesis gas. Syngas or synthesis gas is produced by coal gasification, biowaste gasification or by natural gas or hydrocarbon reforming. Dimethyl ether synthesis in the vapor phase suffers from low per-pass conversions, mandated in part the debilitating effects of high temperature on the catalysts. Synthesis of DME in the gas phase has been studied in detail at Mobil Oil [30,31]. Gas phase DME synthesis processes, in general, suffer from the drawbacks of low hydrogen and CO conversions per pass, along with low yield and selectivity of DME coupled with a high yield of carbon dioxide. These processes are typically expensive due to high capital costs for reactors and heat exchangers, and high

recycle rates [29,32]. Using an inert liquid as a heat sink for highly exothermic reactions offers a number of opportunities in syngas processing. Heat generated by the exothermic reactions is readily accommodated by the inert liquid medium. This enables the reaction to be run isothermally, minimizing catalyst deactivation, which is commonly associated with the more adiabatics gas phase technologies.

Methanol dehydration to DME as described in patent literature occurs on γ-Al_2O_3 and γ-Al_2O_3 modified with phosphates or titanates [33]. Temperature in the range 250 – 400 $^{\circ}$C and pressure up to 1.04 MPa have been claimed. Many other catalysts have been reported for alcohol dehydration, including zeolites, silicas alumina, mixed metal oxides, and ion – exchange resins and three catalysts were reviewed recently [34,35]. DME formation has also been reported over a 1 wt% Pd/ Al_2O_3 catalyst with 90 % selectivity at 71 % methanol conversion [20]. The reaction was performed at 200 $^{\circ}$C and 0.1 MPa. When the Pd was supported on ZnO, the product was primarily methyl formate, whereas on various other supports, including SiO_2, Cr_2O_3 and MgO, only CO was produced.

Both Lewis and Bronsted acidity are involved in the dehydration reaction over acid catalysts, and selectivity control to limit the dehydration of DME to olefins and aromatics requires that the surface acidity not be too high and the reaction temperature be below 300 $^{\circ}$C [34]. The olefins are generally thought to be produced by a consecutive reaction in which methanol is first converted to DME, which in turn is converted to olefins and aromatics. Reaction mechanisms for DME formation have been proposed by various investigators. According to Kubelkova et al.[37], the mechanism over Si-Al zeolites involves protonation of the hydroxyl group reacts with a gas-phase methanol molecule to from DME at 180-300 $^{\circ}$C and $C_2 - C_5$ aliphatics and aromatics above 300 $^{\circ}$C . According to these authors, Lewis acid sites (Al_n–OH), associated with nonskeletal alumina, can also form methoxyls according to the reaction

$$Al_n-OH \ + \ CH_3OH \ \leftrightarrow \ Al_n-OCH_3 \ + \ H_2O \quad\quad\quad (1)$$

$$Al_n- OCH_3 \ + \ CH_3OH \ \leftrightarrow \ (CH_3)_2O \ + \ H_2O \ + \ Al_n \quad\quad\quad (2)$$
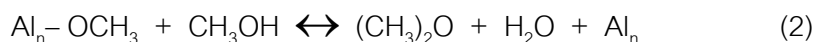
Bandeira and Naccache [22] proposed a duel acid-base mechanism in which CH_3OH reacts on a Bronsted acid site and another methanol molecule reacts at an adjacent O^{2-} site. Thus a bimolecular Langmuir – Hinshelwood reaction mechanism is proposed according to the following reaction steps:

$$CH_3OH \ + \ H^+ \ \leftrightarrow \ [CH_3OH_2]^+ \quad\quad\quad (3)$$

$$CH_3O\text{-}H \ + \ O^{2+} \ \leftrightarrow \ [CH_3O]^- \ + [OH]^- \quad\quad\quad (4)$$

$$[CH_3OH_2]^+ \ \leftrightarrow \ [CH_3]^+ + H_2O \quad\quad\quad (5)$$

$$[CH_3]^+ \ + \ [CH_3O]^- \ \leftrightarrow \ CH_3OCH_3 \quad\quad\quad (6)$$
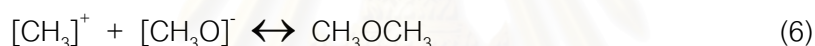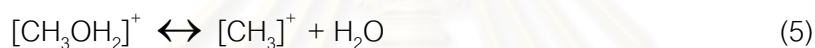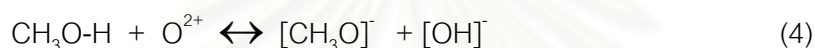
And reaction (6) is the rate limiting step.

Most recently, methanol dehydration kinetics were examined over a $\gamma\text{-}Al_2O_3$ catalyst at 0.15 MPa in the temperature range 290 – 360 $^\circ$C. A kinetic equation assuming surface reaction control with dissociative adsorption of methanol gave the best fit to the experimental results [39]. The dissociative adsorption is consistent with many previous kinetic models in which the rate of DME formation is found to proportional to the square root of the methanol concentration. A high selectivity to DME can be obtained by suitable choice of the catalyst and reaction conditions. It has been shown that weak acid sites favor methanol dehydration [40] and that strong acid sites, although having high turnover frequency, are less selective than weak acid sites [34]. Controlled dealumination of the zeolite is therefore one way of achieving high DME selectivity. DME selectivity and yield have also been shown to increase with time on-stream, presumably because of coking of the strong acid sites, as shown by the data in Table 2.6 for SAPO-

11 catalyst [41]. Acidity control is most effective with zeolite catalysts, and these appear to be the most promising catalysts for this synthesis

Table 2.5 Effect of Coking on Dimethyl ether Yield over SAPO-11 Catalysts [41]

	Methanol feed rate (g methanol/g/h)			
	0.050		0.031	
Time on-stream, h	0.12	1.1	0.17	1.5
Methanol conversion, %	35.3	43.4	38.9	68.0
DME selectivity, %	41.2	67.1	5.1	86.6
DME yield, %	17.9	17.9	3.5	33.7

The single step, liquid phase DME synthesis process incorporates the sequential reaction of methanol synthesis and methanol dehydration in a slurry phase reactor system. Combining these reversible reactions in a single step drives each reaction thermodynamically by utilizing its inhibiting products as reactant in the subsequent reactions. Apart from the superior heat management allowed by the liquid-phase operation, the synergistic effect of these reactions occurring together yields higher quantities of DME than could be obtained from sequential processing [29,32,42]. A number of processes have been developed to convert coal- or natural gas-based syngas into DME. The prominent ones include those by Haldor Topsoe, NKK Corporation, Air Products, Toyo Engineering Company and the University of Akron, Electric Power Research Institute. A brief description of these processes are given below.

2.5.1. Haldor Topsoe Process

The chemical reactions involved in synthesis of DME from natural gas are as follows:

Reforming:

$$CH_4 + 3/2O_2 = CO + 2H_2O$$

$$CH_4 + H_2O = 3H_2 + CO$$

$$CO + H_2O = CO_2 + H_2$$

Dimethyl ether synthesis:

$$3H_2 + CO = CH_3OH + H_2O$$

$$H_2O + CO = H_2 + CO_2$$

$$2CH_3OH = CH_3OCH_3 + H_2O$$
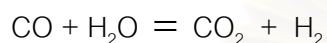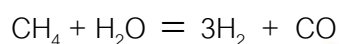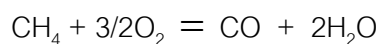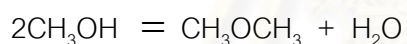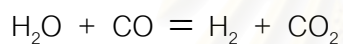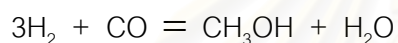
Haldor Topsoe has conducted a considerable amount of research for the purpose of developing DME as a diesel fuel from natural gas. They developed a new process, which is an integrated process from production of methanol from synthesis gas generated from various feed stocks ranging from natural gas to coal and biomass, followed by its subsequent conversion into DME in one single plant.
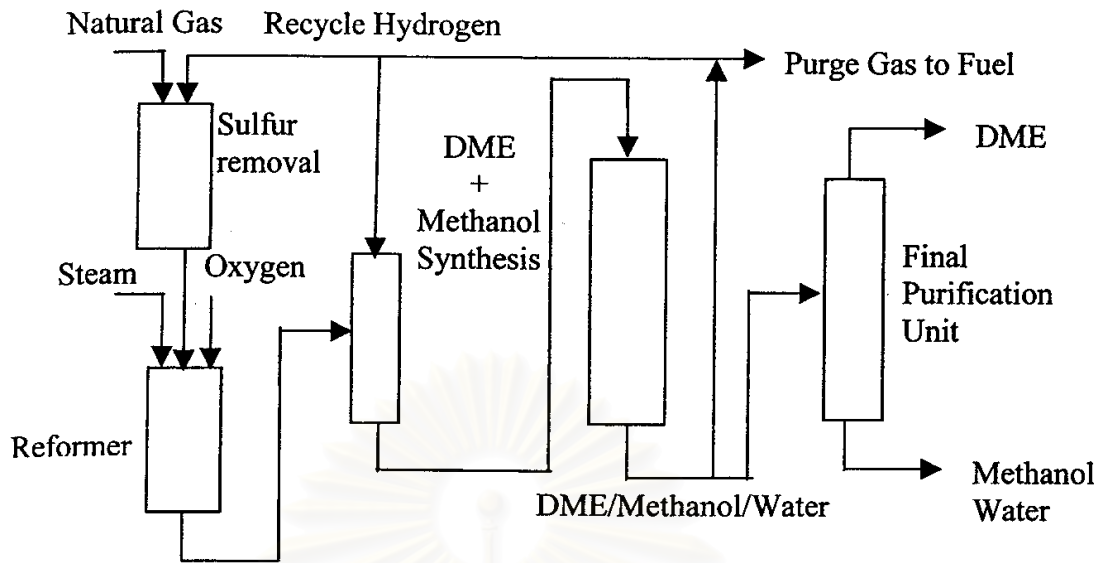
Figure 2.7 Haldor Topsoe technology for DME synthesis [43]

The Haldor Topsoe process can produce neat DME or a raw fuel grade DME that can be specific blends of DME, methanol and water. As shown in Fig.2.7, the process consist of the following main steps: synthesis gas preparation, methanol and DME synthesis and final purification unit. The synthesis gas preparation process uses autothermal reforming (ATR), consisting of a specifically designed burner (CTS burner). In this process, oxygen is added to desulfurize natural gas and stream. The steam to carbon ratio in the ATR is low (as low as 0.6) and the exit temperature is high. This ensures a favorable synthesis gas composition and low methane content. Synthesis of methanol and conversion of methanol into DME takes place in two separate reactors, which allows both parts of sequential reaction to be carried out at optimal conditions. Methanol synthesis, which is a more exothermic reaction than DME synthesis, is carried out in a cooled reactor where reaction exotherm is continuously removed. Dimethyl ether synthesis takes place over a proprietary multiple-function methanol/DME catalyst in a loop comprising three adiabatic fixed-bed reactors in series. These have interstage cooling to achieve a high conversion of CO to CO_2. The product mixture of DME/methanol/water is then condensed and separated. The unconverted synthesis gas

is split into a recycle stream and a purge stream, which is used as fuel and as hydrogen

recycle. Dimethyl ether is purified by distillation in the final purification unit [43,44].

2.5.2. NKK Process or JFE Process

Researchers at NKK Corporation have developed a process for DME synthesis

from coal-bed methane using a slurry-bed reactor technology, utilizing a proprietary

highly active catalyst for producing DME directly from the syngas at high yields.The

success of this technology has been demonstrated since 1999 [45].

2.5.2.1. DME synthesis reaction and equilibrium conversion

Table 2 shows reactions concerning with direct DME synthesis and their reaction

heats. There are mainly two overall reaction routes that synthesize DME from synthesis

gas (syn-gas: H2+CO gas), re-action (a) and (b). The reaction (a) synthesizes DME in

three steps, which are methanol synthesis reaction (c), dehydration reaction (d) and

water-gas shift reac-tion (e). When the shift reaction does not take place, reaction (c)

and (d) are combined to the reaction (b), which is the other DME synthesis route. Haldor

Top-soe A/S and some other direct DME syntheses follow reaction (b) [3]. JFE direct

DME synthesis follows reaction (a).

Table 2.6 Reaction formulas concerning DME synthesis.

	Reaction	Reaction heat (kJ/mol)
(a)	$3CO+3H_2 \rightarrow CH_3OCH_3+CO_2$	-246
(b)	$2CO+4H_2 \rightarrow CH_3OCH_3+H_2O$	-205
(c)	$2CO+4H_2 \rightarrow 2CH_3OH$	-182
(d)	$2CH_3OH \rightarrow CH_3OCH_3+H_2O$	-23
(e)	$CO+H_2O \rightarrow CO_2+H_2$	-41

Since both reaction (a) and (b) generate two molecules of products from six molecules

of syn-gas, the higher reaction pressure gives higher syn-gas con-version. In

consideration of process design, JFE Direct DME Synthesis reaction pressure is around

3 to 7 MPa, and its standard pressure is 5 MPa. Methanol synthesis is an equilibrium-restricted reaction. However when the dehydration reaction (d) takes place simultaneously, the syn-gas conversion rises dramatically. Figure 2.8 shows stoichiometric equilibrium syn-gas conversion of DME synthesis (a) and (b) under 5 MPa, and methanol synthesis (c) under 5 and 9 MPa. Compared DME synthesis reaction (a) with reaction (b), reaction (a) gives much higher syn-gas conversion in all temperature conditions.
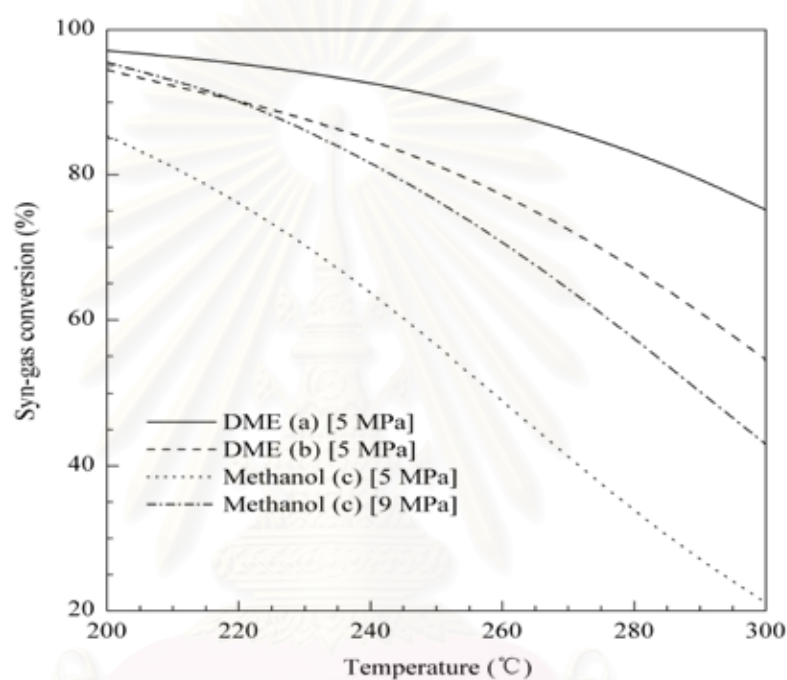
Figure 2.8 Stoichiometric equilibrium conversion of DME and methanol synthesis

Figure 2.9 shows equilibrium conversion of synthesis gas (CO conversion plus H_2 conversion) calculated at 260°C and 5 MPa for DME synthesis reaction (1) and methanol synthesis reaction (2) as a function of hydrogen/carbon monoxide ratio (H_2/CO) of the synthesis gas. In each reaction, the equilibrium conversion has its maximum peak where H_2/CO ratio corresponds to the stoichiometric value, that is, with H_2/CO ratio of 1.0 for DME synthesis reaction (1) and 2.0 for methanol synthesis reaction (2). The maximum equilibrium conversion for DME synthesis reaction (1) is much higher than that for methanol synthesis reaction (2).
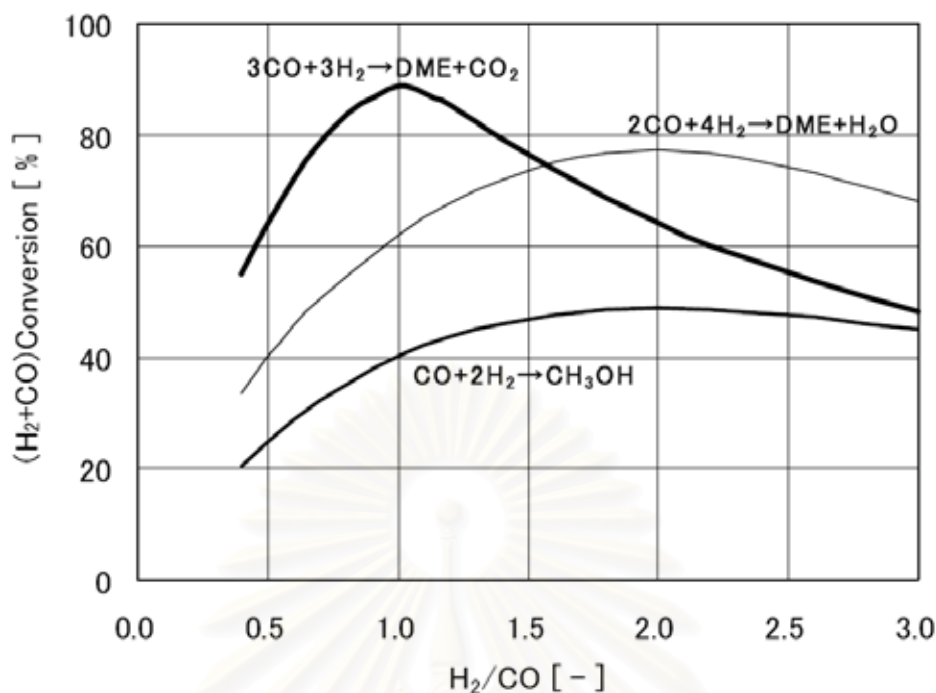
Figure 2.9 Equilibrium conversion of synthesis gas (260°C, 5 MPa) [45]

As the reaction of DME synthesis is highly exothermic, it is more important to control the reaction temperature than that in the case of methanol synthesis, because the higher equilibrium conversion of DME synthesis gives much more reaction heat, and hot spot in the reactor could damage the catalyst. In the slurry which is composed of an inert solvent and fine catalyst particles, the reactant gas forms bubbles and diffuses into the solvent, and chemical reaction takes place on the catalyst. The reaction heat is quickly absorbed by the solvent, which has a large heat capacity, and thanks to the high effective heat conductivity, the temperature distribution in the slurry could be homogeneous. There is less restriction on the shape and strength of the catalyst in the slurry phase reactor than that in the fixed-bed reactor. Catalyst is replaceable even during operation. In the slurry phase reactor, as catalyst particles are surrounded by the solvent, mass transfer mechanism of reactants and products is different from that in the fixed bed reactor. In this connection, a catalyst system adequate to the slurry phase reactor has been developed. In order to enable a large scale test, a catalyst mass production technology has been also developed. There is an additional merit that the

slurry phase reactor for DME synthesis is simpler than that of FT synthesis. It is because DME synthesis reaction products are all in gas phase at the reactor outlet and liquid product and catalyst separation is not required By-product of reaction (1) is CO_2, actually with methanol and a very small amount of water, separation of liquid product and unreacted synthesis gas is efficiently done at chilled temperature($-39^{o}C$). CO_2 can be removed by dissolving in product DME.

The synthesis gas (H_2/CO=1) adequate for DME synthesis can be produced in an autothermal reformer (ATR) with O_2 and recycled CO_2 from DME synthesis itself by the following reaction;

$$2CH_4+O_2+CO_2 \longrightarrow 3CO+3 H_2+ H_2O \qquad \Delta H = - 30.4 kJ/mol \qquad (5)$$
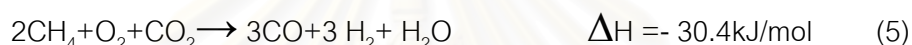
The burner top structure and furnace inner profile were designed to enhance mixing of feed in order to realize both higher thermal efficiency and much lower soot formation and residual methane at the same time. Water cooled burner and well designed refractory works are applied to keep its robustness. Reforming catalyst bed is located at the lower part of ATR to have role of completing reforming and having better gas distribution. Synthesis gas going out of ATR is rapidly quenched to prevent Boudouard reaction. Synthesis gas production (5) and DME synthesis reaction (1) give the following overall reaction:

$$2CH_4+O_2 \longrightarrow CH_3OCH_3+ H_2O \qquad \Delta H = - 276.4 kJ/mol \qquad (6)$$

which indicates that DME and water is generated by a kind of partial oxidation of methane. Table 2.6 shows a comparison of "Direct synthesis" and "Indirect synthesis". Indirect synthesis is two step process of methanol synthesis by reaction (2) from synthesis gas and DME production by dehydration reaction (3).The synthesis gas (H_2/CO=2) adequate for methanol synthesis can be produced in an autothermal reformer (ATR) with O_2 and steam by the following reaction;

$$2CH_4 + O_2 + H_2O \longrightarrow 2CO + 4H_2 + H_2O \qquad \Delta H = -71.4 \text{kJ/mol} \qquad (7)$$

Table 2.7 Characteristics of two DME processes [45]

Process	Direct (JFE)	Indirect (Two Step)	
		Methanol	Dehydration
Reaction pressure(MPa)	5	8-10	1-2
Reaction temperature($^{\circ}$C)	240-280	180-270	300-340
One through conversion(%)	50	38	70
Reaction by-product	CO_2	-	Water
(Water+MeOH)/DME (molar ratio)	0.1	-	1.9
Reactor	Slurry Phase	Fixed Bed	Fixed Bed
Cold gas efficiency(%) ( ) – Theoretical cold gas efficiency(%)	71(83)	57(83)	
		66(84)	87(98)

The combination of (7),(2) and (3) gives the same overall reaction formula (6). The methanol synthesis is done actually at pressure 8-10 MPa because the equilibrium conversion of the methanol synthesis is low at pressure 5 MPa as shown in Figure 2.9. Dehydration reaction is conducted at 300-340°C and 1-2 MPa. Once through conversion is high, around 70 %, but energy requirement for evaporation of liquid methanol and separation of three components, DME, by-product water and unreacted methanol is so large. Taking account of this energy requirement, the cold gas efficiency of dehydration process goes down to 87 % and the overall cold gas efficiency of DME production from natural gas is estimated as about 57 %. The calculated theoretical value of cold gas efficiencies of the DME production from methane, the methanol production from methane, and the dehydration of methanol is shown in Table 2.7. In this table, estimated values for actual plant are also indicated; an evaluated value from operation results of an actual plant of the methanol synthesis, a predicted value by process simulation for the methanol dehydration and the direct DME synthesis. It is understood that the direct synthesis could have big advantages of the lower synthesis pressure and the higher cold efficiency over the indirect synthesis.

2.5.2.2. Advantage of Slurry Phase Reactor for DME Synthesis

A fixed bed is generally used for catalytic reaction. For such exothermic reaction as methanol synthesis, various design ideas are applied to control the temperature in the reactor. The reaction of DME synthesis is highly exothermic, it is more important how to control the reaction temperature than in the case of methanol synthesis, because the higher equilibrium conversion of DME synthesis could give higher reaction heat, and hot spot in the reactor could damage the catalyst. As shown in Figure 2.10, the slurry phase reactor is an apparatus in which the reactant gas forms bubbles, and chemical reaction takes place during the bubbles rise in the slurry: a solvent containing fine catalyst particles. The heat of the reaction is quickly absorbed by the solvent, which has a large heat capacity, and thanks to the high heat conductivity. The temperature within the reactor vessel can be easily controlled in order to achieve higher conversion with longer catalyst life. There are fewer restrictions on the shape and strength of the catalyst in the slurry phase reactor than in the fixed bed reactor. In the slurry phase reactor, however, as catalyst particles are surrounded by the solvent, it is required to develop an efficient catalyst.
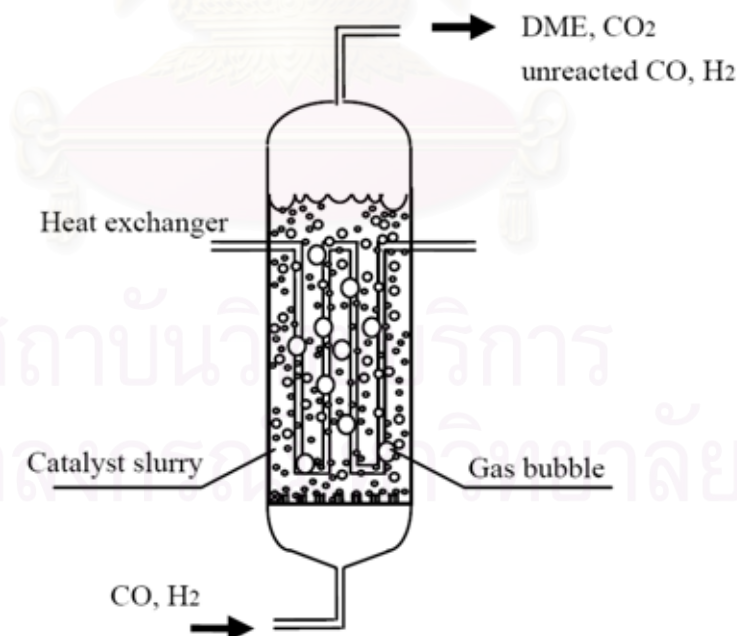
Figure 2.10 Concept of slurry phase reactor for DME synthesis [45]

2.5.2.3 DEVELOPMENT OF JFE'S DME SYNTHESIS PROCESS

The basic features of the JFE process are its slurry phase reactor in which the temperature can be easily controlled thanks to the high effective heat convection and its newly developed catalyst system adequate to the slurry phase reactor which realizes the reaction of formula (1). JFE (formerly NKK Corporation) has developed new efficient catalyst and slurry phase process for DME synthesis in the fundamental research since 1989 [17]. On these fundamental results, JFE conducted five years development project using a 5 tons/day pilot plant, started since 1997 with funds provided by the Ministry of Economy, Trade and Industry [45]. In 2001, conceptual design of 100 tons/day-scale plant was carried out. In 2002, five years development project using 100 tons/day-scale demonstration plant has started by DME Development Co., Ltd. with funds provided by the Ministry of Economy, Trade and Industry. DME Development Co., Ltd. was established in December 2001 in order to promote the development of DME direct synthesis technology by JFE, Nippon Sanso Corporation, Toyota Tsusho Corporation, Hitachi Ltd., Idemitsu Kosan Co., Ltd, Marubeni Corporation, INPEX Corporation, LNG Japan Corporation, Total S.A. and Japex Co., Ltd .

The 5 tons-DME/day pilot plant was designed and constructed by JFE in 1999 at Taiheiyo Coal Mining's site in Hokkaido. The synthesis gas is produced by reforming reaction in auto thermal reformer of coal mine gas (CH_4 40%, Air 60%) and propane with oxygen, steam and recycled carbon dioxide to vary its hydrogen/carbon monoxide ratio widely. Propane is added to reduce the nitrogen content of the synthesis gas. The produced synthesis gas is cooled, compressed and separated carbon dioxide by amine absorption and enters the DME synthesis reactor. The dimension of the reactor is 55 cm in inner diameter and 15 m in height. The effluent of the reactor is cooled and chilled to be separated from unreacted gas, which is recycled to the reactor. The liquid stream from the separator is separated into three products, DME, CO_2 and methanol in the two distillation columns. From September 1999 to December 2000, five test operations of DME synthesis were conducted including long term continuous operation for two months. The operations were very stable for both synthesis gas production and DME synthesis. Test using only coal mine gas was conducted successfully, though the synthesis gas contains nitrogen at higher than 40 %. During the operation, a certain

amount of spent catalysts was drawn out of the reactor and fresh ones were charged without any troubles. Figure 2.11 shows an example of the observed temperature profile in the reactor. The temperature was well controlled almost constant to the target value (260 $^{\circ}$C) and there was no hot spot. Figure 2.12 shows one-through and total synthesis gas conversion as a function of the recycle ratio (recycle gas flow rate / make-up gas flow rate) in the reactor. Total conversion increases up to higher than 95 % with increasing the recycle ratio while one-through conversion is almost constant. The production of H_2O is very small; $H_2O/(DME+CH_3OH+H_2O)=0.013$ by hydrogen-mole base. This confirms that the overall reaction follows the reaction formula (1). The purity of product DME is higher than 99.9 % and the total content of water and methanol as impurity is lower than 100 ppm.
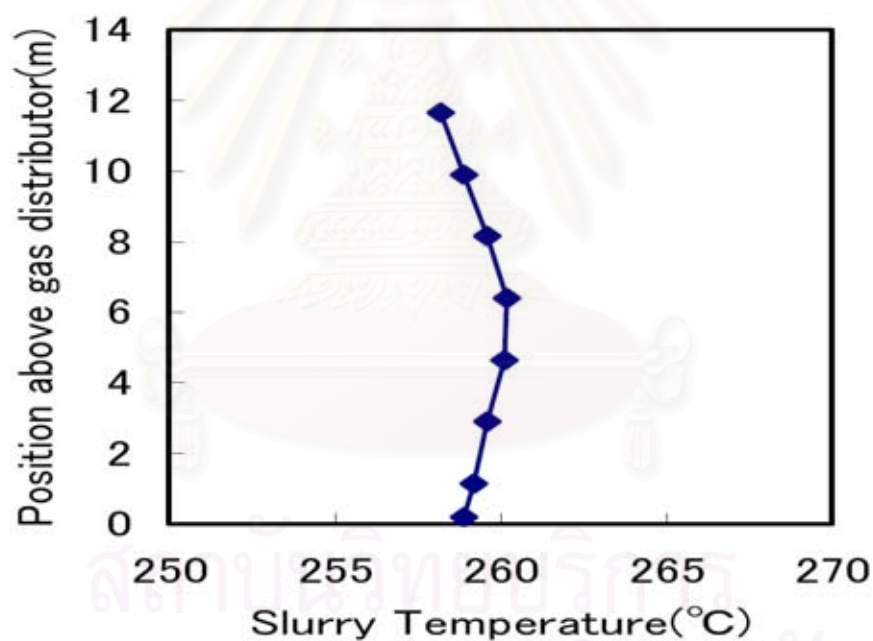
Figure 2.11 Slurry temperature distribution [45]
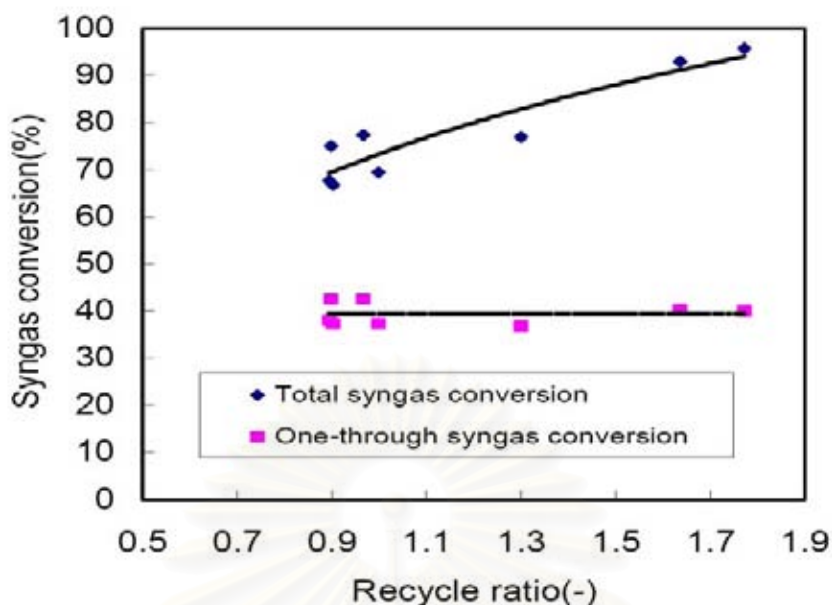
Figure 2.12 Syngas conversion as a function of Recycle ratio [45]

Figure 2.13 shows one-through CO conversion and ratio W/F of weight of catalyst charged (W) and gas flow rate (F) in the slurry phase reactor under the same temperature and pressure condition for laboratory scale autoclave (DME synthesis amount: 1 kg/day), small scale bench plant that is bubble column reactor heated from outside (50 kg/day) and large scale bench plant in which heat exchange coils are installed (5 tons/day). In spite of 5,000 times difference of scale among those three reactors, CO conversion data vary coherently with W/F. This suggests that the synthesis reaction rate is mainly controlled by reaction itself and the production is proportional to the amount of catalyst in the reactor. The flow phenomena in the slurry phase reactor is affected as shown in Figure 2.10 by the size of bubble generated through gas distributor, slurry depth (Hs) and its ratio (Hs/D) to reactor diameter (D). Figure 2.14 shows changes of Hs/D as the reactor is scaled up in enlarging the reactor diameter with constant W/F and constant slurry depth. With smaller Hs/D, lateral flow should be taken into account.

According to feasibility study of commercial plant, the minimum production scale is evaluated to be 2,500 tons/day. Fabricator informs that the maximum diameter of the

pressure vessel of DME synthesis is 8 m, beyond which the production scale-up is realized by increasing the slurry depth.
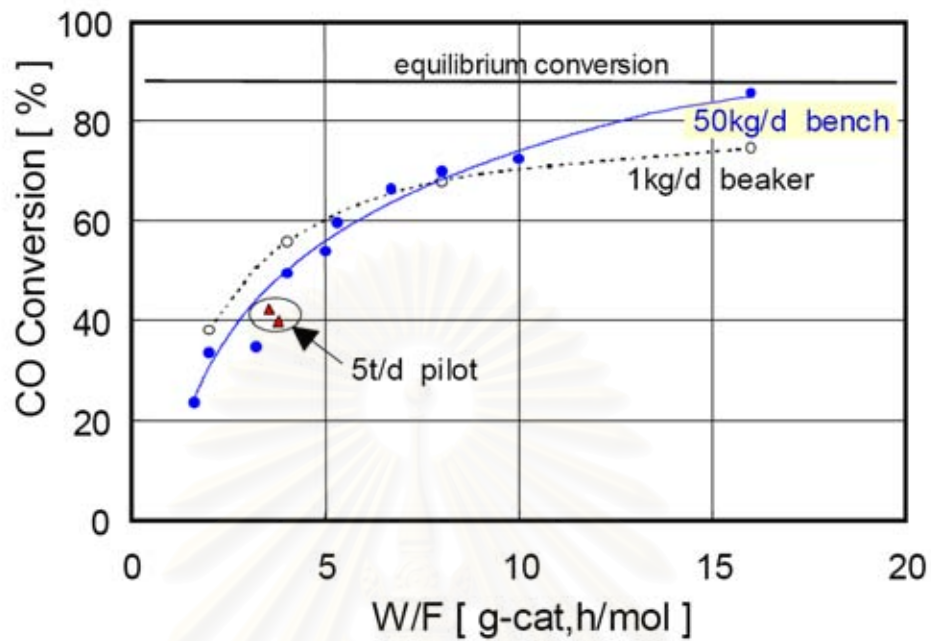
Figure 2.13 Effect of W/F on one-through CO conversion [45]
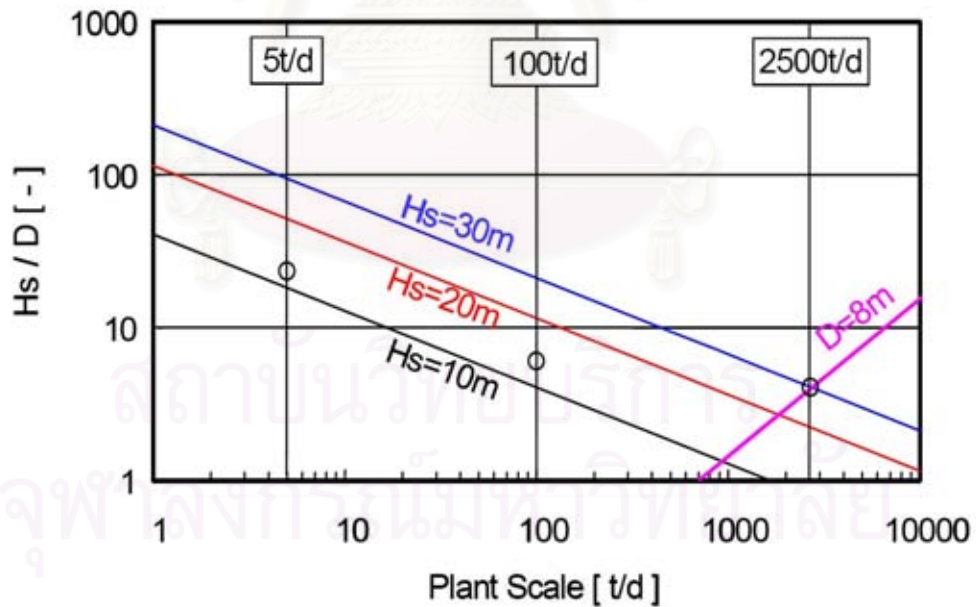
Figure 2.14 Scaling-up of Slurry Phase Reactor (W/F=Constant) [45]

In Figure 2.14, the values of Hs/D are indicated by round mark for 5 tons/day, 100 tons/day and 2,500 tons/day reactor designs. As the value of Hs/D for 100 tons/day

reactor is as low as that of 2,500 tons/day reactor, the flow could be similar between these two cases. Provided the process performance is confirmed in 100 tons/day reactor of which the scale is 20 times of 5 tons/day, the similar scale-up principle can be applied to 2,500 tons/day reactor since it is 25 times larger of 100 tons/day.

The design, manufacturing and construction of 100 tons/day demonstration plant have started in 2002 and will be completed in November 2003. The commissioning will start in December 2003. From 2004 to 2006, two to three month continuous operations will be made five times to confirm the viability of the technology and to obtain various engineering data aimed to establish the scale up technology of commercial scale plant. In order to examine the design and operational conditions of 100 tons/day plant and to support the analysis of operational data, small scale experiments will be done. On the basis of the operational data, conceptual design and feasibility study will be made for 2500 tons/day-scale commercial plant. As for raw materials, natural gas, coal, bio-mass and so on will be studied. Schematic process flow diagram of 100 tons/day demonstration plant is shown in Figure 2.15. The reactor is 2.3 m in inner diameter and 22 m in height. Reaction heat is used to generate steam. The standard reaction condition is temperature: 260 $^{\circ}$C and pressure: 5 MPa as the same as that of 5 tons/day plant. The effluent of the reactor is cooled and chilled to be separated from unreacted gas, which is recycled to the reactor. DME is purified in two distillation columns and stored in pressurized tank (1,000 tons). By-produced methanol is returned to the DME synthesis reactor after water removal to be converted into DME. The product DME will be supplied for various development projects of DME utilization technology.
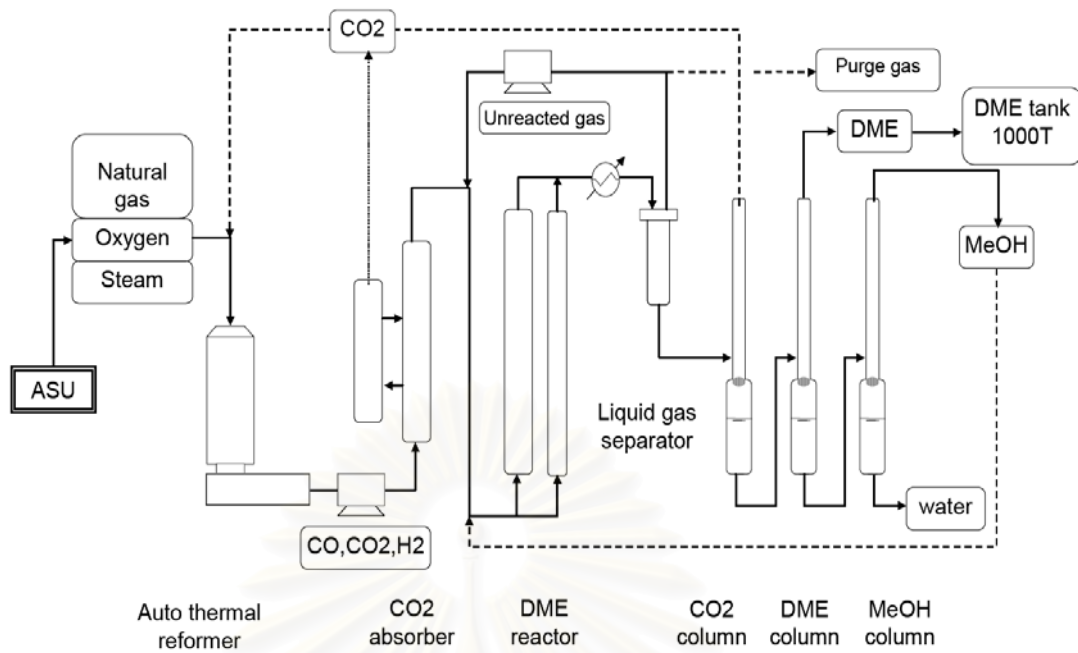
Figure 2.15. Process Flow Diagram of 100 tons/day DME Synthesis Plant [45]

Natural gas is reformed in an auto-thermal reformer at the condition; the outlet temperature is 1000-1200 $^{\circ}$C and the inner pressure is 2.3 MPa with oxygen, steam and carbon dioxide recycled from a carbon dioxide removal unit and a purification unit to give synthesis gas of H_2/CO=1. The synthesis gas is cooled, compressed and carbon dioxide is removed by a methanol absorption and supplied into DME synthesis reactor. There are two reactors in parallel; main reactor is 2.3 m in inner diameter and 22 m in height, small reactor is 0.65 m in inner diameter and 28m in height. The small reactor is equipped to get various engineering data with higher gas velocity conditions. Reaction heat is removed by internal heat exchanger coils to generate steam. The standard reaction condition is temperature: 260 $^{\circ}$C and pressure: 5 MPa. The effluent of the reactor is cooled and chilled to separate DME from unreacted gas, which is recycled to the reactor. DME is purified in two distillation columns and stored in pressurized tank (1,000 tons). By-product methanol is recycled to the DME synthesis reactor after water removal to be converted into DME.

2.5.2.4 Fluid dynamic phenomena in slurry phase reactor

The flow regime of slurry phase reactor varies as a function of reactor diameter and gas superficial velocity in the reactor as shown in Figure 2.16. The operating points of pilot plant (5tons/day, diameter: 0.55m), demonstration plant (100tons/day, diameter: 2.3 m and 0.65 m) and also planned commercial plant (3,000 tons/day, diameter: 7 m) are located in the same region of heterogeneous flow. The gas hold up (ε_g) was measured in increasing gas velocity (U_g) up to 40 cm/s. Within this range, the gas hold up increased smoothly without any sudden change as shown in Figure 2.17. As for the synthesis reaction with higher gas velocity, DME production yield by catalyst weight is almost constant up to 40 cm/s. The gas hold-up decreases by 0.05 with slurry concentration increasing 20% to 30%.There is no clear dependence of the gas hold up on the reactor diameter. According to Krishna [46], the ratio of gas bubble size (db) to reactor diameter (D) is smaller than 0.125, reactor diameter has no effect on the gas holdup. In our case, the ratio (db/D) is less than 0.05; for D=0.65-2.3 m, db=5-30 mm (estimated by a fluid dynamic simulation with increasing Ug)
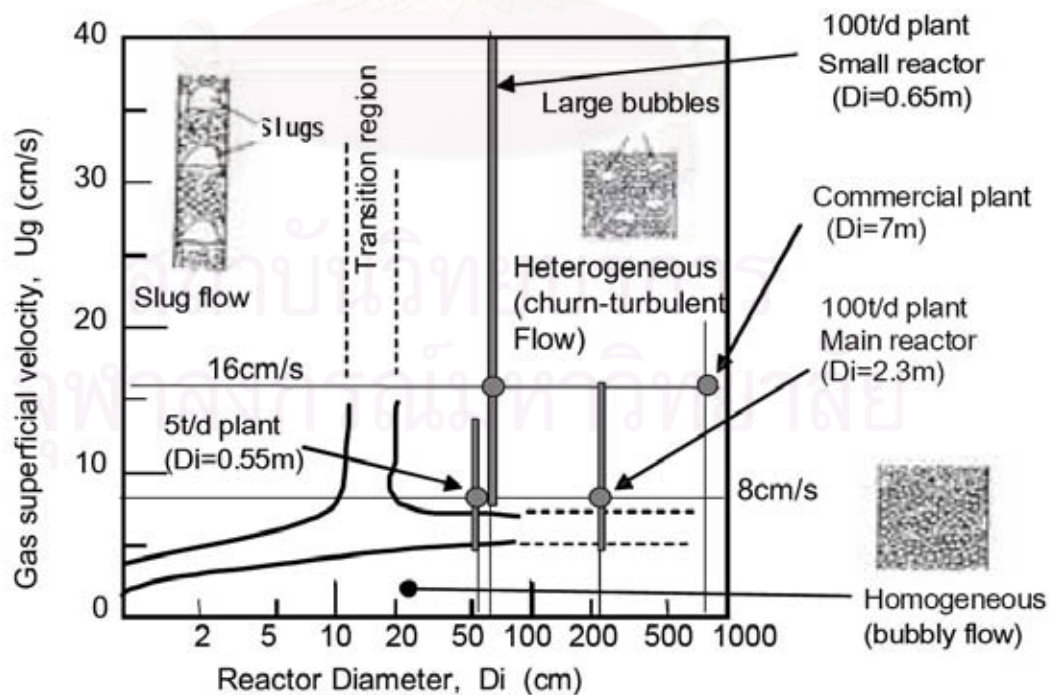
Figure 2.16 . Flow Regime Map [45]
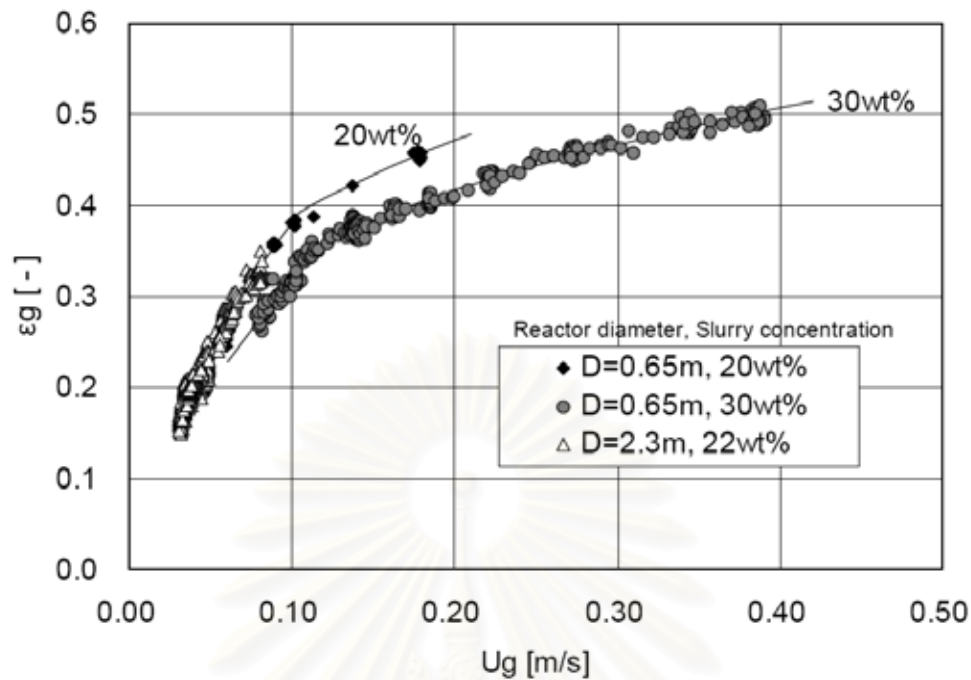
Figure 2.17 Effect of Superficial Gas Velocity on Gas Hold-up [45]

The mixing diffusion coefficient in liquid phase was estimated by one dimensional reactor model from measured temperature distribution data and also by a fluid dynamics model for liquid and gas bubbles movement. Figure 2.18 shows a comparison of the temperature distribution measured and simulated. In this one dimensional simulation, the reaction and heat transfer was simulated in changing a factor for the mixing diffusion coefficient calculated by Deckwer equation. With factor of 0.5-1.0, the simulated temperature distribution and conversion at the outlet is similar to the measured ones. The heat transfer coefficient from the slurry to heat exchanger tubes was also evaluated from heat balance data of the reactor as shown in Figure 2.19. In this figure, Deckwer equation for heat transfer coefficient agrees with the operational data with some allowance. Based on these data, the commercial scale production of 3,000 tons/day could be realized by a single reactor with 7 m in diameter and 44 m in height. Figure 2.19 shows an example of simulation for a commercial scale reactor, the

temperature distribution is homogeneous and the synthesis conversion is sufficiently high.
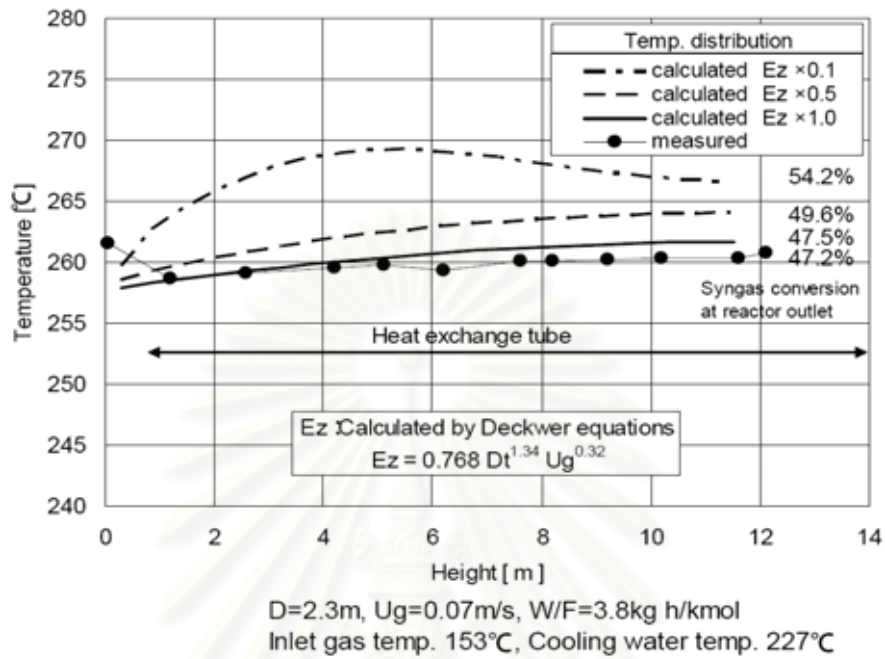
Figure 2.18. Comparison of Measured with Calculated by 1-D Reactor Simulator [45]
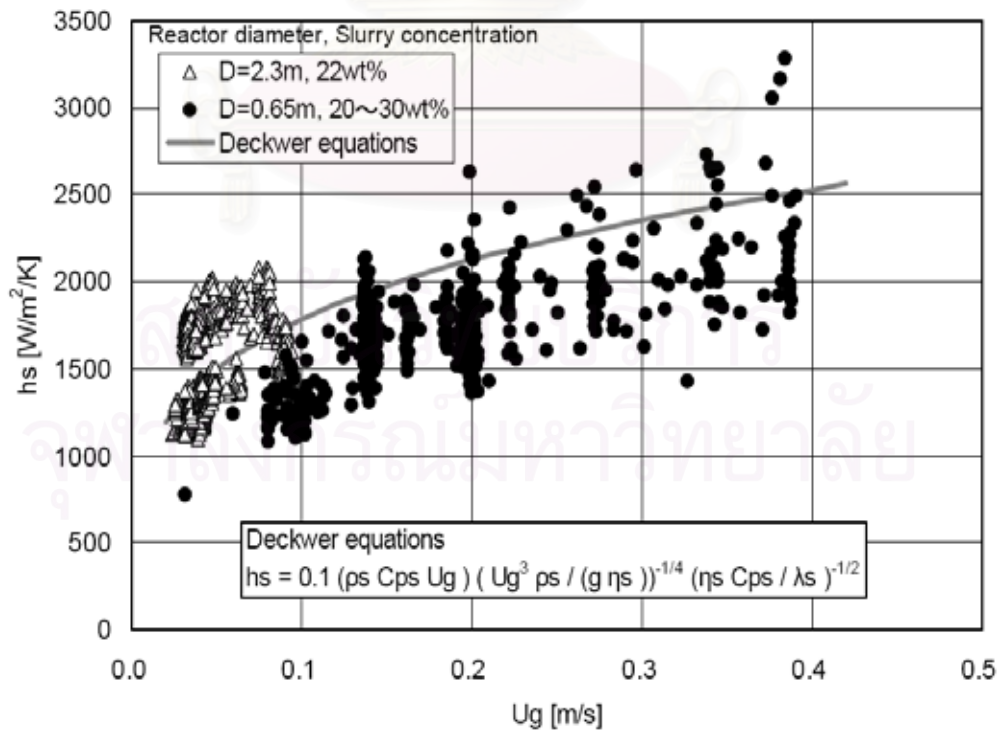
Figure 2.19 Effect of Superficial Gas Velocity on Slurry Heat Transfer Coefficient [45]
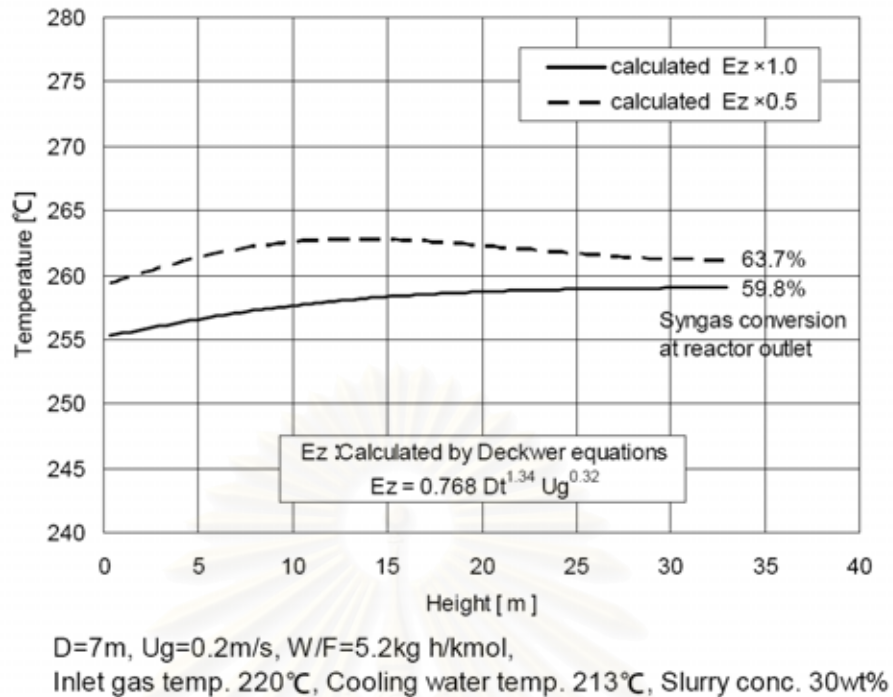
Figure 2.20 Example of 1-D Reactor Simulation for commercial scale plant [45]

2.5.3. Air Products Process

Air Products has developed a single-step process for the direct synthesis of DME from synthesis gas with or without coproduct methanol in the liquid phase. This process can handle syngas with higher than 50 vol% CO, as is the syngas composition from advanced coal gasification. This process gives higher syngas conversion per pass than can be achieved by methanol synthesis alone. Selectivity of DME and methanol is optimized by varying reaction conditions catalyst compositions, and /or ratios of suit specific process applications. Conversion of syngas to DME involves three separate reactions. All three reactions are equilibrium limited and exothermic in nature. Based on what they claim, the reaction chemistry is :

$$xCO + xH_2O = xCO_2 + xH_2 \qquad \text{water gas shift reaction}$$

$$yCO + 2yH_2 = yCH_3OH \qquad \text{Methanol synthesis}$$

$$2CH_3OH = CH_3OCH_3 + H_2O \qquad \text{Methanol dehydration}$$

$(x+y)CO + (2y-x)H_2 \rightleftharpoons CH_3OCH_3 + CO_2 + (y-2)CH_3OH + (1-x)H_2O$ Net reaction
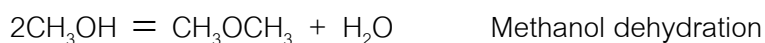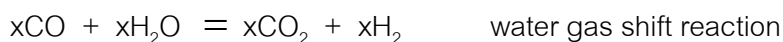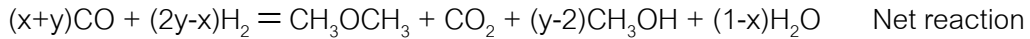
The single–stage synthesis of DME is carried out in a slurry-phase reactor, equipped with six-bladed draft tube impellers. The catalysts used are powdered commercial catalysts BASF S3-85 and BASF S3-86 for methanol synthesis, γ-alumina catalyst for methanol dehydration, and copper-based BASF K3-110 as a shift catalyst. These catalyst are slurried in either degassed Witco-70 or DRAKEOL-10 mineral oils with slurry concentrations in the range of 15-30 wt% catalyst. As shown in Fig. 2.21, three potential commercial modes of operation to produce DME have been investigated by Air Products. The first operating mode an oxygen-blown coal gasifier with recycle of the synthesis gas. The co-product of this process mode are methanol and DME, which have applications in the fuel and petrochemical industry. Per-pass CO conversion was 70 % at 1200 L/kg of catalyst per hour.
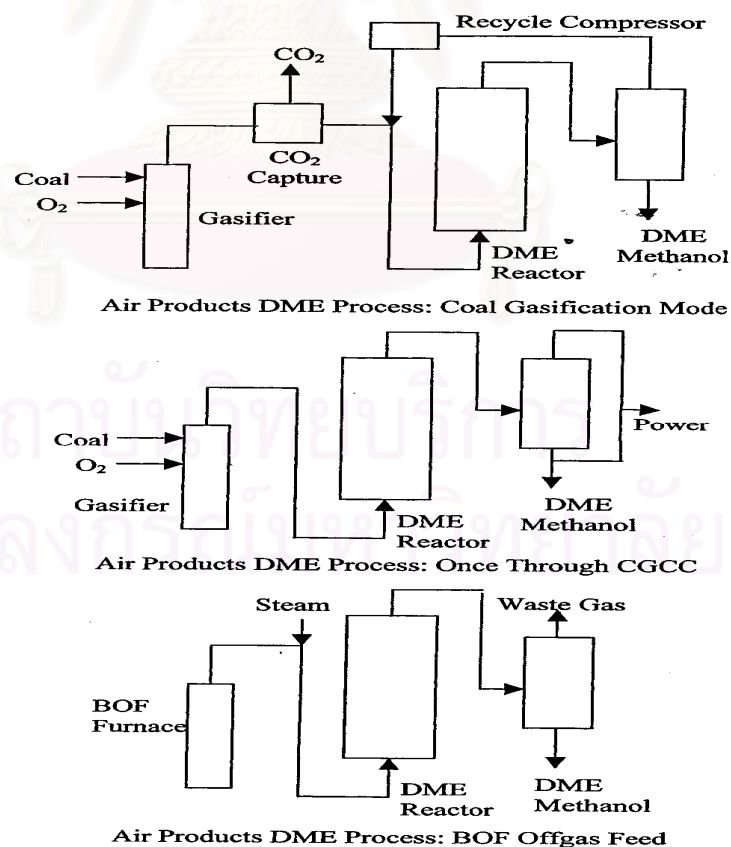
Figure 2.21 Air Products LPDME process (commercial modes of operation) [29]

The second operating mode uses the once-through approach of coal-derived syngas. Dimethyl ether and methanol are recovered, and unreacted gas is fired to a turbine. The third operating mode also uses the once-through process, but uses basic oxygen furnace (BOF) off-gas as the feed stream. The hydrogen to carbon monoxide ratio of BOF off-gas is essentially zero, thereby making it imperative for steam to be co-fed to the reactor. This processes enables the use of off-gases with unfavorable compositions, which are currently recovered only for their fuel value, and upgrading them into more valuable liquid products [29,32].

2.5.4. Toyo Engineering Corporation Process

Toyo Engineering Corporation has developed a jumbo DME plant from natural gas using existing proven technologies. Toyo Engineering Corporation has developed a number of large-scale methanol synthesis plant in the world. Chemical reactions involved in DME synthesis by TEC's process, as claimed, are shown below:

$CO + 2H_2 = CH_3OH$ Methanol synthesis

$CO_2 + 3H_2 = CH_3OH + H_2O$ Methanol synthesis

$2CH_3OH = CH_3OCH_3 + H_2O$ Methanol dehydration

$CO + CO_2 + 5H_2 = CH_3OCH_3 + 2H_2O$ Net reaction
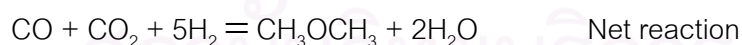
The configuration of a 7000 MTPD DME plant is based on the combination of methanol synthesis and methanol dehydration. Attractive feature of this process include lesser total investment cost and lesser oxygen consumption when compared with the methanol/DME co-production route or direct DME synthesis routé. Also, carbon dioxide is not produced in the DME synthesis step of this process, As shown in Fig. 2.22 , this process utilizes a steam reformer, TEC's TAF-X reactor, oxygen reformer, TEC's MRF-Z methanol reactor and TEC's DME reactor.
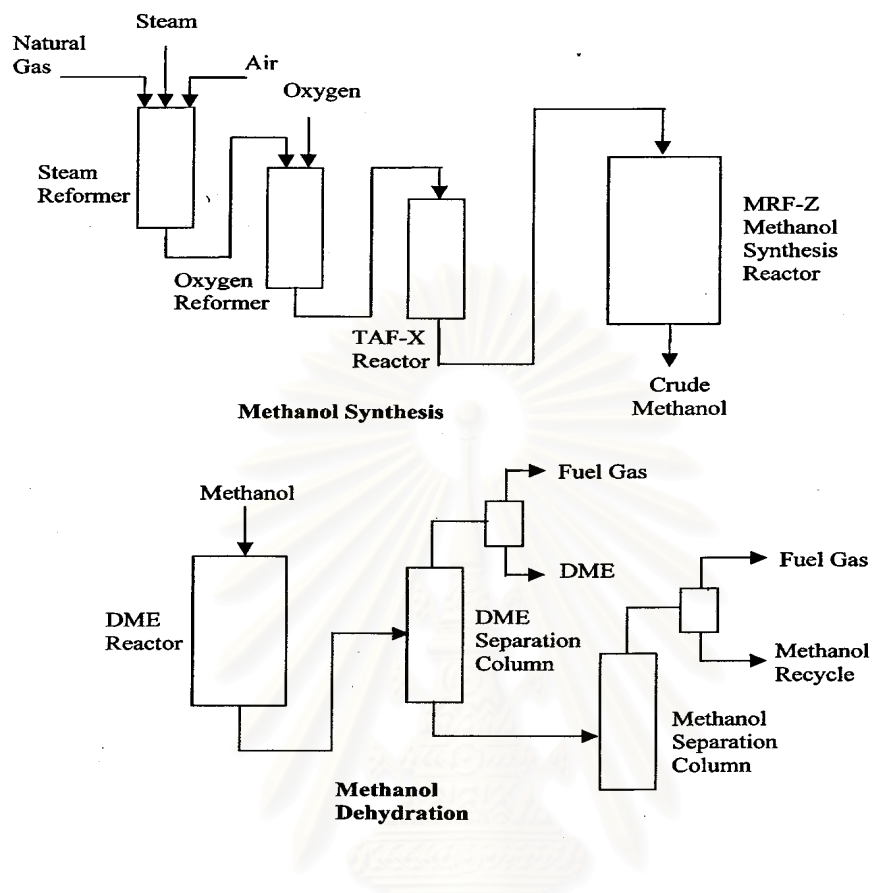
Figure 2.22 Toyo Engineering Corporation DME process [30]

2.5.5. Electric Power Research Institute (UA-EPRI) Process

Researchers at the University of Akron, in conjunction with the Electric Power Research Institute, have developed a novel liquid-phase process that produces DME in a single stage from CO-rich syngas [59,60]. A process schematic of the DME minipilot plant is shown in Fig. 2.23 The process chemistry for the novel one-step synthesis of DME in the liquid phase is as follows:

$$CO_2 + 3H_2 = CH_3OH + H_2O \qquad \text{Methanol synthesis}$$

$$CO + H_2O = CO_2 + H_2 \qquad \text{water gas shift reaction}$$
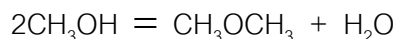
$$2CH_3OH \;=\; CH_3OCH_3 \;+\; H_2O \qquad\qquad \text{Dimethyl ether synthesis}$$
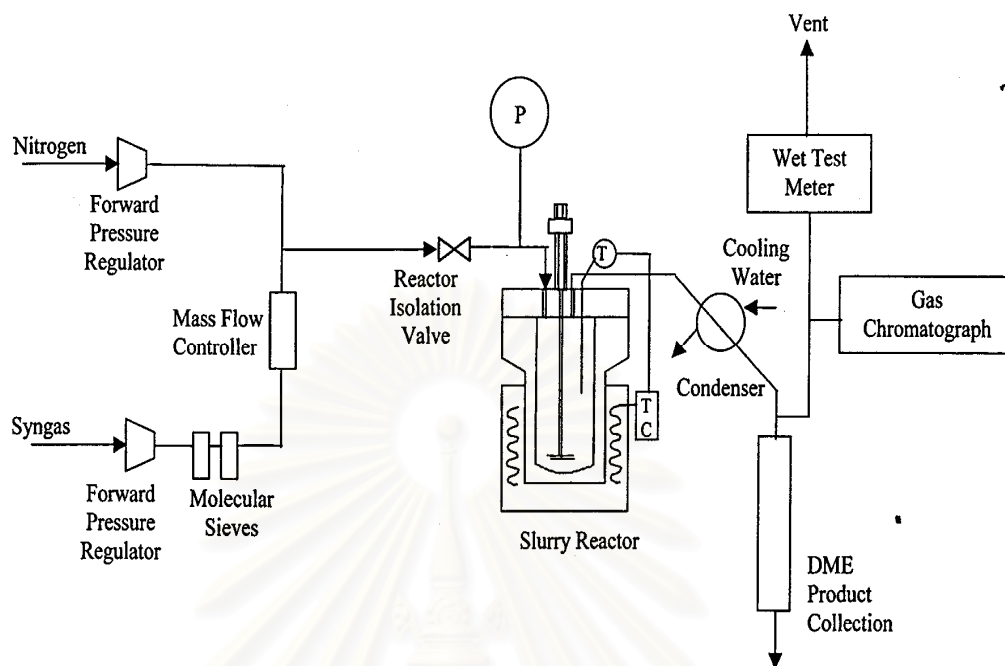
Figure 2.23 Process schematic of the UA-EPRI liquid-phase DME experimental process

   Unit [42]

The methanol synthesis reaction and water gas shift reaction take place over the co-precipitated $Cu/ZnO/Al_2O_3$ catalyst, and the methanol dehydration reaction takes place over a γ-alumina catalyst. The reactions are carried out at 250 $^{\circ}$C and 70 atm in a liquid phase involving inert oil, such as Witco-40, Witco-70 or Freezene-100 oil.

The single-stage reactor productivity was increased by as much as 60 % when the co-production of methanol and DME was used, as compared to methanol synthesis alone. Per-pass syngas conversion when using the co-production of methanol and DME approach was increased by as much as 50 % over that of methanol synthesis only. At high slurry ratios, when methanol concentration in the liquid phase is very high, the percent increase in single-stage reactor productivity could be as high as 80 % . The above fact is very significant from a commercial perspective as almost all the

commercial reactors in the liquid phase synthesis are operated in the gas-to-liquid mass transfer limited region. The process is capable of co-producing methanol and DME in any fixed proportion, at significant synthesis rates of both methanol and DME. The process feasibility has been well demonstrated on their minipilot plant system [42,47].

2.6. Kinetics of dimethyl ether synthesis from synthesis gas

Direct synthesis of DME from syngas involves two steps, methanol synthesis followed by in situ methanol dehydration, Eqs. (1) - (4), which in turn requires two functionally independent catalysts, i.e. a methanol forming component and a dehydration component. An inherent advantage of the co-production of methanol and DME is the alleviation of the equilibrium limitation of the methanol synthesis [19,49,50,51,52,53], which results in a significant increase in total methanol production.

$$CO + 2H_2 = CH_3OH \qquad (1)$$

$$CO_2 + 3H_2O = CH_3OH + H_2O \qquad (2)$$

$$CO + H_2O = CO_2 + H_2 \qquad (3)$$

$$2CH_3OH = CH_3OCH_3 + H_2O \qquad (4)$$
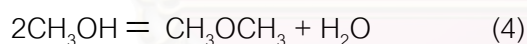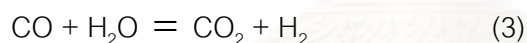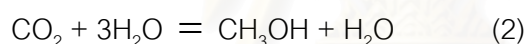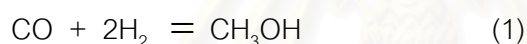
Reactions (1)-(3) are catalyzed by a methanol synthesis component (e.g. $CuO/ZnO/Al_2O_3$) and reaction (4) is catalyzed by an acidic component (e.g. c-alumina). Reactions (1)-(4) show a high degree of synergy provided the operating conditions are optimized such that the methanol produced is efficiently removed. Water formed in reaction (2) and (4) is removed via the water-gas shift reaction (3) to produce hydrogen which kinetically favours the production of methanol. A wide range of possible feed and other operating conditions can be used in the combined synthesis process. The source of syngas, the type of reactor configuration, feed policy and the loading of the two functionally independently catalysts are closely interrelated. For example, the use of a

CO rich hydrogen lean syngas derived from coal gasification is best suited to a CSTR configuration, such that in the liquid-phase di-methyl ether process (LPDME) which provides good mixing and efficient heat management in the slurry-bubble column reactor. Additionally, the LPDME synthesis process also ensures that the catalyst system is exposed to a higher CO_2 content for the same syngas compared to the conventional fixed-bed-type reactor. Synthesis gas from natural gas can be converted either in a CSTR or fixed-bed reactor, but in this case the CO_2 management needs are different. A fixed-bed type reactor would suit a graded catalyst bed in which the methanol-to-dehydration catalyst ratio varied along the length. Clearly, there is a range of plausible process variables which can be explored in the design of a combined synthesis process. However, the main focus of most published scientific literature has been on the catalyst development rather than the detailed kinetic work necessary to underpin the reaction engineering. The previously study investigates some key process variables which influence the reaction kinetics of the dual catalytic methanol + DME synthesis process. Reported here are the effects of CO_2 feed concentration, CO_x/H_2 ratio and the catalyst loading ratio. This data have been used to test a kinetic model of the combined synthesis based on proposed models for the component reactions [39,54,55,56].

Kinetics were measured in an internal recycle reactor (300 cm^3 volume, 100 cm^3 catalyst basket) at 5 MPa and 250 $^\circ$C using a impeller speed of 1500 rpm. For DME synthesis, the c-alumina catalyst (supplied by Norton Chemicals Co.) and commercial $CuO/ZnO/Al_2O_3$ catalyst were crushed and sieved to size 250 - 500 mm. The catalysts were stacked in two beds in the same catalyst basket, $CuO/ZnO/Al_2O_3$ on top of γ-alumina, with a layer of quartz wool physically separating them. The catalyst ratio of methanol forming and dehydration catalyst was typically 2 : 1 unless otherwise stated. The catalyst was activated in situ by reduction using a flow of 5 % H_2 in N_2 at 250 $^\circ$C approached at 1 $^\circ$C min^{-1} from room temperature for 12 h. Both internal and external particle diffusion resistance were confirmed absent. Two thermocouples were inserted

central and at the bottom of the catalyst bed; a third was in the gas phase. The temperature difference between the thermocouples inserted into the catalyst bed and the bulk gas phase was always ±0.75 $^{\circ}$C or less. This was in agreement with calculation which gave a temperature difference between the catalyst surface and the bulk gas phase of less than 1.0 $^{\circ}$C [57,58]. The intraparticle temperature difference was calculated to be less than 0.53 $^{\circ}$C.The required feed gas mixtures were obtained by blending a wide range of syngas compositions, CO_x:H_2 ratio=1 : 1 to 1 : 4, (Air Products, CP grade) using a suite of mass flow controllers. 10% of helium was added as an internal analytical standard. The feed gas mixture was passed through a carbonyl trap (to remove Fe and Ni carbonyls) before entering the reactor. To avoid condensation of liquid products, the downstream line from the reactor was trace heated. A small fraction of the reactor effluent was piped to a GC for on-line analysis. Since hydrogen was used as the carrier gas, to utilize the He standard, hydrogen in the reactor outlet was not measured. The carbon balances of all experiments closed to 5 % and in 90 % of the experiments the balances closed to within 2.2%. The calculation of total methanol yield was based on the following:

Total methanol yield, Y_{TM}

$$Y_{TM} = \left\{ \frac{n_{CH_3OH} + 2 \times n_{CH_3OCH_3}}{[n_{CO} + n_{CO_2}]_{in}} \right\} \times 100\% \tag{5}$$

The simulation of methanol and/or DME synthesis reactions was based on a CSTR model. Several kinetic models for methanol synthesis and methanol dehydration reactions were tested under both independent and combined synthesis conditions. From the initial screening, the model for methanol synthesis proposed by Vanden Bussche and Froment [54] based on a strictly sequential reaction mechanism of CO to CO_2 to CH_3OH via surface carbonate, and the dehydration model proposed by Bercic and Levec [39] based on reaction of dissociatively adsorbed methanol, were selected

for analysis and simulation of the combined process. Parameter estimation was based on the minimization of the objective function (6).

$$\min_{\theta} \Phi = \sum_{i=1}^{I} w_i^2 \sum_{k=1}^{k} \left(z_{ik,pred.} - z_{ik,expt.} \right)^2 \tag{6}$$

Steady-state operation were modelled using gPROMS[1] (together with gEST) which utilised Eq. (6) and the mass conservation equations to determine the value of parameter θ that minimizes the weighted, w_i, sum of the squares of residuals. The component balance equations used to construct the kinetic model were:

$$F^o y_i^o - F y_i = w \sum_j \left[v_{ij} r_j \right] \tag{7}$$

for all reactants, products and inert, with the exception of exit hydrogen for which no analysis was made. The methanation reaction was ignored. The kinetic rate equations, r_j, for methanol synthesis and dehydration were Eqs. (8) - (10).

$$r_{CO2,\,hydrogenation} = \left[\frac{k_1 (p_{H_2} p_{CO_2})[1 - (1/Keq)(p_{CH_3OH} p_{H_2O})/(p_{CO_2} p^3_{H_2})]}{(1 + K_2(P_{H_2O}/P_{H_2}) + \sqrt{K_3 P_{H_2}} + K_4 P_{H_2O})^3} \right] \tag{8}$$

$$r_{RWSG} = \left[\frac{k_5 p_{CO_2}[1 - (1/Keq)(p_{CO} p_{H_2O})/(p_{CO_2} p_{H_2})]}{(1 + K_2(P_{H_2O}/P_{H_2}) + \sqrt{K_3 P_{H_2}} + K_4 P_{H_2O})} \right] \tag{9}$$

$$r_{MeOH} = \left[\frac{C^2_{CH_3OH} - ((C_{H_2O} C_{DME})/Keq)}{(1 + 2\sqrt{K_{CH_3OH} C_{CH_3OH}} + K_{H_2O} C_{H_2O})^4} \right] \tag{10}$$

Methanol synthesis was performed over the commercial $CuO/ZnO/Al_2O_3$ catalyst. Steady state was achieved within 24 h from start up and kinetic experiments were typically carried out over a duration of 100 h during which catalysts deactivation was insignificant, except when using a CO_2 free CO/H_2 feed., steady state, activity profile of

methanol (only) synthesis obtained by gradually replacing CO_2 with CO in the $1CO_2$: $4H_2$ feed [41]. The maximum methanol production was obtained using synthesis gas with 2-5% CO_2, a common industrial feed condition. The methanol synthesis model, including the water-gas shift reaction, proposed by Vanden Bussche and Froment (1996)[38] fitted our kinetic data reasonably well. A sensitivity analysis of the kinetics to parameters k_1 to k_5, revealed that the adsorption constant of hydrogen, K_3, strongly affects the magnitude and position of the local maximum at the low CO_2 content feed while the adsorption constants, K_2 and K_4, mainly responded to feed conditions where high water concentration is found for example in the CO_2 rich feed gas region. Methanol production is of course proportional to the magnitude of reaction rate constant, k_1, over entire range of different carbon oxide feed. Rate constant, k_5, has only slight effect on the overall methanol production rate provided the shift reaction is sufficiently fast.The parameters $B(i)$ were set to the values (Table 2.8) reported by Vanden Bussche and Froment,[38], since the present study used a similar catalyst and was carried out at a single temperature. The data for a CO_2 free CO/H_2 feed gas were not included in the parameter estimation in the kinetic model due to the observed catalyst deactivation problem [43]. Only minor changes to the parameters of the original rate equations were required (Table 2.8). The solution was independent of the initial approximation of the parameters. Verification that the parameters in Table 2.8 were not bound dependent was achieved by varying the upper and lower bounds of the solution constraint for each of the parameters, k_1 to k_5, over a wide range. Data dependence tests were performed by randomly excluding data points and by allowing for the error in the carbon balances.

Table 2.8 Kinetic parameters for methanol synthesis [54]

| Parameters* | $A(i) \exp((B(i)/RT)$ | |
	$A(i)$	$B(i)$
k_1	1.65	36,696
K_2	3.61×10^3	0
K_3	0.37	17,197
K_4	7.14×10^{-11}	124,119
k_5	1.09×10^{10}	$-94,765$
$Keqm1$	Twigg (1986)	
$Keqm2$	Twigg (1986)	
K_{CH_3OH}	7.9×10^{-4}	70,500
k_6	3.7×10^{10}	$-105,000$
K_{H_2O}	0.84×10^{-1}	41,100
$Keqm3$	Stull et al. 1969	

*See Eq. (8)–(10); values for $B(i = 1...5)$ are taken from Vanden Bussche and Froment, 1996 and B ($i = 6$, CH_3OH and H_2O) from Bercic and Levec (1992).

2.7. Synthesis gas

Synthesis gas (Syngas) is a gaseous mixture containing mainly hydrogen, carbon monoxide and carbon dioxide in various amounts. In most cases, these three compounds constitute more than 90 % of the syngas, but other components including methane and inert gases such as nitrogen and argon are often present in the mixture. Syngas is only seldom a product by itself, and its major role is as a key intermediate in the synthesis of a range of chemicals. Syngas may in principle be produced from any carbon-containing feedstock, but today only coal and hydrocarbons are used as raw materials to any significant extent. New plants are normally designed based on natural gas of other hydrocarbon feedstock, because the investment is only about one-third of that of a plant based on coal. Today, synthesis gas is mainly used for the production of ammonia (120 x 10^6 ton/year) and methanol (30 x 10^6 ton/year) followed by pure hydrogen for hydrotreating in refineries. Other current application are in the production of higher alcohols by hydroformulation and a number of products including acetics acid,

formaldehyde, dimethyl ether (DME), and methyl-tert-buthyl ether (MTBE); in all cases methanol is used as a co-reactant.

2.8. Literature reviews

G.R. Moradi. et al. [60] studied the synthesis gas to dimethylether (STD) conversion was examined on various hybrid catalysts prepared by seven different methods. These catalysts had the same general form as $CuO/ZnO/Al_2O_3$ with theoretical weight ratio 31/16/53, respectively. A novel preparation method for hybrid catalyst namely sol–gel impregnation has also been developed which showed better performance in comparison with the other methods. Also, in order to find out the effect of various alumina contents at a fixed CuO/ZnO ratio on the performance of the hybrid catalyst, a series of catalysts with different contents of alumina have been prepared by sol–gel impregnation method. The optimum weight ratio for $CuO/ZnO/Al_2O_3$ catalyst has been found to be about 2:1:5, respectively. These catalysts characterized by TPR, XRD, XRF, BET, TGA, N_2O absorption. The catalysts performance were tested at 240 ^{O}C, 40 bar and space velocity 1000 ml/gcat.h, with the inlet gas composition $H_2/CO/N_2$ = 64/32/4 in a micro slurry reactor.

L. Wang. et al. [61] studied a series of CuO-ZnO catalysts (with different Cu/Zn molar ratios) and evaluated under the reaction conditions of syngas-to-dimethyl ether (DME) with three sorts of feed gas and different space velocity. The catalysts were characterized by X-ray diffraction (XRD) and temperature programmed reduction (TPR). The experiment results showed that the reaction conditions of Syngas-to-DME process greatly affected the methanol synthesis and WGS reaction. The influence caused by Cu/Zn molar ratio was quite different on the two reactions; increasing of percentage of CO_2 in feed gas was unfavorable for catalyst activity, and also inhibited both reactions; enhancement of reaction space velocity heavily influenced the performance of the

catalyst, and the benefits were relatively less for methanol synthesis than for the WGS reaction.

J. Fei. et al. [62] studied the activity of Cu–Mn–Zn/zeolite-Y catalysts for dimethyl ether (DME) synthesis from syngas can be affected by the content of copper in the catalyst. The appropriate ratio of $Cu/(Cu + Mn + Zn)$ for catalyst activity was above 0.6, and the conversion of CO and the selectivity of DME reached 78 % and 67 %, respectively, under the reaction conditions of 2.0 MPa, 250 $^{\circ}$C, 1500 h^{-1}. The results of catalyst characterization by powder X-ray diffraction (XRD), temperature-programmed reduction (TPR) and temperature- programmed desorption (TPD) showed that the excess CuO in conjunction with mixed oxide was easier reduction, much more beneficial to the activation of CO at lower temperature and higher catalytic activity for DME synthesis.

J. Erena. et al. [63] studied effect of operating conditions (time on stream, temperature, pressure and space time) on the conversion of CO and CO_2, selectivity to dimethyl ether (DME), yield of DME and product distribution is studied in the DME synthesis from H_2, CO and CO_2 in a single reaction step on a CuO-ZnO-Al_2O_3/NaHZSM-5 bifunctional catalyst. CO conversion is total at 275 $^{\circ}$C and 40 bar, with a selectivity to DME of 80% and a yield of DME of 78%, for a space time of 67 (g of catalyst) h/mol of (H_2 + CO) and for a feed made up of H_2/CO = 2/1. Catalyst deactivation under these conditions is insignificant, even when CO_2 is fed and there is a high water concentration in the medium.

D. Mao. et al. [64] studied a series of γ-Al_2O_3 samples modified with various contents of sulfate (0–15 wt.%) and calcined at different temperatures (350–750 $^{\circ}$C) were prepared by an impregnation method and physically admixed with CuO–ZnO–Al_2O_3 methanol synthesis catalyst to form hybrid catalysts. The direct synthesis of dimethyl ether (DME) from syngas was carried out over the prepared hybrid catalysts

under pressurized fixed-bed continuous flow conditions. The results revealed that the catalytic activity of $SO_4^{2-}/\gamma\text{-}Al_2O_3$ for methanol dehydration increased significantly when the content of sulfate increased to 10 wt.%, resulting in the increase in both DME selectivity and CO conversion. However, when the content of sulfate of $SO_4^{2-}/\gamma\text{-}Al_2O_3$ was further increased to 15 wt.%, the activity for methanol dehydration was increased, and the selectivity for DME decreased slightly as reflected in the increased formation of byproducts like hydrocarbons and CO_2. On the other hand, when the calcination temperature of $SO_4^{2-}/\gamma\text{-}Al_2O_3$ increased from 350 °C to 550°C, both the CO conversion and the DME selectivity increased gradually, accompanied with the decreased formation of CO_2. Nevertheless, a further increase in calcination temperature to 750 °C remarkably decreased the catalytic activity of $SO_4^{2-}/\gamma\text{-}Al_2O_3$ for methanol dehydration, resulting in the significant decline in both DME selectivity and CO conversion. The hybrid catalyst containing the $SO_4^{2-}/\gamma\text{-}Al_2O_3$ with 10 wt.% sulfate and calcined at 550 °C exhibited the highest selectivity and yield for the synthesis of DME.

F. Yaripour. et al. [65] studied a series of solid–acid catalysts with different content of components to prepared by co-precipitation (sol–gel) method. These samples comprised silica–titania and modified $\gamma\text{-}Al_2O_3$ with phosphorus. To determination of optimum ones, the effects of various contents of phosphorus have been investigated. Dehydration of methanol to dimethyl ether (DME) on solid–acid catalysts was studied in a fixed-bed reactor at a temperature of 300 °C under atmospheric pressure and a GHSV of 15,600 h⁻¹. The catalysts have been characterized using BET, XRD, FT-IR, NH_3–TPD and elemental analysis techniques and also the results were reported. According to the experimental results, silica–titania catalysts have exhibited low activity for DME synthesis. Phosphorus-modified catalysts have shown better performance compared to the untreated $\gamma\text{-}Al_2O_3$. It was found that surface areas increase with increasing in the molar ratio of aluminium-to-phosphorus at aluminium

phosphate catalysts. Also, by modifying alumina with phosphorus, it was observed that the surface acidity of aluminium phosphate catalysts decrease with increasing in the molar ratio of Al/P at aluminium phosphate catalysts. The sample of non-stoichiometric aluminium phosphate (molar ratio of Al/P = 2) have exhibited the best conversion without any by-product.

Q. Zhang et al.[66] studied the effect of palladium on the performance of Cr/ZnO catalyst to investigated for the synthesis of methanol from synthesis gas. Hydrogen adsorption on the Pd-Cr/ZnO well fits the equation combination of Langmuir isotherm equation and Freundilich isotherm equation while CO adsorption well fits Freundilich model. Addition of palladium in Cr/ZnO promoted the activity and selectivity of methanol synthesis.

G. Yang et al. [67] studied three kinds of H-ZSM-5 zeolite capsule catalysts were prepared by a direct hydrothermal synthesis method, where directly synthesized H-ZSM-5 membrane was coated perfectly onto Co/SiO_2 catalyst pellets of different sizes. SEM, EDS and XRD were used to characterize the catalyst morphology and to identify the H-ZSM-5 structure of zeolite capsules. Surface acidity and pore property of these catalysts were tested by NH_3-TPD and gas adsorption. The results showed that smaller Co/SiO_2 pellets with large external surfaces were favorable for zeolite capsule growth under the same synthesis conditions. The Fischer–Tropsch synthesis (FTS) reactions using the conventional FTS catalyst Co/SiO_2 or the physically mixed catalyst of Co/SiO_2 with H-ZSM-5, or the zeolite capsule catalysts were each conducted. The isoparaffins were selectively obtained on the capsule catalysts and the mixed catalyst. The capsule catalysts exhibited higher selectivity of isoparaffins than the mixed catalyst due to the space confined effect and the shape-selective effect. Especially, capsule catalysts with smaller sizes showed higher CO conversion and higher isoparaffin selectivity. Changing

the substrate pellet size could control the capsule catalysts' structure and their activity as well as their selectivity.

G. Yang et al. [68] studied three kinds of H-ZSM-5 zeolite capsule catalysts were prepared on Ru/SiO$_2$ catalyst pellets with different size. Characterization indicated that defect-free H-ZSM-5 capsule had been constructed on the Ru/SiO$_2$ surface successfully. And small Ru/SiO$_2$ pellet with large external surface was favorable for zeolite capsule growth under the same zeolite synthesis conditions. In the iso-paraffin direct synthesis via Fischer–Tropsch synthesis (FTS) reaction, zeolite capsule catalysts, especially the one with smaller pellet size, realized the higher iso-paraffin selectivity comparing with conventional FTS Ru/SiO$_2$ catalyst, and physically mixed catalyst of Ru/SiO$_2$ with H-ZSM-5 zeolite.

X. Li et al. [69] focuses on the synthesis of iso-paraffin-rich hydrocarbons by Fischer–Tropsch synthesis (FTS) over silica gel supported Co catalyst (Co/SiO$_2$). The basic concept is to isomerize and/or hydrocrack the primary FTS hydrocarbon products. A physical mixture consisting of a small amount of zeolite or Pd/zeolite mixed with Co/SiO$_2$ enhanced the formation of C$_4$–C$_{10}$ iso-paraffins while suppressing the formation of higher molecular hydrocarbons, probably because of the selective cracking of these hydrocarbons on them. In separate experiments, a two-reactor system was used. The first reactor contained a physical mixture of Co/SiO$_2$ and zeolite, and the second reactor contained zeolites or Pd-supported zeolites. The two-reactor system gave sharp C-number distribution within C$_3$–C$_6$ and iso-paraffins-rich products. The hydrocracking of *n*-octane and *n*-decane (model compound simulating products of the FTS reaction) over mixed catalysts composed of various compositions of Pd/SiO$_2$ and H-ZSM-5 in the presence of gaseous hydrogen showed high and stable activity, and produced primarily iso-paraffin-rich hydrocarbons. The isomerization was favored for mixtures rich in Pd/SiO$_2$. The role of Pd was thought to be the inlet of hydrogen spillover to the zeolite surface.

N. Tsubaki et al. [70] studied direct isoparaffin synthesis method from syngas was developed by using a hybrid catalyst composed of Fischer–Tropsch synthesis catalyst, H-ZSM-5 zeolite, and Pd/SiO$_2$, where normal paraffin from Fischer–Tropsch synthesis was hydrocracked in situ on H-ZSM-5 and Pd/SiO$_2$ stabilized zeolite activity effectively even at pressurized steam atmosphere mainly via spillover effect.

CHAPTER III

EXPERIMENTAL PROCEDURES

3.1. Material and reagents

The starting materials were chromium nitrate nanohydrate {$Cr(NO_3)_3.9H_2O$, A.R. Grade, Wako Chemical}, zinc nitrate hexahydrate {$Zn(NO_3)_2.6H_2O$, A.R. Grade, Wako Chemical}, alumimium nitrate nanohydrate {$Al(NO_3)_3.9H_2O$, 99.9 % A.R. Grade, Wako Chemical}, tetrapropylammoniumhydroxide {TPAOH; $C_{12}H_{29}NO$, 10% A.R. Grade, Kanto Chemical}, tetraethyl orthosilicate {TEOS; $Si(OC_2H_5)_4$, 95 % A.R. Grade, Kanto Chemical}, Dehydrated ethanol {C_2H_5OH, 99.5 wt% A.R. Grade, Kanto Chemical} and Nitric acid {HNO_3, 69 wt% A.R. Grade, Kanto Chemical}.

3.2. Catalyst preparation

Chromium and zinc oxide (Cr/ZnO = 1:2) used as the catalyst for the methanol synthesis was prepared by the co-precipitating method as shown in Fig. 3.1 [71]. Aqueous solutions of $Cr(NO_3)_3.9H_2O$ and $Zn(NO_3)_2.6H_2O$ with a Cr to Zn atomic ratio of 1 to 2 were mixed. About 300 mL of the aqueous solution of Na_2CO_3 was slowly added to the mixed solution until the pH value of mixture reached 9.0 and continuously stirred at temperature of 338 K within 60 min. The mixture solution was aged for 30 min under the same conditions. The resulting solid was filtrated and washed with hot de-ionized water (343 K) for elimination residual effect of Na^+ on catalytic activity, dried at 393 K for 12 h. and was calcined at 773 K for 1 h in sequence. The calcined catalyst was pelletized and crashed into particles with a size of 0.85–1.70 mm before loading into the reactor. This catalyst will be noted as CrZnO.

The conventional Co/Al_2O_3 FTS catalyst was prepared by incipient wetness impregnation of γ-Al_2O_3 (JRC-ALO-6, JGC Universal Ltd.; specific surface area: 180.0 m^2/g, pore volume 0.93 cm^3 /g, pellet size 0.35–0.83 mm) with an aqueous solution of $Co(NO_3)_2.6H_2O$. The catalyst precursors were dried in air at 393 K for 12 h after the impregnation and then calcined in air at 673 K for 2 h. The cobalt loading in the samples was 10 wt% [66].

Figure 3.1 Catalyst preparation apparatus [71]

3.3. Capsule catalyst preparation

3.3.1. Cr/ZnO capsule catalyst (For dimethyl ether synthesis)

Capsule catalysts were prepared by a direct hydrothermal synthesis method (Fig.3.2), where directly synthesized H-ZSM-5 membrane was coated perfectly onto Cr/ZnO catalyst [72]. Zeolite capsules have been successfully synthesized on the Cr/ZnO pellets. Using TPAOH (tetrapropylammonium hydroxide) as structure-directing reagent, we were prepared the synthesis sol according to the molar composition of $0.48TPAOH:2TEOS:8EtOH:120H_2O:0.24HNO_3$. Firstly, The mixture of TPAOH with deionized water was dissolved in a Teflon container at room temperature, and then the sol was stirred in the container for several minutes. Secondly, TEOS (tetraethylorthosilicate) was slowly added into the above sol. After stirring at room temperature for 6 h, a homogeneous, clear precursor sol was obtained. Before hydrothermal synthesis, specific size of Cr/ZnO pellets and the precursor sol were sealed in a stainless steel autoclave with a teflon inner tank, and then the autoclave was put inside the hydrothermal synthesis instrument (DRM-420DA, Hiro Company, Japan).

Crystallization temperature and synthesis time were 453 K and 24 hours, respectively while the rotation speed was 2 rpm. After the synthesis, the catalyst separated from the mother liquor were washed by deionized water and dried at 393 K for 12 hr. The catalyst will be named in CrZnO-S where S mean Silicate-I (For first time). Later to continued for the second time, we put the catalyst(CrZnO-S) in the solution base on molar ratio of $0.48TPAOH:2TEOS:8EtOH:120H_2O:0.24HNO_3:0.25Al_2O_3$. The aluminuim resource, $Al(NO_3)_39.H_2O$ (Aluminium nitrate nonahydrate) was used. Hydrothermal synthesis time was 24 hours. After the synthesis, the capsule catalysts separated from the mother liquor were washed repeatedly by deionized water and dried at 393 K for 12 h. Calcination at 773 K for 5 h was conducted in order to remove any organic structure-directing agent that had settled in the zeolite pores. In the following discussion, the capsule catalysts will be noted as CrZnO-S-Z.

3.3.2. Co/Al_2O_3 capsule catalyst (For isoparaffins synthesis)

The conventional FTS catalyst 10 wt% Co/Al_2O_3 was prepared by the incipient wetness impregnation of γ-Al_2O_3 (JRC-ALO-6, 0.35-0.85 mm) with $Co(NO_3)_2 \cdot 6H_2O$ solution. The zeolite membrane synthesis recipe for H-Beta zeolite capsule catalyst preparation was $48.24SiO_2:17.40TEAOH:1.0Al_2O_3: 519.3H_2O$. Hydrothermal synthesis was performed on the Co/Al_2O_3 at 428 K with rotation rate of 2 rpm for 24 h. The final zeolite capsule catalyst after the calcination at 823K for 8 h was named Co/Al_2O_3-B. The zeolite capsule catalyst without calcination was used to prepare the tricomponent zeolite capsule catalyst by incipient wetness impregnation method with dinitrodiammine palladium aqueous solution. The tricomponent zeolite capsule catalyst with 2.5 wt% Pd loading, named Co/Al_2O_3-Pd/B, was obtained after calcinations at 823 K for 8 hr [74].
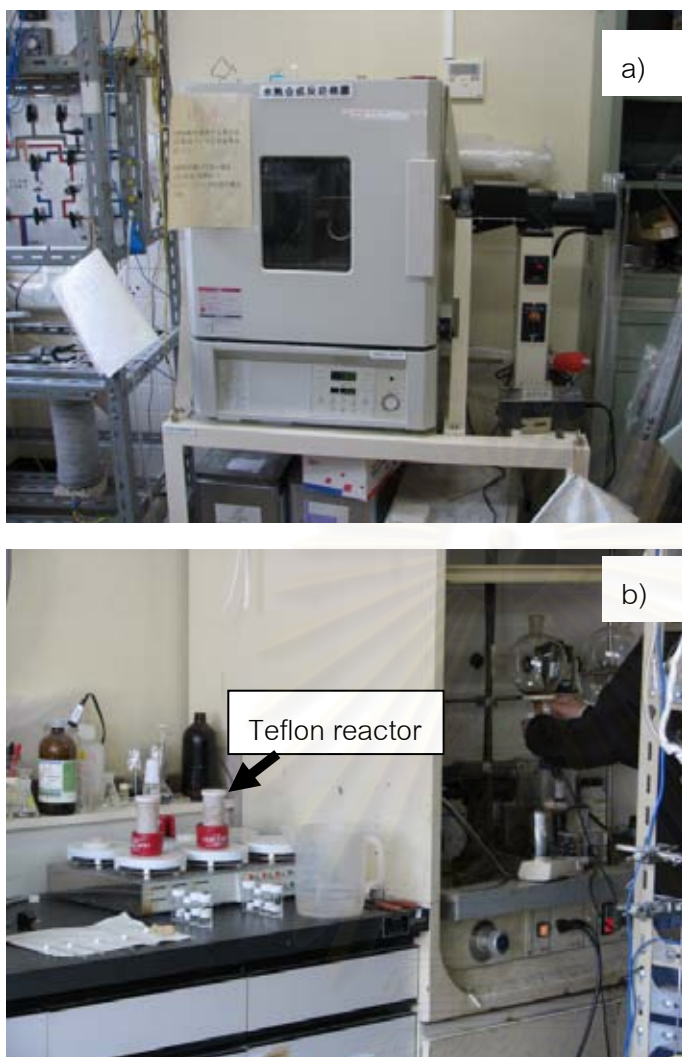
Figure 3.2 Capsules catalyst preparation equipment; a) Hydrothermal synthesis reactor,

b) Teflon reactor for hydrothermal synthesis method [73].

3.4. Physical mixing catalysts

3.4.1. Physical mixing catalysts of Cr/ZnO with H-ZSM-5

A commercial H-ZSM-5 (SiO_2/Al_2O_3 = 100) powder was directly synthesized by the same method as that used for preparing the zeolite membrane capsule catalysts mentioned above, but with no Cr/ZnO pellets inside, and the crystallization time was also 1 day. After a series of similar treatments: separation, washing, drying and calcination, H-ZSM-5 zeolite powder was physically well mixed with the Cr/ZnO (pellet size of 0.85–1.7 mm) and then pressed at 60.0 MPa. After the molding, the weight composition ratio of the new pellets was Cr/ZnO:H-ZSM-5 = 10:1 and the size of new pellets was also

0.85–1.70 mm. This catalyst will be named CrZnO-Z-M where the M means the mechanical mixture of H-ZSM-5 and Cr/ZnO.

3.4.2. Physical mixing catalysts of Co/Al$_2$O$_3$ with H-beta zeolite

A commercial of H-beta zeolite powder and Co/Al$_2$O$_3$ was physically well mixed with the Co/Al$_2$O$_3$ (pellet size of 0.85–1.7 mm) and then pressed at 60.0 MPa. After the molding, the weight composition ratio of the new pellets was Co/Al$_2$O$_3$: H-beta = 5:1 and the size of new pellets was also 0.85–1.70 mm. This catalyst will be named Co/Al$_2$O$_3$-β mix.

3.5. Capsule catalyst characterization

Measurements of the surface area and pore volume of catalysts were performed in an automatic gas adsorption system (Quantachrome, Autosorb-1, Yuasa Co.) by N$_2$ adsorption. Before analysis, the samples were degassed at 573 K and 3.0 Pa for 3 h. (Fig. 3.3a)

The thickness of zeolite capsule as well as compositional analysis and surface morphology observation were obtained by the scanning electron microscopy (JEOL, JSM-6360LV) combined with the energy-diffusive X-ray spectroscopy (EDS) (JEOL, JED-2300). The samples used for this analysis were firstly pretreated by an auto fine coater (JEOL, JFC-1600) to coat a platinum layer. (Fig. 3.3b)

An X-ray diffractometer (RINT 2400, Rigaku. Co.) equipped with Cu Ka radiation (λ = 0.15406 nm) was used to determine chemical structure and to collect the data of crystallite size of chromium oxide. Operations were performed at 40 kV and 40 mA. The average size of chromium oxide in the passivated catalysts was calculated by the Scherrer equation. (Fig. 3.3c)
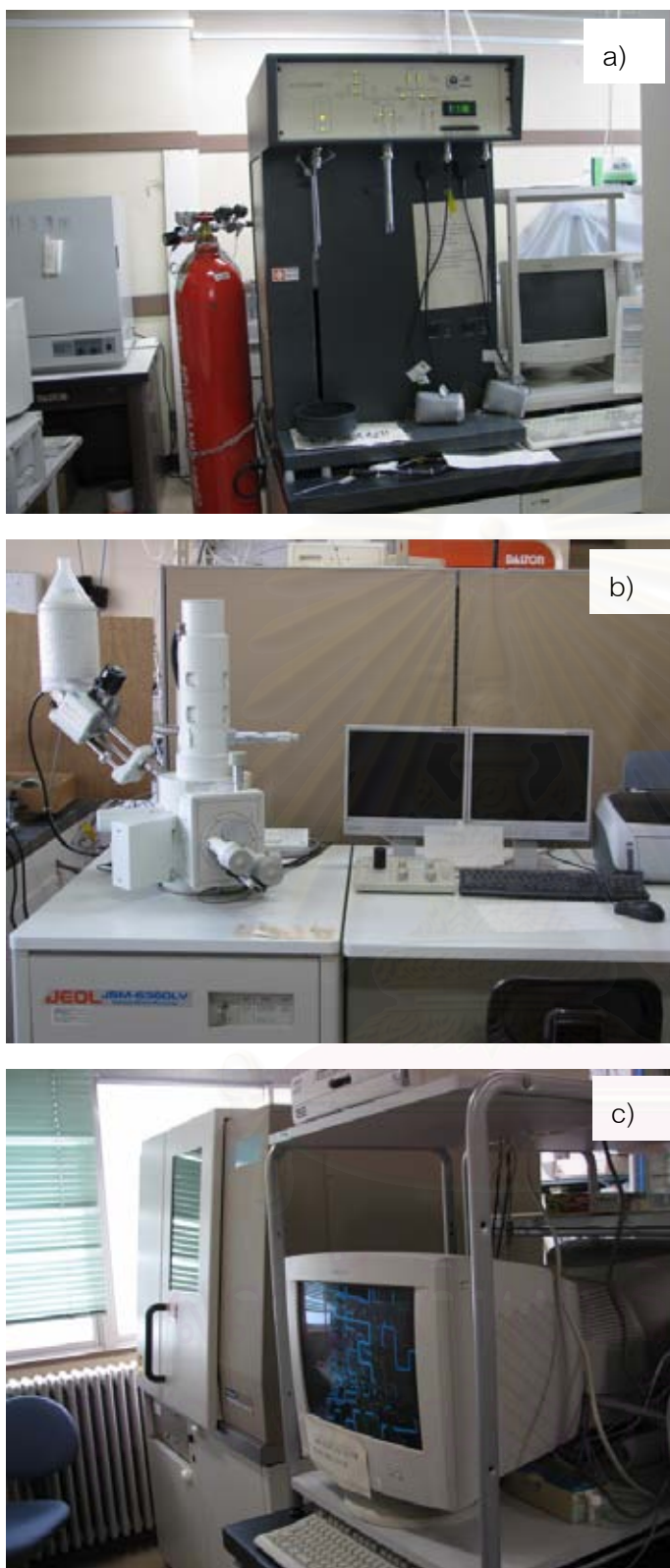
Figure 3.3 Capsule catalyst characterization unit; a) BET surface area (Quantachrome, Autosorb-1, Yuasa Co), b) Scanning electron microscopy (SEM: JEOL, JSM-6360LV) combined with the energy-diffusive X-ray spectroscopy (EDS: JEOL, JED-2300), c) X-ray diffractometer (XRD: RINT 2400, Rigaku. Co.)

3.6. Dimethyl ether synthesis

3.6.1. Dimethyl ether synthesis in a down flow fixed-bed reactor

Dimethyl ether synthesis for testing the catalytic activity of catalysts was performed in a down flow fixed-bed stainless steel reactor as shown in Fig. 3.4. The temperature and the pressure of the reaction were controlled at 573, 598, and 623 K and 5 MPa, W/F = 13.6 g.h/mol, respectively. At the middle of the reactor, the mixtures of catalysts (zeolite capsule catalysts containing 0.5 g Cr/ZnO with 3.0 g quartz sand were held in the fixed-bed reactor. Using a ramp rate of 2 K/min. Firstly, the catalysts were heated in 80 ml/min H_2 flow to 673 K and reduced in situ at this temperature for 3 h prior to reaction [66]. In the reaction system, the effluent products firstly passed through an ice trap where the heavy hydrocarbons were collected by a solvent with an internal standard, installed at the end of the reactor. The zeolite capsule catalysts and physical mixture catalyst were tested for dimethyl ether synthesis. Other light components that could not be captured by ice trap were on-line heated at 398 K and finally analyzed with an online gas chromatograph (Shimadzu, FID, GC-8A) equipped with a column Porapack Q (column temperature 130 $^{\circ}$C). Since the separation of olefins, isoparaffins and DME by the FID was not so satisfying. Furthermore, another online gas chromatograph (Shimadzu,TCD, GC-8A) equipped with an active charcoal column was used to determine the concentrations of CO, CO_2 and CH_4 in the products, where 3% argon in the feed gas acted as the internal standard. At the exit of ice trap, some gas products were collected from 5 to 6 hours, and then were analyzed by Gas chromatography (Shimadzu,TCD, GC-14B) equipped with a capillary column (J&W Scientific GS-Alumina, i.d. 0.53 mm x 30 m) was used to identified the content of propane, because the separation of propane with methanol by PQ column was not so satisfied. The selectivity of hydrocarbons in the reaction products was calculated on the carbon base [72].

Figure 3.4 Schematic view of the dimethyl ether synthesis unit.(1: Mass flow controller, 2: Oven, 3: a down flow fix-bed reactor, 4: Back pressure, 5: GC FID, 6: Ice trap, 7: GC TCD, 8: Gas collector) [72]

3.6.2. Dimethyl ether synthesis in a slurry phase reactor

DME synthesis reaction has been studied in a mechanically agitated slurry reactor. The hybrid catalyst (1 g) slurried in 20 ml n-paraffin oil. A feed gas having the composition of H_2/CO/Ar = 48/48/4 molar ratio was used for all experiments. The temperatures in the bed and on the internal wall of the reactor are controlled by means of a temperature controller. The flow rates of feed gas are controlled by Brooks 5850E mass flow-meters. The feed flow rate was set at 20 ml/gcat.h. The impeller speed was 1200 rpm; independent experiments verified that mass transfer effects were negligible at this impeller speed. The temperature and pressure conditions were set at 300 $^{\circ}$C and 40 bar which are in the range of low pressure process for methanol synthesis (200–300 $^{\circ}$C, 35–55 bar). Before the feed was introduced, the catalysts had been reduced with pure hydrogen at the normal pressure according the following heating program: heated from room temperature to 400 $^{\circ}$C with heating rate 1 $^{\circ}$C/min and was kept for 3 h at this temperature. Then the catalysts were cooled to room temperature at the presence of oxygen flow, and finally analyzed with an online gas chromatograph (Shimadzu, FID, GC-2014) equipped with a column Porapack Q (column temperature 130 $^{\circ}$C). Since the separation of olefins, isoparaffins and DME by the FID was not so satisfying. Furthermore, another online gas chromatograph (Shimadzu,TCD, GC-2014) equipped with an Unibead C column was used to determine the concentrations of CO, CO_2 and CH_4 in the products, A schematic of the slurry reactor system is shown in Fig. 3.5..
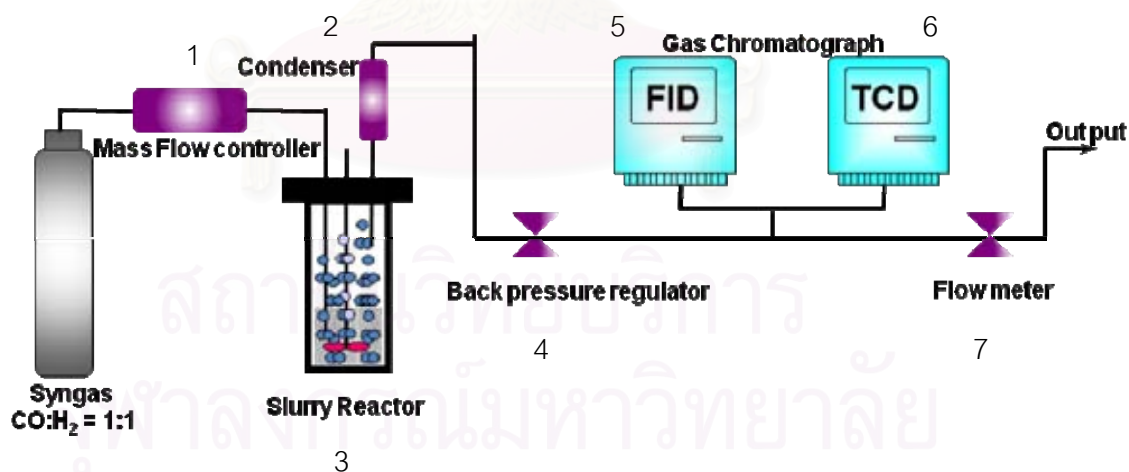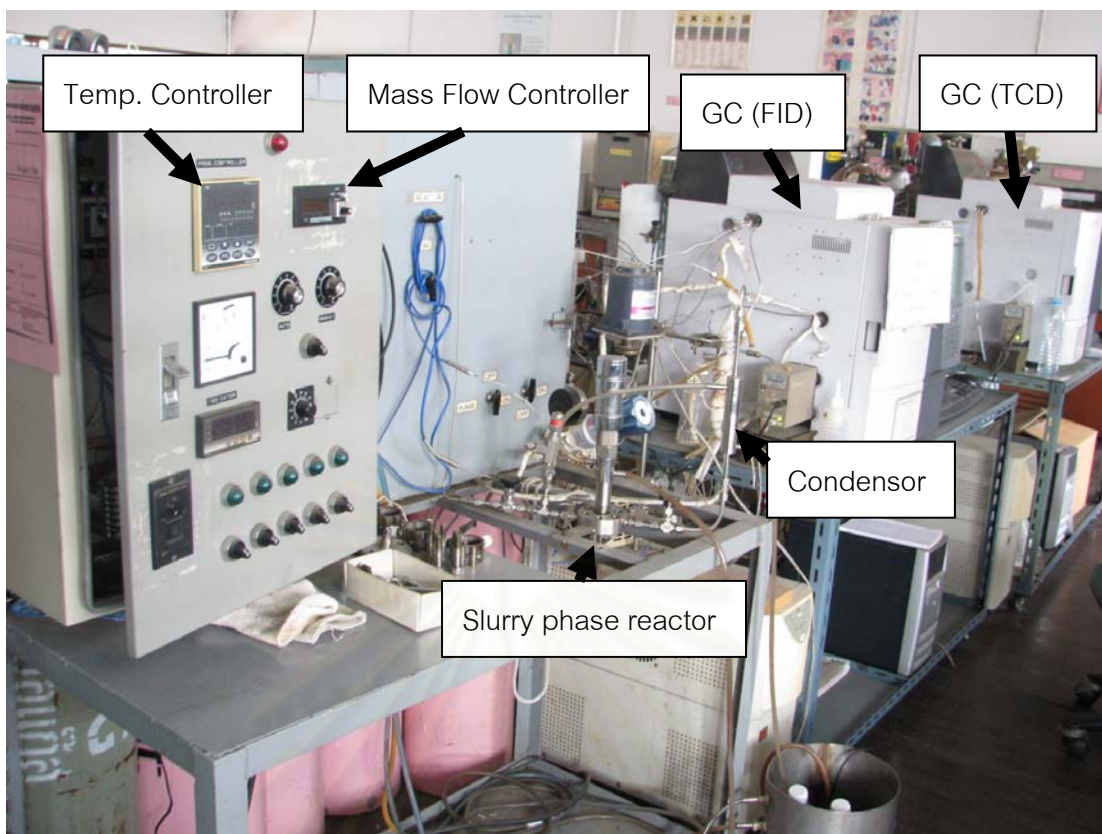
Figure 3.5 schematic view of the dimethyl ether synthesis unit. (1: Mass flow controller, 2: Condensor, 3: a slurry-phase reactor, 4: Back pressure, 5: GC FID, 6: GC TCD, 7: Flow meter)

3.7. Isoparaffins synthesis

Isoparaffins synthesis was performed in a down flow fixed-bed stainless steel reactor as shown in Fig. 3.4. The temperature and the pressure of the reaction were controlled at 533 K and 1 MPa, W/F = 5 g.h/mol, respectively. At the middle of the reactor, the mixtures of catalysts (zeolite capsule catalysts containing 0.5 g Co/Al_2O_3 with 3.0 g quartz sand were held in the fixed-bed reactor. Using a ramp rate of 2 K/min. Firstly, the catalysts were heated in 80 ml/min H_2 flow to 673 K and reduced in situ at this temperature for 3 h prior to reaction [66]. In the reaction system, the effluent products firstly passed through an ice trap where the heavy hydrocarbons were collected by a solvent with an internal standard, installed at the end of the reactor. The zeolite capsule catalysts and physical mixture catalyst were tested for isoparaffin synthesis. Other light components that could not be captured by ice trap were on-line heated at 398 K and finally analyzed with an online gas chromatograph (Shimadzu, FID, GC-8A) equipped with a column Porapack Q (column temperature 130 $^{\circ}$C). Since the separation of olefins, isoparaffins and DME by the FID was not so satisfying. Furthermore, another online gas chromatograph (Shimadzu,TCD, GC-8A) equipped with an active charcoal column was used to determine the concentrations of CO, CO_2 and CH_4 in the products, where 3% argon in the feed gas acted as the internal standard. At the exit of ice trap, some gas products were collected from 5 to 6 hours, and then were analyzed by Gas chromatography (Shimadzu,TCD, GC-14B) equipped with a capillary column (J&W Scientific GS-Alumina, i.d. 0.53 mm x 30 m) was used to identified the content of propane, because the separation of propane with methanol by PQ column was not so satisfied. The selectivity of hydrocarbons in the reaction products was calculated on the carbon base [72].
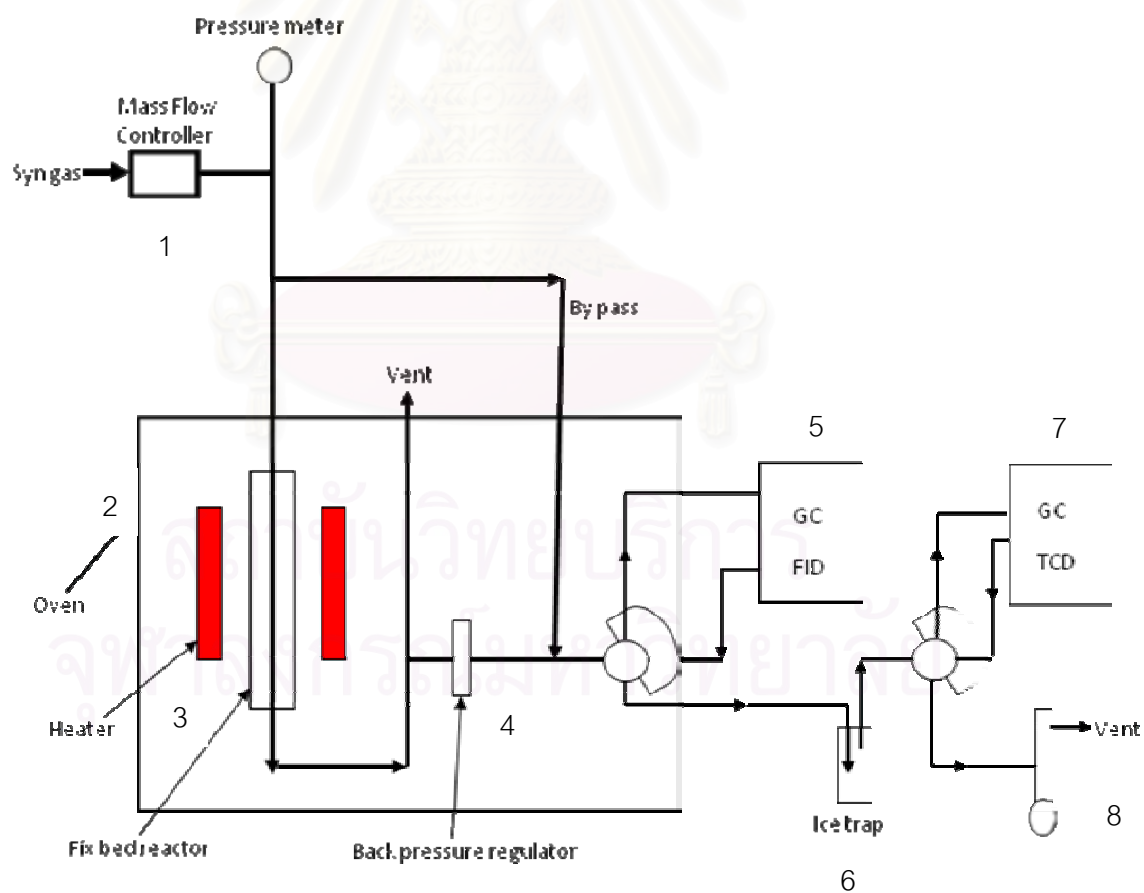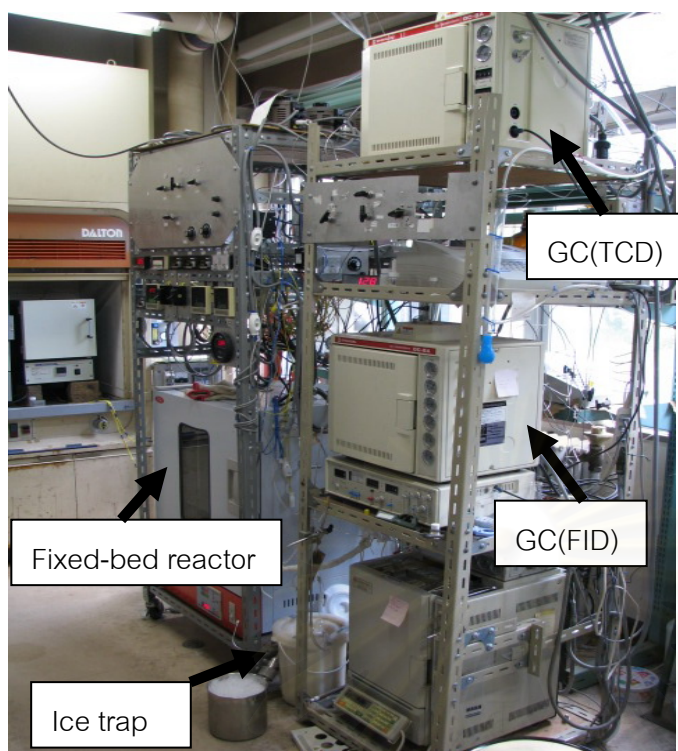
CHAPTER IV

DIMETHYL ETHER SYNTHESIS

In this section work, the experiment is divided into two parts. The first part was prepared the new capsule catalysts by a direct hydrothermal synthesis method, Zeolite membrane was coated on the Fischer-Tropsch synthesis (FTS) catalyst pellet, Cr/ZnO, which were called capsule catalysts. The capsule catalysts were tested the performance of all catalysts in a fixed-bed reactor. The second part was studied the performance of a similar catalysts at 573 K, 4 MPa with a slurry phase reactor and then they were compared with the conventional FTS catalyst and physically mixing catalysts.

4.1. Dimethyl ether synthesis in a down flow fixed-bed reactor

4.1.1. Characterization of catalysts

The conventional FTS catalyst pellets namely Cr/ZnO were synthesized by spontaneous precipitation from metal sources (chromium nitrate nanohydrate and zinc nitrate hexahydrate) in the presence of de-ionized water medium. While capsule catalysts were successfully synthesized by a direct hydrothermal synthesis method, the directly synthesized H-ZSM-5 membrane was coated perfectly onto Cr/ZnO catalyst.

4.1.1.1. X-ray diffraction

The structure of the catalysts were studied by X-ray powder diffraction. Cell parameters were obtained from a least square refinement of the XRD data with the aid of a computer program which corrected for the systematic experimental errors. The XRD patterns of the synthesized catalysts are shown in Figure 4.1. All detectable peaks of the synthesized catalysts are indexed based on the structure in standard data as PDF files. The XRD patterns of synthetic CrZnO catalysts are shown in Figure 4.1a. The standard XRD patterns of CrZnO indicated that the main peaks include $ZnCr_2O_4$(PDF #22-1107) and ZnO_2(PDF#77-2414), respectively. The XRD patterns of a commercial H-ZSM-5 zeolites are shown in Figure 4.1d. The standard XRD patterns of H-ZSM-5 (PDF #88-0808) indicated that the main peaks were H-ZSM-5 (PDF #88-0808) two peaks at 7θ

and 8θ for the H-ZSM-5 zeolites. Some changes can be observed from the XRD patterns, a capsule catalysts (CrZnO-S-Z) in Figure 4.1c and physically mixing catalyst (CrZnO-Z-M) in Figure 4.1b with different XRD pattern compared with the CrZnO and the XRD peaks between 10θ and 30θ had disappeared, which should be attributed to the capsule catalyst calcinations at 500 °C. However, the XRD pattern confirmed presence of two peaks at 7θ and 8θ for the zeolite capsule catalysts, suggesting that H-ZSM-5 zeolite membrane had been coated on the CrZnO catalysts surface successfully. [67].
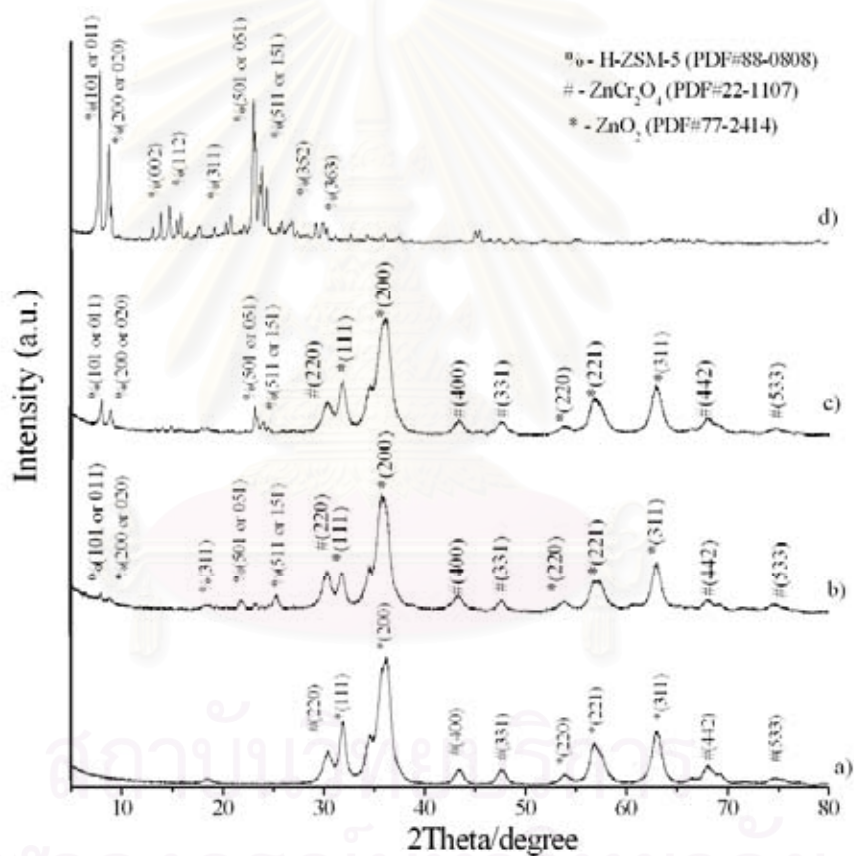
Figure 4.1 XRD patterns of catalysts; a) CrZnO, b) CrZnO-Z-M(10:1), c) CrZnO-S-Z

(10:1)and d) H-ZSM-5 [67].

.

4.1.1.2. BET analysis

The pore properties of the conventional FTS catalyst (CrZnO), physical mixing catalyst (CrZnO-Z-M), capsule catalyst (CrZnO-S-Z) and H-ZSM-5 zeolite were compared in Table 4.1. The surface area from CrZnO to CrZnO-Z-M increased from 90.4 m^2/g to 148.2 m^2/g because HZSM-5 zeolite was penetrated into CrZnO. For the zeolite capsule catalysts (CrZnO-S-Z) enwrapped by zeolite shell, the surface area was increased from 90.4 m^2/g to 187.8 m^2/g and the pore volume decreased from 0.306 cm^3/g to 0.222 cm^3/g, because of the hydrothermal synthesis and calcination effect, It was increased after the coating of H-ZSM-5 membrane. Furthermore, the pure H-ZSM-5 had more specific surface area (595.6 m^2/g) and pore volume (0.308 cm^3/g), and these properties was determined the increasing surface area and decreasing pore volume of the capsule catalysts [68].

Table 4.1 Physical properties of catalyst and capsule catalyst

Sample	Surface area $[m^2g^{-1}]$	Pore volume $[cm^3g^{-1}]$	Average pore diameter [nm]
CrZnO	90.4	0.306	13.5
CrZnO-S-Z	187.8	0.222	5.9
CrZnO-Z-M	148.2	0.297	10.5
H-ZSM-5	595.6	0.308	3.4

4.1.1.3. SEM and EDS analyses of capsule catalyst surfaces

Figure 4.2a and 4.2b were shown the surface SEM images of the conventional FTS catalyst (CrZnO) and zeolite capsule catalyst (CrZnO-S-Z), respectively. In Fig. 4.2b, H-ZSM-5 crystallites constructing the zeolite capsule on the surface of CrZnO substrates can be observed clearly, while there are no crystals on the CrZnO pellet in Fig. 4.2a. Slight differences in the size and shape of H-ZSM-5 crystallites can be found if this capsule catalyst is compared with the zeolite capsule catalyst hydrothermally synthesized for 2 days reported in the previous papers [72], [73] and [74], the latter zeolite capsule had a larger size and more regular shape than the H-ZSM-5 crystallites. These results should be attributed to the crystallization time. The surface element analysis of the conventional FTS (CrZnO) by EDS in Figure 4.3a, on the CrZnO surface, Zn Kα and Cr Kα signals had been shown that the Cr and Zn analysis were indicated molar ratio of Cr 32.73 %, Zn 67.27 %, respectively. It was close to the original catalyst preparation content. In Figure 4.3b was shown the surface elemental analysis of zeolite capsule catalyst CrZnO-S-Z. The surface EDS analysis of this zeolite capsule catalyst indicated that the signals of Cr Kα and Zn Lα were zero, confirming the integrity of the zeolite membrane enwrapped the CrZnO pellet, suggesting that there was no pinhole or crack in the zeolite capsule and that this zeolite membrane preparation was successful with the SiO_2/Al_2O_3 ratio equal 89 from EDS analysis. (Figure 4.3).
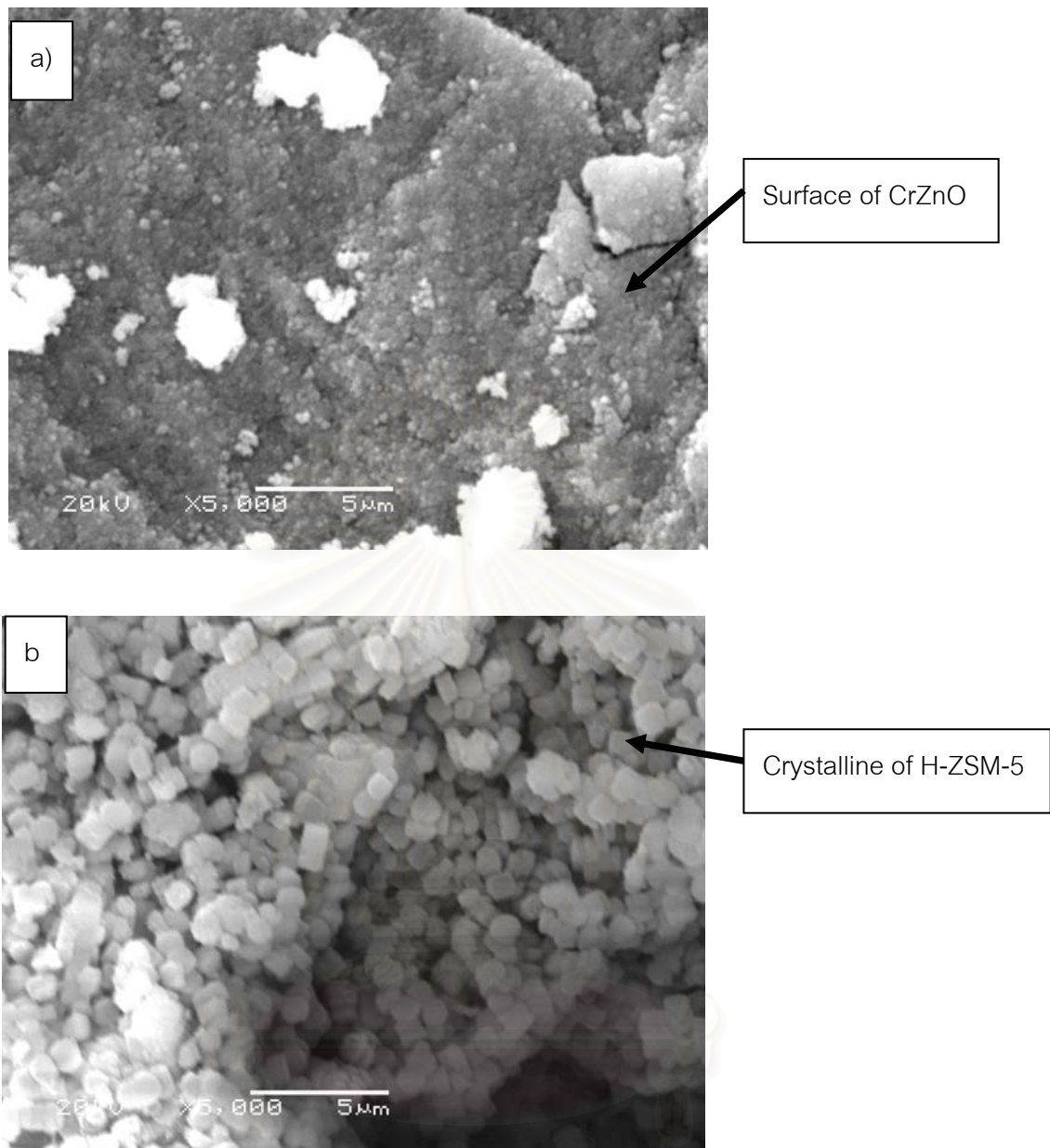
Figure 4.2 Surface SEM images of the CrZnO pellet and zeolite capsule catalyst pellet, and the EDS analysis result. a) CrZnO ; b) CrZnO-S-Z. [72,73]
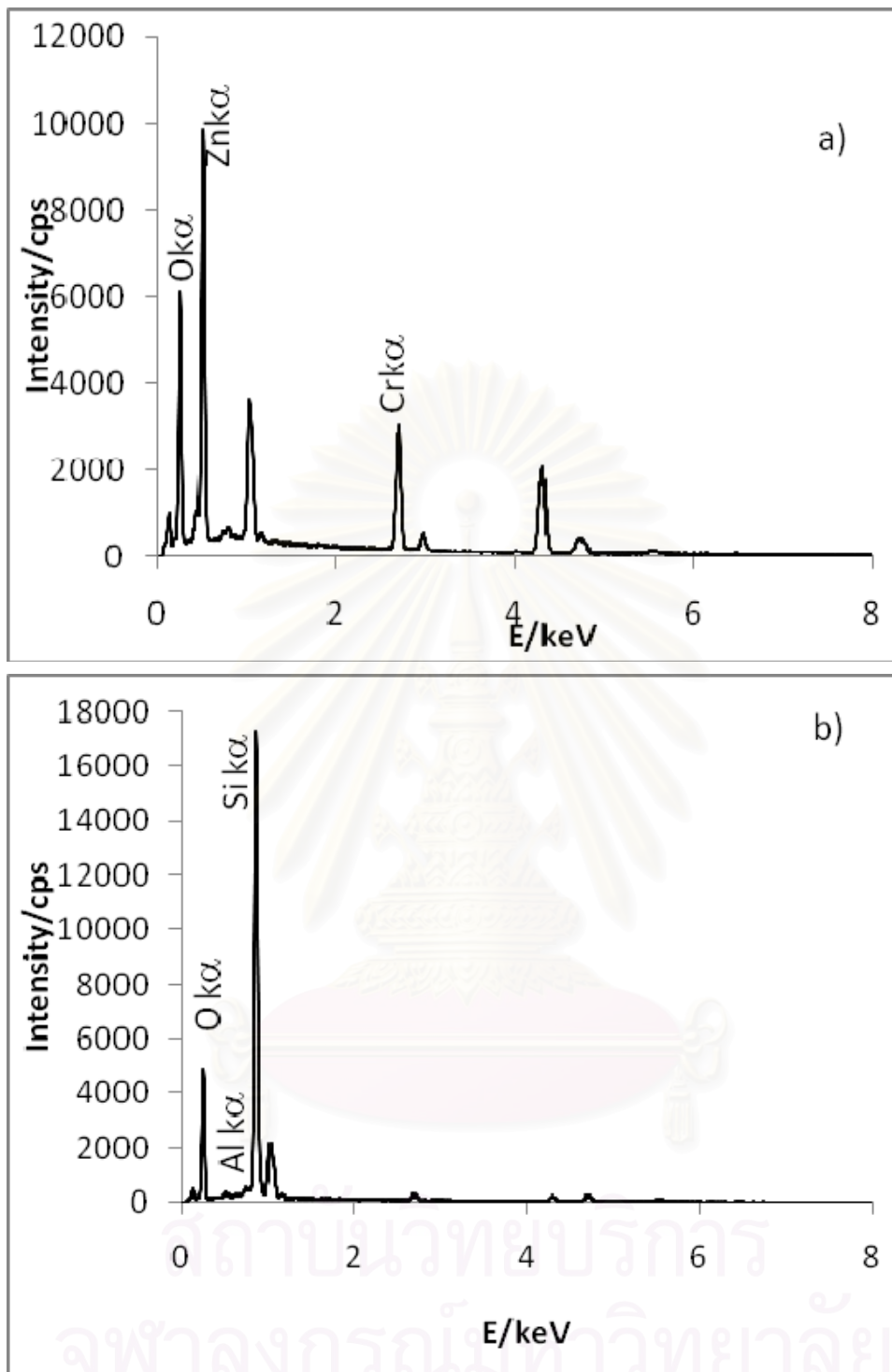
Figure 4.3 Elemental composition of the external surface of the CrZnO pellet and the

capsule catalyst pellet from EDS analysis. a) CrZnO; atomic ratio: Cr 32.73 %,

Zn 67.27 % ; b) CrZnO-S-Z; atomic ratio: Al 1.03 %, Si 98.97 % [72,73]

4.1.1.4. SEM and EDS characterization of cross-section of capsule catalysts

Fig. 4.4 shows the SEM image and EDS line analysis of the cross-section of zeolite capsule catalyst (CrZnO-S-Z). A compact H-ZSM-5 shell can be clearly observed on the surface of the conventional FTS catalyst (CrZnO substrate), indicating that a zeolite membrane was synthesized on the surface of CrZnO pellets successfully. For the EDS analysis, the Si Kα and Al Kα peaks were clearly detected. At the interface of the CrZnO substrate and the H-ZSM-5 capsule, the radial distribution of Si dropped suddenly while that of Al increased a little, indicating a phase change from CrZnO to H-ZSM-5 phase. However, Al composition was not zero inside the CrZnO substrate which proved that some H-ZSM-5 entered the pores of CrZnO. The thickness of zeolite capsule of this sample was about 18 nm by using the radical distribution profiles. The experimental results above confirmed that a compact H-ZSM-5 membrane without cracks was directly synthesized on the surface of all CrZnO pellets. Furthermore, there was no signal of Cr and Zn on any part of the zeolite capsule, showing that no chromium and zinc on the surface of FTS catalyst dissolved during the hydrothermal synthesis process [67].
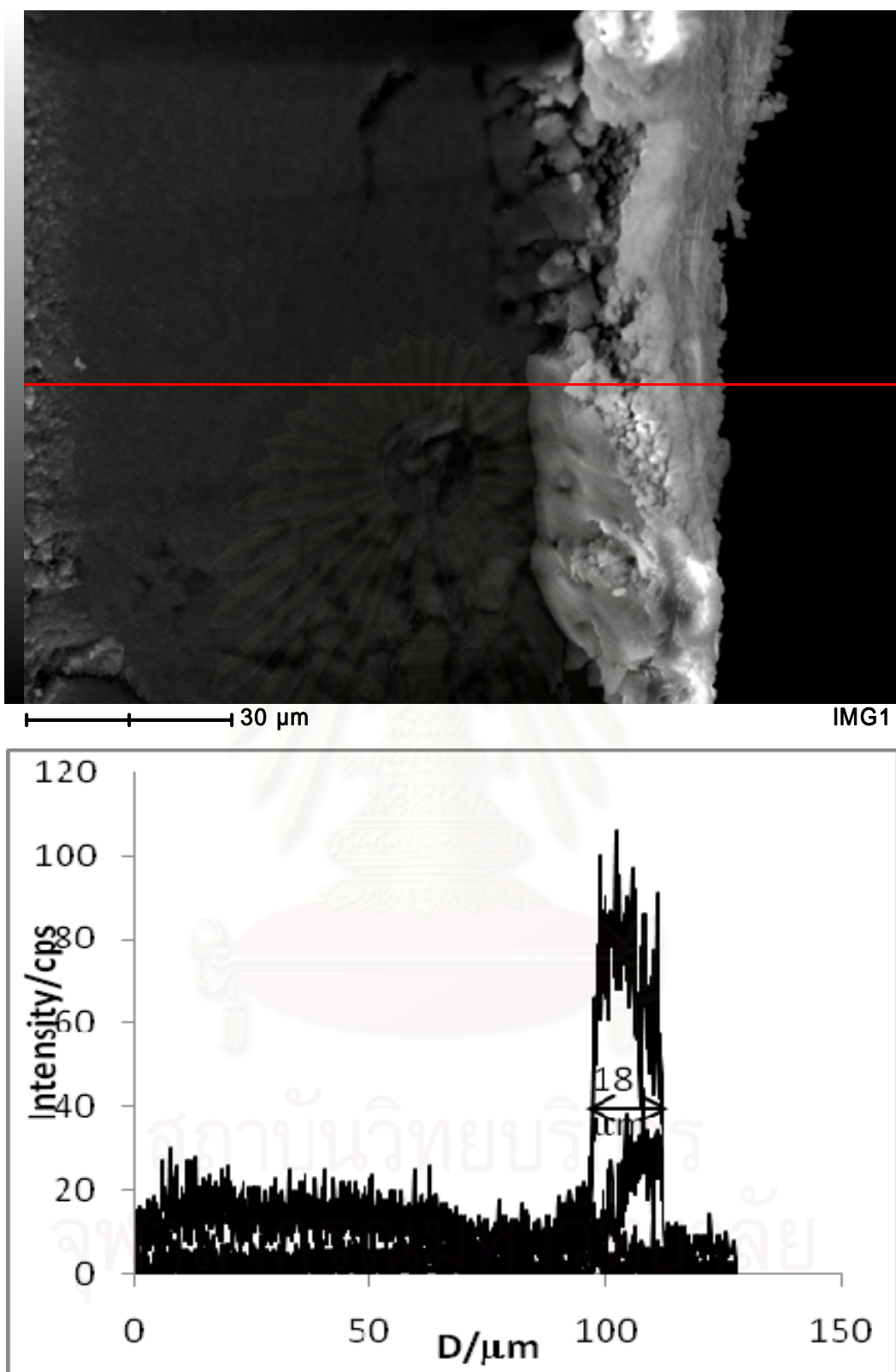
Figure 4.4 Cross-sectional SEM images and the redial elemental distribution of Al and Si

by the EDS analysis of zeolite capsule catalyst CrZnO-S-Z [67].

4.1.2. Catalytic performance of catalysts

The catalytic performance of the conventional FTS catalyst (Cr/ZnO), capsule catalyst (CrZnO-S-Z) and mixed catalyst (CrZnO-Z-M) are shown in Table 4.2. It is clear that the conventional FTS catalyst (Cr/ZnO) exhibits a wide product distribution in which methanol is the main products. When mixed with H-ZSM-5 zeolite, the product distribution strays from the ASF law and the selectivity for isoparaffins and olefins increases. The zeolite-coated catalyst gives a completely different product distribution to the other two samples as the product distribution deviates from the ASF law. Furthermore, the dimethyl ethers are now the main products. This difference is caused by the unique core/shell structure of the zeolite-coated catalyst. Zeolite capsule catalyst (CrZnO-S-Z) gave a lower CO conversion than that of (Cr/ZnO), probably because of the zeolite coated on the surface of Cr/ZnO might partly decrease the syngas diffusion rate while passing through the zeolite shell. For the mixture of Cr/ZnO and zeolite, there is no spatial restriction between the FTS and hydrocracking/isomerization reactions, which means that this is a random process and the two reactions occur independently. Thus, the hydrocarbons desorbed from the FTS site might therefore leave the catalyst directly without undergoing dehydrating at the zeolite sites. In contrast, the core/shell structure of the zeolite-coated catalyst provides an integrated, confined reaction environment.

At 598 K, for the traditional FTS catalyst CrZnO, the CO conversion was 7.26 %. The CH_3OH, CH_4 and C_2-C_3 selectivity were 80.58%, 7.75 % and 11.04%, respectively. But the physically mixing catalyst (CrZnO-Z-M) had a different hydrocarbon distribution. The fractions of C_{4+} was increased, suppressing the formation of heavy hydrocarbons, suggesting that the heavy hydrocarbons cannot be hydrocracked and isomerized completely. For FTS reaction, the main products are methanol, normal paraffins and olefins, which can enter the zeolite channels; then, on the acidic sites of zeolite, long-chain hydrocarbons can be converted into lighter ones by the isomerization and cracking. However, the physically mixing catalyst (CrZnO-Z-M) could be occured only random cases of hydrocracking and isomerization. A part of FTS hydrocarbons might have no chance to contact zeolite catalyst or might only approach the outer surface of zeolite. Consequently, heavy hydrocarbons($>C_4^+$) still existed in the final products [67,68]

Table 4.2. Reaction performance of the conventional and zeolite capsule catalysts[a]

Catalysts	Temp	% CO conversion			Selectivity(%)				
	(K)	CO	CO_2	Total	CH_4	C_2-C_3	CH_3OH	DME	C_{4+}- HC
CrZnO	573	5.43	3.38	5.15	2.42	10.14	87.44	0.00	0.00
	598	7.26	0.48	6.33	7.75	11.04	80.58	0.63	0.00
	623	7.68	-5.43	5.89	14.11	19.47	63.05	3.37	0.00
CrZnO-S-Z[b] (10:1)	573	2.27	6.97	2.91	7.78	11.18	35.62	45.42	0.00
	598	6.03	0.04	5.21	4.80	15.98	33.89	45.33	0.00
	623	9.53	-14.70	6.22	11.23	18.27	20.39	50.11	0.00
CrZnO-Z-M[c] (10:1)	573	9.30	-9.42	6.74	4.23	64.34	15.39	10.65	5.39
	598	25.25	-64.96	12.93	3.73	38.75	12.00	0.77	44.75
	623	45.16	-122.21	22.29	7.03	21.51	11.14	0.43	59.89

[a]Reaction condition: W/F = 13.6 g.h/mol, 4 hr; Pressure 5.0 MPa; Syngas composition: Ar 3.02 %, CO 32.6%, CO_2 5.16 %, Balance H_2.

[b]"S" and "Z" in this catalyst name expressed that firstly Silicate-1 membrane and then followed by H-ZSM-5 membrane synthesis on the support of CrZnO.

[c]"Z" stand for the H-ZSM-5 zeolite, M means the physically mixed catalyst of CrZnO with H-ZSM-5 (SiO_2/Al_2O_3 = 100)

The catalytic activity and product selectivity of the capsule catalysts (CrZnO-S-Z) showed slightly lower CO conversion values than those of CrZnO catalyst and physically mixing catalyst (CrZnO-Z-M), which might be attributed to the fact that the surface site were covered by zeolite during the hydrothermal synthesis. In addition, in order to react on the zeolite capsule catalyst core, syngas must first pass through the zeolite shell, which may lead to diffusion restrictions, comparing with that of the traditional FTS catalyst. CO conversions of zeolite capsule catalyst was 6.03% for CrZnO-S-Z, indicating that the main rate-controlling step was not the diffusion of syngas through the zeolite capsule under the reaction conditions. The syngas containing H_2 and CO passed through the zeolite capsule. However, dissimilar molecular diffusivity values of these two gases had been meant that they would pass through the zeolite shell at different diffusion rates. As a result, the final partial pressures of H_2 and CO in the core part of capsule catalysts were not the original pressure value of the Syngas, and we

estimated that there existed the enhanced partial pressure ratio of H_2 to CO when the core was covered by zeolite capsule.

The CO conversion, DME, CH_4 and C_2-C_3 selectivity on the capsule catalyst were increased with temperature. After desorption from the active site on CrZnO surface, methanol was occurred with dehydration and the hydrocarbon undergo hydrocracking reaction at the acidic sites of H-ZSM-5. At elevated temperature, the reaction was accelerated, consequently n-paraffin and olefin increased. After the active sites of capsule catalyst core on the FTS reaction and desorption of the hydrocarbons formation, normal hydrocarbons with linear structure would pass through the channels of the zeolite capsule to escape. The dehydration and cracking was occurred during their diffusion process. Different from that on the mixed catalyst, C_{4+} hydrocarbons were completely decomposed due to the confined space effect of the capsule catalyst and highly membrane surface to core volume ratio. Inside the zeolite capsule catalysts have a large external surface area, having more zeolite quantity per unit reactor volume, which is reason for the high selectivity and activity. It is easier for long-chain normal hydrocarbons to be hydrocracked [75]. Long-chain hydrocarbons have larger molecular sizes, and they will stay for longer times inside the zeolite capsule. Therefore, it is sufficient for them to be cracked and isomerized. Our results prove that CrZnO-S-Z had higher activity and excellent DME selectivity. The external surface area and hydrothermal synthesis method during preparation of this catalyst were well adjusted to achieve high yield of DME under the reaction conditions.

4.2. Dimethyl ether synthesis in a slurry phase reactor

The catalytic performance of the conventional FTS catalyst (Cr/ZnO) and physically mixing catalyst (CrZnO-Z-M) were also tested in a slurry phase reactor. Table 4.3 presented the reaction performance of these catalysts. The mixed catalyst (CrZnO-Z-M) gave a higher CO conversion than that of (Cr/ZnO), probably because of the syngas diffusion rate directly passing through the core catalyst and zeolite enhance increased the catalyst activity.

Table 4.3 Reaction performance of the conventional and the physically mixing catalysts[a]

Catalysts	Temp (K)	% CO conversion	Selectivity(%)					
		CO	CH_4	C_2-C_3	CH_3OH	DME	C_{4+} - HC
CrZnO	573	2.89	81.66	12.86	5.03	0.00	0.45
CrZnO-Z-M[b]	573	3.79	5.77	42.98	4.57	45.94	0.74

[a]Reaction condition: Temp. 573 K, 4 hr; Pressure 4.0 MPa; Syngas composition: Ar 4.00 %, CO 48.0% Balance H_2.

[b]"Z" stand for the HZSM-5 zeolite, M means the physically mixed catalyst of CrZnO with HZSM-5 (SiO_2/Al_2O_3 = 100)

At 573 K, for the conventional FTS catalyst (CrZnO) exhibits a wide product distribution in which straight-chain hydrocarbons are the main products, the CO conversion was 2.89 %. The CH_3OH, CH_4 and C_2-C_3 selectivity were 5.03 %, 81.66 % and 12.86 %, respectively. When it was compared to the physically mixing catalyst (CrZnO-Z-M), the product distribution strays from the ASF law and the selectivity for isoparaffins and olefins increases, the physically mixing catalyst (CrZnO-Z-M) had a different hydrocarbon distribution, especially DME. The CO conversion, DME, CH_4 and C_2-C_3 selectivity on the physically mixing catalysts were showed to 3.79 %, 45.94 % and 42.98 %, respectively . After desorption from the active site on CrZnO surface, methanol was occurred with dehydration and the hydrocarbon undergo hydrocracking reaction at the acidic sites of H-ZSM-5. However, the capsule catalyst (CrZnO-S-Z) decrease catalytic activity when zeolite membrane was separated from core shell. Therefore, these catalyst was not suitable and applied for a slurry phase reactor [72].

CHAPTER V

ISOPARAFFINS SYNTHESIS

5.1. Characterization of catalysts

The conventional FTS catalyst pellets namely Co/Al_2O_3 were prepared by incipient wetness impregnation from metal sources (cobalt nitrate hexahydrate) in the presence of de-ionized water medium. While capsule catalysts were successfully synthesized by a direct hydrothermal synthesis method, where directly synthesized H-beta membrane was coated perfectly onto Co/Al_2O_3 catalyst.

5.1.1. X-ray diffraction

The structure of the catalysts were studied by X-ray powder diffraction. Cell parameters were obtained from a least square refinement of the XRD data with the aid of a computer program which corrected for the systematic experimental errors. The X-ray diffraction (XRD) patterns of these solids, zeolite-coated Co/Al_2O_3, and pure Co/Al_2O_3 are shown in Figure 5.1, where it can clearly be seen that these solids are H-beta zeolite that has crystallized from solution. Diffraction peaks assigned to H-beta zeolite are also observed for the coated Co/Al_2O_3 pellets along with those for Co species and Al_2O_3, thereby indicating that the zeolite has successfully been coated onto the surface of the FTS catalyst. The XRD patterns of synthetic Co/Al_2O_3 catalysts are shown in Figure 5.1b. The standard XRD patterns of Co/Al_2O_3 indicated that the main peaks include Co_3O_4 and Al_2O_3, respectively. The XRD patterns of a commercial H-beta zeolites are shown in Figure 5.1a. The standard XRD patterns of H-beta indicated that the main peaks were two H-beta peaks at 7θ and 22θ. Some changes can be observed from the XRD patterns, a zeolite coated Co/Al_2O_3 in Figure 5.1c with different XRD pattern compared with the Co/Al_2O_3 and the XRD peaks between 10θ and 30θ had disappeared, which should be attributed to the capsule catalyst calcinations at 550 $^\circ$C. However, the XRD pattern confirmed presence of two peaks at 7θ and 22θ for the zeolite capsule catalysts, suggesting that H-beta zeolite membrane had been coated on the Co/Al_2O_3 catalysts surface successfully [74].
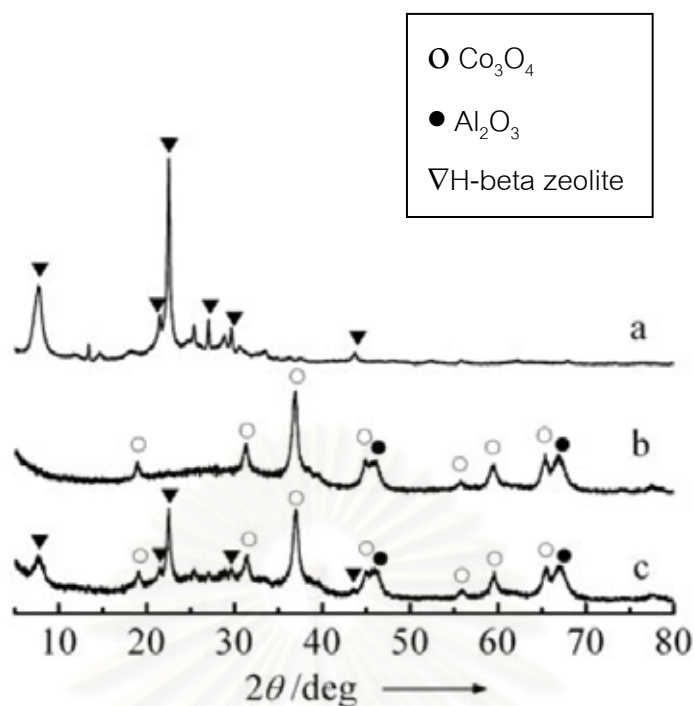
Figure 5.1 XRD patterns of a) H-beta zeolite, b) Co/Al_2O_3, and c) zeolite coated
Co/Al_2O_3 [74].

5.1.2. EDS analyses of capsule catalysts

The surface elemental distributions of the Co/Al_2O_3 pellet before and after the zeolite coating are shown in Figure 5.2. The analytical results confirm the integrity of the zeolite membrane on the Co/Al_2O_3 pellet. The surface element analysis of the conventional FTS (Co/Al_2O_3) by EDS in Figure 5.2a, on the Co/Al_2O_3 surface, Co Lα and Co Kα signals had been shown that the Al and Co analysis had molar ratio of Al 91.24 % and Co 8.76 %, respectively. It was close to the original catalyst preparation content. In Figure 5.2b gives the surface elemental analysis of zeolite coated Co/Al_2O_3. The surface EDS analysis of this zeolite capsule catalyst was shown that the signals of Co Lα and Co Kα were zero, confirming the integrity of the zeolite membrane enwrapped the Co/Al_2O_3 pellet, suggesting that there was no pinhole or crack in the zeolite capsule and that this zeolite membrane preparation was successful with the SiO_2/Al_2O_3 ratio equal 47 from the EDS analysis, which is almost the same as that of the precursor solution.

Figure 5.2 The surface EDS analysis results: a) Co/Al$_2$O$_3$ pellet; atomic ratio: Al 91.24%, Co 8.76%; b) after the hydrothermal synthesis; atomic ratio: Al 4.08%, Si 95.92% [74].

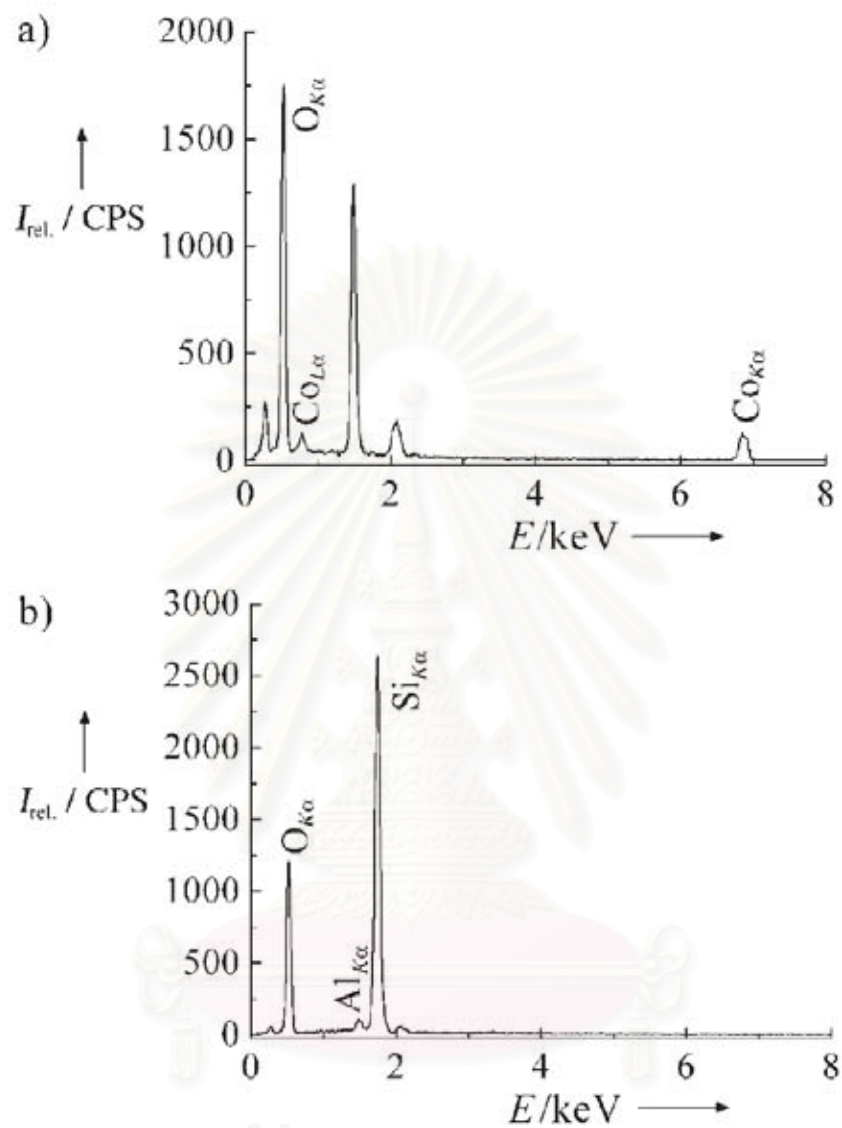### 5.1.3. SEM and EDS characterization of cross-section of capsule catalysts

Figure 5.3 was shown the SEM images and the elemental distribution of a coated Co/Al$_2$O$_3$ pellet. A compact H-beta zeolite shell can be observed crystallized on the surface of the Co/Al$_2$O$_3$ pellet., indicating that a zeolite membrane was synthesized on the surface of Co/Al$_2$O$_3$ pellet successfully. For the EDS analysis, the CoKα and CoLα peaks were clearly detected. At the interface of the Co/Al$_2$O$_3$ pellet and the H-beta capsule, the changes of the Al and Si signal intensities at the interface between the Co/Al$_2$O$_3$ pellet and the zeolite layer indicate a change from Al$_2$O$_3$ to H-beta zeolite. The Si signal inside the FTS catalyst is caused by diffusion of the zeolite precursor solution into the pores of Co/Al$_2$O$_3$. Furthermore, there was no signal of Co on any part of the zeolite capsule, showing that no cobalt on the surface of FTS catalyst dissolved during the hydrothermal synthesis process. The distribution gradient of the SiO$_2$/Al$_2$O$_3$ ratio inside the zeolite shell has been suggested to be related to the basicity of the solution used to synthesize the zeolite.[76] In this case, the high pH value of the synthesis solution means that the surface Al of the core pellet dissolves to a small extent and the resulting Al species diffuse away from the interface and establish a concentration profile. These Al species are incorporated into the zeolite during the synthesis and the concentration gradient in solution leads to a composition gradient inside the zeolite framework. The distribution gradient of the SiO$_2$/Al$_2$O$_3$ ratio reflects the fact that the zeolite membrane is crystallized directly onto the surface of the pellet.

The experimental results confirm that H-beta zeolite membrane without cracks can be directly synthesized on the surface of a Co/Al$_2$O$_3$ pellet by a hydrothermal method. It should be noted, however, that the Co/Al$_2$O$_3$ pellets need to be heated under reflux in TEAOH and soaked in ethanol before mixing with the hydrothermal synthesis precursor solution as no H-beta zeolite can be coated onto the FTS catalyst without this pretreatment. This process activates the surface Al-OH groups of the pellet with which the Al-OH and Si-OH groups in the zeolite can easily react to form Al-O-Al and Al-O-Si bonds between the substrate and the membrane. The surface Al-OH groups of the Co/Al$_2$O$_3$ pellet therefore anchor the zeolite membrane to the pellet [74].
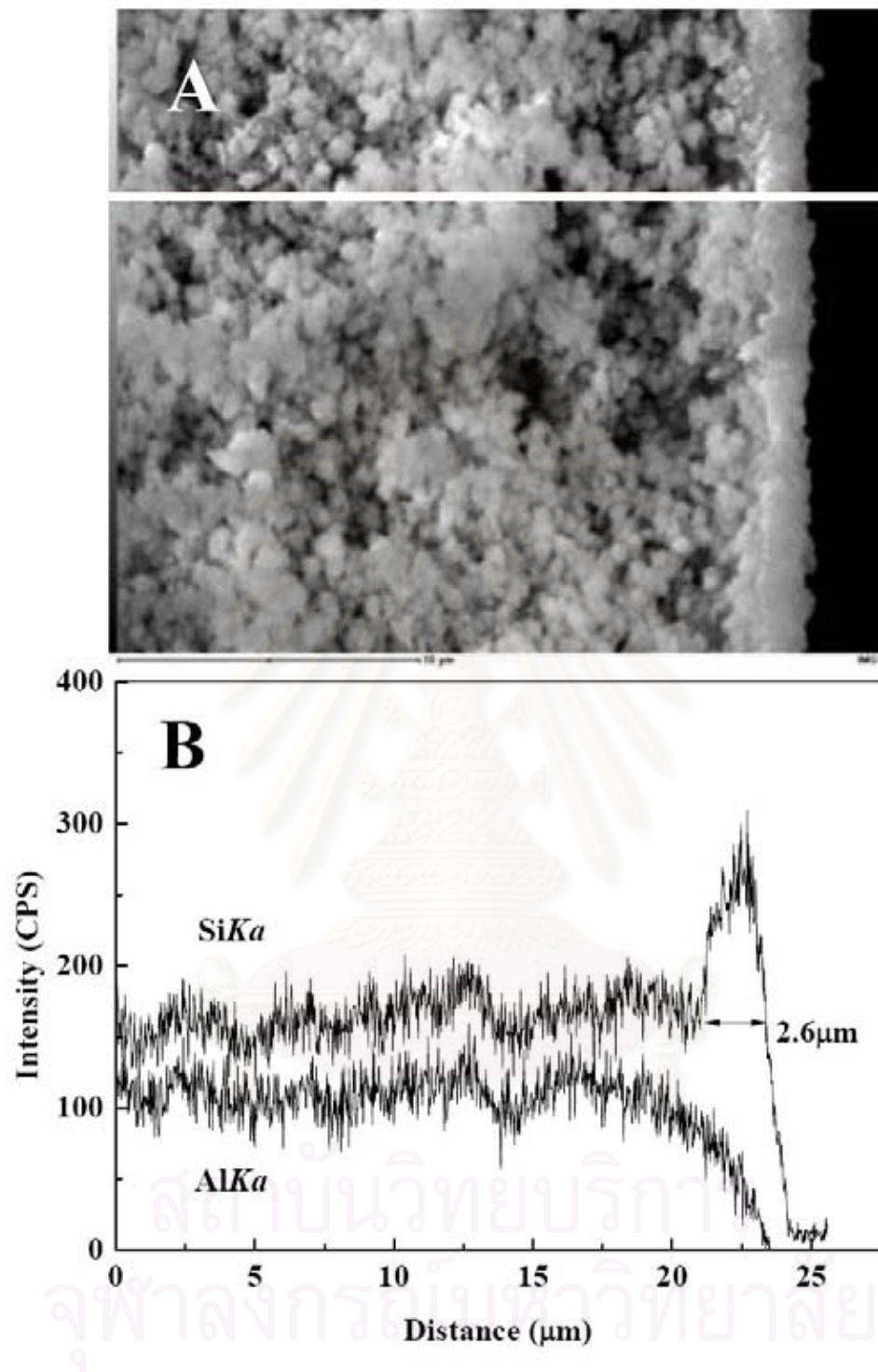
Figure 5.3 A) Cross-sectional SEM image of the coated Co/Al$_2$O$_3$ pellet

B) EDS analysis of the coated Co/Al$_2$O$_3$ pellet

5.2. Catalytic performance of catalysts

The capsule catalysts were prepared by a direct hydrothermal synthesis method, Zeolite membrane was coated on the Fischer-Tropsch synthesis (FTS) catalyst pellet, Co/Al_2O_3. The performance of H-Beta zeolite capsule catalyst (Co/Al_2O_3-B) and tricomponent zeolite capsule catalyst (Co/Al_2O_3-Pd/B), the conventional FTS catalyst of 10 wt% Co/Al_2O_3 was also tested. Table 5.1 presented the reaction performance of these catalysts. Zeolite capsule catalyst (Co/Al_2O_3-B) gave a lower CO conversion than that of Co/Al_2O_3, probably because of the partial coverage of Co active sites on the core by zeolite crystal during the hydrothermal synthesis process.   For Co/Al_2O_3-Pd/B, the palladium loaded on the surface of Co/Al_2O_3-B might partly decrease the syngas diffusion rate while passing through the zeolite shell. As a result, Co/Al_2O_3-Pd/B exhibited the lowest catalyst activity of 32.35 % than other catalysts. Table 5.1 shows the catalytic performance of these catalysts and the product distributions are presented in Figure 5.5.

Table 5.1 Reaction performance of zeolite capsule catalyst, tricomponent zeolite capsule catalyst[a] [76].

Catalyst	Conv.% CO	Select. % CH$_4$	Select. % CO$_2$	C_{iso}/C_n[b]	$C_=/C_n$[c]
Co/Al_2O_3	97.60	22.11	11.09	0.20	0.16
Co/Al_2O_3-B	85.25	11.45	3.08	0.38	0.74
Co/Al_2O_3-Pd/B	32.35	10.81	0.00	0.96	0.23

[a] Reaction conditions: 523 K, 1.0 MPa, $H_2/CO = 2$, $W_{Co/Al2O3}/F_{CO+H2}$ =15g·h/mol.

[b] C_{iso}/C_n is the ratio of iso-paraffin to n-paraffin of C_{4+}.

[c] $C_=/C_n$ is the ratio of olefin to n-paraffin of C_{2+}.

For the isoparaffin synthesis, Co/Al$_2$O$_3$ gave the lowest C$_{iso}$/C$_n$ ratio of 0.20, although with the highest catalytic activity. For Co/Al$_2$O$_3$-B, the C$_{iso}$/C$_n$ ratio was 0.38, proving its effectiveness for isoparaffin direct synthesis with the spatial consecutive reaction model. However, the selectivity of olefins increased along with the production of isoparafin undergoing the cracking reaction. Based on the hydrogenation of olefins by the palladium loaded on the zeolite shell, tricomponent zeolite capsule catalyst Co/Al$_2$O$_3$-Pd/B with the core/shell/paint structure exhibited the highest isoparaffin selectivity of 0.96. All the reactions, FTS, cracking, isomerization and hydrogenation can be accomplished simultaneously only using this single catalyst. Tricomponent H-beta zeolite capsule catalyst with core/shell/paint structure explored a new way for simple synthesis of multiple step reactions.

As illustrated in Figure 5.4, syngas passes through the zeolite membrane channel to reach the core catalyst, where it forms normal paraffins (by FTS). These hydrocarbons must diffuse through the zeolite membrane to leave the catalyst, and those with a straight-chain structure have a chance of being cracked at the acidic sites of the zeolite. Since the hydrocarbon diffusion rate in the membrane depends on the chain length, the longer the chain length is, the longer the hydrocarbons will stay inside the zeolite, and the higher the chance that they will be cracked, which leads to a high
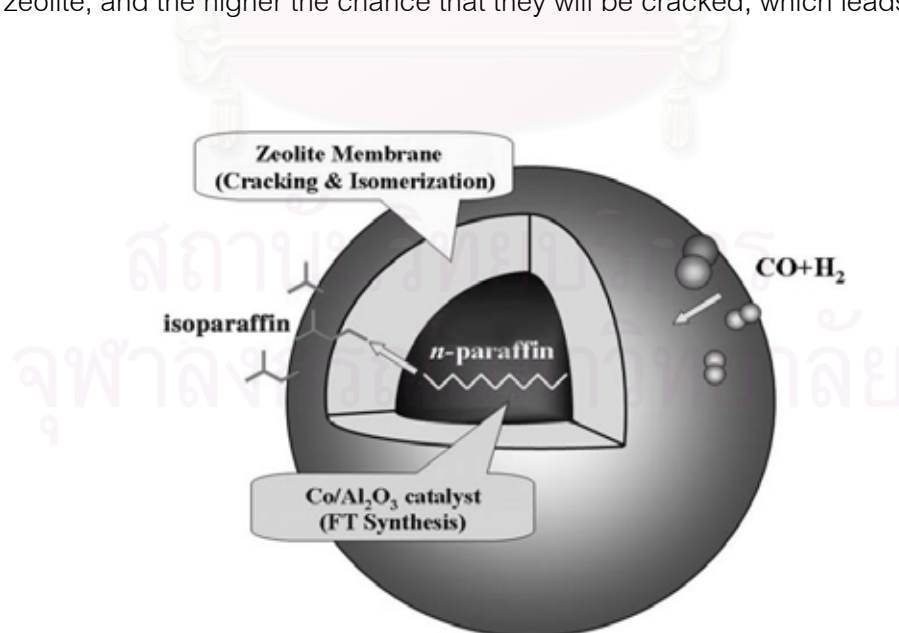

Figure 5.4. Representation of the core/shell catalyst.

C_{iso}/C_n ratio and a narrow product distribution. It is also important to note that the zeolite-coated Co/Al_2O_3 catalyst shows a highly desirable lower methane selectivity than that of the normal FTS catalyst, this selectivity might be related to the hydrophilicity of the zeolite. It is well known that the hydrophilicity of a zeolite increases as the Si/Al ratio decreases [77]. The SiO_2/Al_2O_3 distribution in the zeolite membrane of the membrane coated catalyst is not uniform and there is a distribution gradient. The part near the Al_2O_3 substrate has a relatively high Al content, which suggests a high hydrophilicity. As a result of the solubility rule (that, like dissolves like) the presence of water can promote the accumulation of CO, which leads to a higher CO/H_2 ratio in the interior of the catalyst and might lower the methane selectivity [78]. Furthermore, some of the isoparaffins and olefins formed in the membrane channels might diffuse in the reverse direction back to the surface of the core catalyst, where they can easily recombine with the adsorbed CH_2 intermediate on Co/Al_2O_3 [79]. This process is driven by the concentration gradient and also suppresses methane formation owing to hydrogenation of the CH_2 species. The CO conversion of the zeolite-coated Co/Al_2O_3 catalyst is slightly lower than with the other catalysts, which can be ascribed to coverage of some of the Co active sites by the zeolite coating. The zeolite membrane might therefore restrict the adsorption of CO and H_2 onto the Co active sites to some extent. The membrane-coated catalyst has a much larger membrane area per unit reactor volume than conventional membrane reactors, which is another reason for the high selectivity for isoparaffins. Furthermore, the simple preparation method of this membrane-coated catalyst has great potential for practical applications.

CHAPTER VI

CONCLUSIONS

This work focuses on the development of a new capsule catalyst system Cr/ZnO and Co/Al$_2$O$_3$ were prepared by the hydrothermal method and evaluated to dimethyl ether and isoparaffins synthesis, respectively. The synthesized capsule catalyst and the conventional FTS catalyst were characterized by X-ray diffraction (XRD), scanning electron microscopy (SEM) and an energy-diffusive X-ray spectroscopy (EDS). In these respect, the aim of this work are studied the characterization of all catalysts and evaluated in dimethyl ether and isoparaffins synthesis with a new capsule catalysts, are summarized as follows:

6.1 Dimethyl ether synthesis

6.1.1. Characterization of catalysts

The conventional FTS catalyst pellets (Cr/ZnO) were synthesized by spontaneous precipitation from metal sources (chromium nitrate nanohydrate and zinc nitrate hexahydrate) in the presence of de-ionized water medium. While capsule catalysts were successfully synthesized by a direct hydrothermal synthesis method, where directly synthesized H-ZSM-5 membrane was coated perfectly onto Cr/ZnO catalyst. The XRD results indicate that the XRD pattern confirmed presence of two peaks at 7θ and 8θ for the zeolite capsule catalysts, suggesting that H-ZSM-5 zeolite membrane had been coated on the CrZnO catalysts surface successfully. and its morphology indicates porosity on the surface due to thermal decomposition process. A compact HZSM-5 shell can be clearly observed crystallizing on the surface of CrZnO substrate and the radial elemental analysis we can draw the conclusions of the thickness of the zeolite HZSM-5, as revealed by SEM and EDS investigations confirm the formation of nanocrystalline of H-ZSM-5. The EDS analysis above results confirmed that a compact HZSM-5 membrane without cracks was directly synthesized on the surface of all Cr/ZnO pellets. Furthermore, there was no signal of Cr and Zn on any part of the zeolite capsule, showing that no chromium and zinc on the surface of FTS catalyst

dissolved during the hydrothermal synthesis process. The current simple, cost-effective and environmental friendly synthetic method using de-ionized water can be extended to prepare nanoparticles.

6.1.2. Catalytic performance of catalysts in a down flow fixed-bed reactor

The experimental results confirm that a complete H-ZSM-5 membrane without cracks was successfully coated onto the surface of CrZnO catalysts by following an improved hydrothermal synthesis method. The zeolite capsule catalyst shown indicates better performance for the direct synthesis of DME than compared to the physically mixing catalysts. Although the total CO conversion on the capsule catalysts was slightly lower, they were exhibited a better selectivity for DME and light hydrocarbon synthesis, especially for DME synthesis from syngas is better than the physically mixing of the catalyst. It is clear from the results of catalytic performance that the conventional FTS catalyst (Cr/ZnO) exhibits a wide product distribution in which straight-chain hydrocarbon and methanol are main products. When mixed with HZSM-5 zeolite, the product distribution strays from the Anderson–Schultz–Flory (ASF) law and selectivity for isoparaffins and olefins increase, although heavy paraffins are still present. The capsule catalyst (CrZnO-S-Z) gives a completely different product and the formation of long chain hydrocarbon($>C_4$) was suppressed completely by the zeolite membrane in this confined reaction. Furthermore, DME is now the main products. This difference is caused by the unique core/shell structure of the zeolite coated catalyst, there is no spatial restriction between the FTS and hydrocracking/isomerization reaction, which mean that this is a random process and the two reactions occur independently. Thus, the hydrocarbon desorbed from the FTS site might therefore leave the catalyst directly without undergoing cracking at the zeolite sites, In contrast, the core/shell structure of the zeolite coated catalyst provides an integrated, confined reaction environment [58]. A successfully improved hydrothermal synthesis of capsule catalyst, a new reaction with better selectivity for DME synthesis may be the other choice for catalysis process. However, the modification of the membrane catalyst and the core catalyst or optimizing the reaction condition might further enhance the catalytic activity and selectivity of the capsule catalysts.

6.1.3. Catalytic performance of catalysts in a slurry phase reactor

Above results shown indicates the physically mixing catalyst (CrZnO-Z-M) have shown the CO conversion, DME, CH_4 and C_3H_8 selectivity with 3.79 %, 45.94 % and 39.95 %, respectively. The product distribution strays from the Anderson–Schultz–Flory (ASF) law. After desorption from the active site on CrZnO surface, DME was occurred with dehydration and the hydrocarbon undergo hydrocracking reaction at the acidic sites of H-ZSM-5. However, catalytic performance of the capsule catalyst (CrZnO-S-Z) was not good in a slurry phase reactor because structure of the zeolite membranes are delicated in a slurry phase. Therefore, The catalyst is not suitable for slurry phase or fluidized bed reactor.

6.2. Isoparaffins synthesis

6.2.1. Characterization of catalysts

The conventional FTS catalyst pellets (Co/Al_2O_3) were synthesized by incipient wetness impregnation of γ-Al_2O_3 with an aqueous solution of Cobalt nitrate hexahydrate in the presence of de-ionized water medium. While capsule catalysts were successfully synthesized by a direct hydrothermal synthesis method, where directly synthesized H-beta membrane was coated perfectly onto Co/Al_2O_3 catalyst. The standard XRD patterns of H-beta indicated that the main peaks were H-beta two peaks at 7θ and 22θ for the H-beta zeolites. Some changes can be observed from the XRD patterns, a zeolite coated Co/Al_2O_3 with different XRD pattern compared with the Co/Al_2O_3 and the XRD peaks between 10θ and 30θ had disappeared, which should be attributed to the capsule catalyst calcinations at 550 $^{\circ}$C. However, the XRD pattern confirmed presence of two peaks at 7θ and 22θ for the zeolite capsule catalysts, suggesting that H-beta zeolite membrane had been coated on the Co/Al_2O_3 catalysts surface successful. And its morphology indicates porosity on the surface due to thermal decomposition process. A compact H-beta zeolite shell can be clearly observed crystallizing on the surface of Co/Al_2O_3 substrate and the radial elemental analysis we can draw the conclusions of the thickness of the zeolite H-beta, as revealed by SEM and EDS investigations the formation of nanocrystalline of H-beta zeolite and confirming the integrity of the zeolite

membrane enwrapped the Co/Al$_2$O$_3$ pellet, suggesting that there was no pinhole or crack in the zeolite capsule and that this zeolite membrane preparation was successful.

6.2.2. Catalytic performance of catalysts

A compact, complete H-beta zeolite membrane has been directly coated onto the surface of Co/Al$_2$O$_3$ catalyst pellets to form a core/shell structure following an improved hydrothermal synthesis method. The conventional Co/Al$_2$O$_3$ FTS catalyst exhibits a wide product distribution in which straight-chain hydrocarbons are the main products. When mixed with H-beta zeolite, the product distribution strays from the ASF law and the selectivity for isoparaffins and olefins increases, although heavy paraffins up to C$_{20}$ are still present. The zeolite-coated catalyst gives a completely different product distribution to the other two samples as the product distribution deviates from the ASF law and the formation of heavy paraffins (C$_{12+}$) is completely suppressed. Furthermore, the middle isoparaffins are now the main products. This difference is caused by the unique core/shell structure of the zeolite-coated catalyst. On the hydrogenation of olefins with the palladium loaded on the zeolite shell, tricomponent zeolite capsule catalyst Co/Al$_2$O$_3$-Pd/B with the core/shell/paint structure exhibited the highest isoparaffin. Tricomponent H-beta zeolite capsule catalyst with core/shell/paint structure explored a new way for simple synthesis of multiple step reactions. This core/shell membrane catalyst provides a tailor-made confined reaction environment that results in spatially confined effects and shape selectivity, which can be extended to various consecutive reactions as the shell and core components are independent catalysts of different reaction.

6.3. Advantage of capsule catalysts

The advantage of capsule catalysts are shown in Table 6.1, when comparing with mixing catalysts.

Table 6.1 Advantage of capsule catalysts and comparing with the hybrid catalysts (physical mixing catalysts)

Type of catalyst	Advantage	Disadvantage
Capsule catalysts	1. To combine FT reaction, isomerization, hydrocracking in a single pellet. 2. To reduce equilibrium shift effect, high shape selectivity, space confined effect and continuous reactive space. 3. Integration of nano structure and microstructure to a microreactor. 4. Reaction heat of exothermal reaction 1 might be utilized by endothermal reaction 2 in consecutive regime.(A→B→C) 5.To control a various consecutive as the shell and core components are independent catalysts of different reaction.	1. To prepare large-surface area membrane which easily form pinhole or crack. 2. Zeolite membrane was very difficult to prepare with hydrothermal method.
Hybrid catalysts (physical mixing catalysts)	1. Easy to prepare a physical mixing catalysts. 2. Easy to Adjust the best reaction temperature of each catalyst completely separate. 3. A wide product distribution	1.Wax accumulation and catalyst deactivation 2. Complicated multiple steps. 3.High cost of operation.

6.4. The further work

Studies on the thermodynamics, mechanisms and kinetics of methanol dehydration to DME are a challenging and difficult task with complexity resulting from the great variety of factors with diverse effects such as catalytic methanol synthesis,

dimethyl ether synthesis process, ratio of syngas , diffusion of gaseous reagents or reaction products, materials heat conductance, static or dynamic character of the environment, feed of flow rate, layer thickness of capsule catalyst, specific area and porosity, type of reactor, amount and distribution of the active centers on catalyst surface, etc. Additionally, the specificity of thermal decomposition kinetics was characterized by identification of the bonds to be selectively activated due to energy absorption at vibrational level, These results were used to identify the kinetic parameters. The results obtained from such studies can be directly applied in starting materials for the preparation of various metals. The extension on the thermodynamic data calculation from the kinetic data is expected to be the useful data for further applications.

ACKNOWLEDGEMENTS

REFERENCES

1. Yoneyama, Y.; He, J.; Morii, Y.; Azuma, S.; Tsubaki, N. Direct synthesis of isoparaffin by modified Fischer–Tropsch synthesis using hybrid catalyst of iron catalyst and zeolite. Catalysis Today 104(2005): 37–40.

2. Anderson, R.B. The Fischer-Tropsch synthesis. Orlando, Florida: Academic Press, 1984.

3. Hindermann, J.P.; Hutchings, G.J.; Kiennemann, A. Mechanistic aspects of the formation of hydrocarbons and alcohols from CO hydrogenation. Catalysis Reviews: Science & Engineering 35(1993): 1-127.

4. Van der Laan, G.P.; Beenackers, A.A.C.M. Kinetics and selectivity of the Fischer-Tropsch synthesis: A literature review. Catal. Rev., Sci. Eng., 44(1999): 255.

5. Adesina, A.A. Hydrocarbon synthesis via Fischer-Tropsch reaction: Travails and Triumphs. Appl. Catal. A 138(1996): 345-367.

6. Schulz, H.; Claeys, M. Reactions of α-olefins of different chain length added during Fischer-Tropsch synthesis on a cobalt based catalyst in a slurry reactor. Appl. Catal. A 186(1999): 71-90.

7. Hindermann, J.P.; Hutchings, G.J.; Kiennemann, A. Mechanistic aspects of the formation of hydrocarbons and alcohols from CO hydrogenation. Catalysis Reviews: Science & Engineering 35(1993): 1-127.

8. Steynberg, A.P.; Espinoza, R.L.; Jager, B.; Vosloo, A.C. Low temperature Fischer-Tropsch synthesis from a Sasol perspective. Appl. Catal. A 186(1999): 13-26.

9. Shi, B.; Davis, B.H. 13C tracer study of the Fischer-Tropsch synthesis: another Interpretation. Catal. Today 58(2000): 255-261.

10. Iglesia, E.; Reyes, S.C.; Madon, R.J.; Soled, S.L. Selectivity control and catalyst design in the Fischer-Tropsch synthesis: Sites, pellets, and reactors. Academic Press, 39(1993a): 221-302.

11. Dry, M.E. Practical and theoretical aspects of the catalytic Fischer-Tropsch Process. Appl. Catal. A 138(1996): 319-344.

12. Eilers, J.; Posthuma, S.A.; Sie, S.T. The SHELL middle distillate synthesis process. <u>Catal. Letters</u> 7(1990): 253-270.

13. Geerlings, J.J.C.; Wilson, J.H.; Kramer, G.J.; Kuipers, H.P.C.E.; Hoek, A.; Huisman, H.M. Fischer-Tropsch Technology - from active site to commercial process. <u>Appl. Catal. A.</u>, 186(1999): 186: 27-40.

14. Eisenberg, B.; Fiato, R.A. EXXON's advanced gas-to-liquids technology. <u>Stud. Surf. Sci. Catal.</u> 119(1998): 943-948.

15. Wilson, G.R.; Carr, N.L. Natural gas to hydrocarbon liquids: Selection of process components, 2nd international conference on refinery processing, AIChE Spring National Meeting, Houston, 1999; 436-442.

16. Benham, C.B.; Bohn, M.S. Maximization of diesel fuel production from a Iron-based Fischer-Tropsch catalyst, 2nd international conference on refinery processing, AIChE Spring National Meeting, Houston, 1999; 431-435.

17. Ohno, Y.; Shikada, T.; Ogawa, T.; Ono, M.; Mizuguchi, M. New clean fuel from coal dimethyl ether. Clean Fuels Symposium, American Chemical Society (ACS) Meeting, Sanfrancisco, CA, Apr 1997.

18. Fleisch, T.. Move on dimethyl ether: case is building for DME as clean diesel fuel. <u>Diesel Prog. Engines Drives.</u> 1(1995): 42-45.

19. Rouhi, A.M. Amoco Haldor Topsoe develop dimethyl ether as alternative diesel fuel. <u>Chem.Eng. News.</u> 26(1995): 37-39.

20. Kato, Y. Trends in energy and environment in the Asian region and feasibility of new clean fuels. Presentation to Asian Economy Joint Study Association, Nov 5, 1999.

21. Fleisch, T. GTL perspectives. In 21st World gas Conference, Nice, France, 2000.

22. Basu, A.; Wainwright, J. DME as a power generation fuel: performance in gas turbines. Petrotech 2001 Conference, New Delhi, India, Jan 2001.

23. Muller, J.; Urban, P.; Holderich, W.; Colbow, K.; Zhang, J.; Wilkinson, D. Electro-oxidation of dimethyl ether in a polymer-electrolyte-membrane fuel cell. <u>J. Electrochem. Soc.</u> 147(2000): 4058-4060.

24. Bhattacharyya, A.; Basu, A. Process for Hydroshifting Dimethyl ether U.S. Patent 5, 626, 794, 1997.

25. Galvita, V. Production of hydrogen from dimethyl ether. Appl. Catal. A Gen. (2001): 85-90.

26. Mills, G. Conversion of synthesis gas to liquid fuels. Fuel 1994.

27. Sardesai, A.; Tartamella, T.; Lee, S. Synthesis of hydrocarbon from dimethyl ether: selectivities toward light hydrocarbons. Fuel Sci. Technol. Int. 1996; 14(5):703-712.

28. Lee, S. U.S. Patent, 5, 459, 166, 1995.

29. Brown, D.M.; Bhatt, B.L.; Hsuing, T.H.; Lewnard, J.J.; Waller, F.J. Novel technology for the synthesis of dimethyl ether from syngas. Catal. Today. 8(1991): 279-304.

30. Bell, W.; Chang, C.; Shinnar, R. Method for Generating Power upon Demand. U.S. Patent, 4, 341, 069, 1982.

31. Zahner, J. Conversion of Modified Synthesis Gas to Oxygenated Organic. Chemicals U.S. Patent, 4, 011, 275, 1977.

32. Lewnard, J.; Hsuing, T.; White, J.; Brown, D. Single-step synthesis of dimethyl ether in slurry reactor. Chem. Eng. Sci. 45(1990): ISCRE 11.

33. Brake, L.D. U.S. Patent, 4, 595, 785(2986).

34. Spivey, J.J. Deehydration catalysts for the methanol/dimethyl ether reaction. Chem. Eng. Commun. 110(1991): 123-142.

35. Sofianos, A.C., and Scurrel, M.S.. Conversion of synthesis gas to dimethyl ether over bifunctional catalytic systems. Ind. Eng. Chem. Res. 30(1991): 2372-2378.

36. Iwasa, N.; Yamamoto, O.; Akasawa, T.; Ohyama, S.; Takezawa, N. Dehydrogenation of methanol to methyl formate over palladium / zinc oxide catalysts. J. Chem. Soc. 18(1991): 1322-1323.

37. Kubelkova, L., Novakova, J., Nedomova, K.. Reactivity of surface species on zeolites in methanol conversion. J. Catal. 124(1990): 441-450.

38. Bandeira, J. and Naccache, C. Kinetics of methanol dehydration on dealuminated H-mordenite: Model with acid and basic active centres. Appl. Catal. 69(1991): 139-148.

39. Bercic G. and Levec J. Intrinsic and global reaction rate of methanol dehydration over γ-Al_2O_3 pellets. Ind. Eng. Chem. Res. 31(1992): 1035-1040.

40. Hocevar, S., and Levec, J.. J. Catal. 135(1992): 518-532.

41. Marchi, A.J. and Froment, G.F. Catalytic conversion of methanol to light alkenes on SAPO molecular sieves. Appl. Catal. 71(1991): 139.

42. Lee, S.. Dimethyl ether synthesis process, Final Report, Project 317-6, EPRI TR-100246, Electric Power Research Institute: Palo Alto, CA, Feb 1992.

43. Wilson, R. DME shows promise as drop-in replacement for diesel fuel. Diesel Prog. Engines Drives. 1(1995): 108-109.

44. Jones, G., Jr., Holm-Larsen, H., Romoni, D., Sills, R.. How is DME manufactured in large-scale plants. PETROTECH-2001, New Delhi, India, Jan 2001.

45. Ohno, Y.; Inoue, N.; Ogawa, T.; Ono, M.; Shikada, T.; Hayashi, H. Slurry phase synthesis and utilization of dimethyl ether. NKK Tech. Rev. (2001): 85.

46. Mii, T. and Hirotani, K. Economic evaluation of a jumbo DME plant. WPC Asia Regional Meeting, Shanghai, China, Sep 17-20, 2001.

47. Lee, S.; Gogate, M.; Kulik, C. A novel single-step dimethyl ether (DME) synthesis in a three-phase slurry reactor from CO-rich syngas. Chem. Eng. Sci. 47(1992): 3769-3776.

48. Keil, F. Methanol-to-hydrocarbons: process technology. Microporous Mesoporous Mater. 29(1999): 49-66.

49 Toseland, B.A.; Underwood, R.P.; Waller, F.J. Proceedings of 1994, DOE Contracts1 Review Conference. (1994): 307-321.

50. Dybkjar, I. and Hansen, J. B. Large-scale Production of Alternative Synthetic Fuels from Natural Gas in Proceedings 4th International Natural Gas Conversion Symposium. Kruger Park, South Africa. 107(1997): 99-116.

51. Fleisch, T.H.; Basu, A.; Gradassi, M.J.; Masin, J.G. Dimethyl Ether: A Fuel for the 21st Century,Natural Gas Conversion IV: Studies in Surface Science and Catalysis. Amsterdam: Elsevier 107(1997): 117.

52. Sam Samdani, G. Chem. Eng. (1995): 17-19.

53. Peng, X.D.; Toseland, B.A.; Underwood, R.P. *Cat*alyst *Deactivation*., In C.H. Bartholomew, & G.A. Fuentes, (Eds.), Studies in surface science and catalysis. Amsterdam: Elsevier. (1997): 175-182.

54. Vanden Busshe, K.M.; Froment, G.F. A Steady-State Kinetic Model for Methanol Synthesis and the Water Gas Shift Reaction on a Commercial $Cu/ZnO/Al_2O_3$ Catalyst. J. Catal. 161(1996): 1-10.

55. Chen, Y.; Sun, Q.; Ge, Z. Chem. React. Engng Technol. 11(1995): 400-404.

56. Skrzypek, J.; Lachowska, M.; Moroz, H. Kinetics of methanol synthesis over commercial copper/zinc oxide/alumina catalysts. Chem Engng Sci. 46*(*1991): 2809-2813.

57. Hougen, O.A. Ind. Engng Chem. 53(1981): 509-515.

58. Yoshida, F.; Ramaswami, D.; Hougen, O.A.   A.I.Ch.E. J. 8(1962): 5-12.

59. Klier, K.; Chatikavaniij, V.; Herman, R.G.; Simmons, G.W. Catalytic synthesis of methanol from CO/H_2 : IV. The effects of carbon dioxide. J.Catal. 74(1982): 343-360.

60. Moradi, G.R.; Nosrati, S.; Yaripor, F. Effect of the hybrid catalysts preparation method upon direct synthesis of dimethyl ether from synthesis gas. Catal.Commun. 8(2007) 598–606.

61. Wang, L.; Fang, D.; Huang, X.; Zhang, S.; Qi, Y.; Liul, Z. Influence of Reaction Conditions on Methanol Synthesis and WGS Reaction in the Syngas-to-DME Process. Journal of Natural Gas Chemistry 15(2006): 38-44.

62. Fei, J.; Hou, Z.; Zhu, B.; Lou, H.; Zheng, X. Synthesis of dimethyl ether (DME) on modified HY zeolite and modified HY zeolite-supported Cu–Mn–Zn catalysts. Applied Catalysis A 30(2006): 49–54.

63. Erena, J.; Garona, R.; Arandes, J.M.; Aguayo, A.T.; Bilbao, J. Effect of operating conditions on the synthesis of dimethyl ether over a $CuO-ZnO-Al_2O_3/NaHZSM-5$ bifunctional catalyst. Catalysis Today 107-108(2005): 467–473.

64. Mao, D.; Yang, W.; Xia, J.; Zhang, B.; Lua, G. The direct synthesis of dimethyl ether from syngas over hybrid catalysts with sulfate-modified γ-alumina as methanol dehydration components. Journal of Molecular Catalysis A: Chemical 250(2006): 138–144.

65. Yaripour, F.; Baghaei, F.; Schmidt, I.; Perregaard, J. Synthesis of dimethyl ether from methanol over aluminium phosphate and silica–titania catalysts. Catal. Commun. 6(2005): 542–549.

66. Zhang, Q.; Li, X.; Fujimoto, K. Pd-promoted Cr/ZnO catalyst for synthesis of methanol from syngas. Applied Catalysis A 309(2006): 28–32.

67. Yang, G.; He a, J.; Yoneyama, Y.; Tan, Y.; Han, Y.; Tsubaki, N. Preparation, characterization and reaction performance of H-ZSM-5/cobalt/silica capsule catalysts with different sizes for direct synthesis of isoparaffins. Applied Catalysis A 329(2007): 99–105.

68. Yang, G.; Tan, Y.; Han, Y.; Qiu, J.; Tsubaki, N. Increasing the shell thickness by controlling the core size of zeolite capsule catalyst:Application in iso-paraffin direct synthesis., Catalysis Communications 9(2008): 2520–2524.

69. Li, X.; Luo, M.; Asami, K. Direct synthesis of middle iso-paraffins from synthesis gas on hybrid catalysts. Catalysis Today 89(2004): 439–446.

70. Tsubaki, N.; Yoneyama, Y.; Michiki, K.; Fujimoto, K. Three-component hybrid catalyst for direct synthesis of isoparaffin via modified Fischer–Tropsch synthesis, Catalysis Communications 4(2003): 108–111.

71. Erena, J. Conversion of syngas to gasoline on bifunctional catalysts. Operating conditions and kinetic modelling. Ph.D. Thesis, University of the Basque Country, Bilbao,1996.

72. He, J., Liu, Z.; Yoneyama, Y.; Nishiyama, N.; Tsubaki, N. Mutiple-functional capsule catalysts: A tailor-made confined reaction environment for the direct synthesis of middle isoparaffins from syngas., Chemistry a European J. 12/32(2006): 8296-8304.

73. He, J.; Xu, B.; Yoneyam, Y.; Nishiyama, N.; Tsubaki, N. Designing a New Kind of Capsule Catalyst and Its Application for Direct Synthesis of Middle Isoparaffins from Synthesis Gas., J. Langmuir. 21(2005): 1699-1702.

74. He, J.; Xu, B.; Yoneyam, Y.; Nishiyama, N.; Tsubaki, N. Designing a New Kind of Capsule Catalyst and Its Application for Direct Synthesis of Middle Isoparaffins from Synthesis Gas., <u>Chemistry Letters</u> 34(2005): 148-149.

75. Leclercq, G.; Leclercq, L.; Maurel, R. Hydrogenolysis of saturated hydrocarbons : II. Comparative hydrogenolysis of some aliphatic light hydrocarbons on platinum-alumina. <u>J. Catal.</u> 44(1976): 68-75.

76. Bao, J.; He, J.; Zhang, Y.; Yoneyam, N.; Tsubaki, N. A Core/Shell Catalyst Produces a Spatially Confined Effect and shape Selectivity in a Consecutive Reaction. <u>Int. J. Gese. Deut. Chem.</u> 47/2(2008): 353-356.

77. Noack, M.; KOlsch, P.; Caro, J.; Schneider, M.; Toussaint, P.; Sieber, I. MFImembranes of different Si/Al ratios for pervaporation and steam permeation. <u>Microporous Mesoporous Mater</u> 35-36(2000): 253 – 265.

78. Jacobs, G.; Das, T.K.; Li, J.L.; Luo, M.S.; Patterson, P.M.; Davis, B.H. Fischer-Tropsch synthesis: influence of support on the impact of co-fed water for cobalt-based catalysts. <u>Stud. Surf. Sci. Catal.</u> 163(2007): 217 – 253.

79. Tsubaki, N.; Yoshii, K.; Fujimoto, K. Anti-ASF Distribution of Fischer–Tropsch Hydrocarbons in Supercritical-Phase Reactions. <u>J. Catal.</u> 207(2002): 371 – 375.

APPENDICES

APPENDIX A

Data of experiment of CrZnO-S-Z capsule catalyst for DME synthesis

Condition of experiment : Temperature 325 $^{\circ}$C

: Pressure 50 Bar

: Feed flow rate 15 ml/min

: Weight of catalyst 0.5 g

: Syngas ; $H_2/CO/CO_2/Ar$ = 59.22/32.60/5.16/3.02

Data from Gas chromatography (TCD)

Syngas	1	2	3	Average
Ar	11975	12120	11765	11953.33
CO	131635	132552	132748	132311.70
CO_2	23203	23248	23144	23198.33
STD gas (TCD)				
Ar	22256	22262	22259	22259.00
CO	21430	21127	21279	21278.67
CH_4	17527	17540	17534	17533.67
CO_2	21753	21707	21730	21730
STD gas (FID)				
CH_4	62795	62902	62849	62848.67

Data from reaction (TCD)

t(min)	30	60	90	120	150	180	210	240	270	300
P(MPa)	5.0	5.0	5.0	5.0	5.0	5.0	5.0	5.0	5.0	5.0
Ar	12279	12491	12574	12634	12693	12708	12728	12734	12740	12745
CO	132237	132454	131987	132028	132069	132088	132449	132459	132469	132495
CH_4	-	-	-	-	-	-	-	-	-	-
CO_2	23269	23501	24551	24362	24730	24403	24774	24703	24567	24545
F_{out} (mol/hr)	0.0296	0.0295	0.0292	0.0297	0.0299	0.0296	0.0298	0.0293	0.0297	0.0295

Data from reaction (FID)

Time(min)	60	120	180	240
CH_4	280	375	281	280
C_2H_4	281	380	432	421
C_2H_6	-	45	48	49
C_3H_6	212	450	421	412
C_3H_8	37	55	52	51
MeOH	2212	2911	2755	2912
DME	4003	5931	5624	5560

APPENDIX B

CALCULATION

1.Calculation of percent CO conversion

$$\%CO = \frac{\left(\dfrac{CO}{Ar}\right)_{in} - \left(\dfrac{CO}{Ar}\right)_{out}}{\left(\dfrac{CO}{Ar}\right)_{in}} \times 100$$

$$\%CO = \frac{\left(\dfrac{132311.70}{11953.33}\right)_{in} - \left(\dfrac{132459}{12734}\right)_{out}}{\left(\dfrac{132311.70}{11953.33}\right)_{in}} \times 100 \qquad ; \text{time at 240 min}$$

$$\%CO = \frac{(11.0690)_{in} - (10.4020)_{out}}{(11.0690)_{in}} \times 100$$

$$\%CO = 6.03\ \%$$

2.Calculation of percent CO_2 conversion

$$\%CO_2 = \frac{\left(\dfrac{CO_2}{Ar}\right)_{in} - \left(\dfrac{CO_2}{Ar}\right)_{out}}{\left(\dfrac{CO_2}{Ar}\right)_{in}} \times 100$$

$$\%CO_2 = \frac{\left(\dfrac{23198.33}{11953.33}\right)_{in} - \left(\dfrac{24703}{12734}\right)_{out}}{\left(\dfrac{23198.33}{11953.33}\right)_{in}} \times 100 \qquad ; \text{time at 240 min}$$

$$\%CO_2 = \frac{(1.9407)_{in} - (1.9399)_{out}}{(1.9407)_{in}} \times 100$$

$$\%CO_2 = 0.04\ \%$$

3. Calculation of Total conversion

$$Total\_conversion = \frac{\left[(\%CO)_{conv} \times (\%CO)_{syngas}\right] + \left[(\%CO_2)_{conv} \times (\%CO_2)_{syngas}\right]}{(\%CO + \%CO_2)_{syngas}}$$

$$Total\_conversion = \frac{\left[(6.03)_{conv} \times (32.60)_{syngas}\right] + \left[(0.04)_{conv} \times (5.16)_{syngas}\right]}{(32.60 + 5.16)_{syngas}} \quad ; \text{ at 240 min}$$

$$Total\_conversion = \frac{[196.578] + [0.2064]}{(37.76)}$$

$$Total\_conversion = 5.21$$

4. Calculation of selectivity of products

$$\%Selectivity = \frac{\sum_{i=1}^{n}(yield\_of\_product)}{(yield\_of\_all\_product)^{n}} \times 100$$

$$Yield = \frac{\left[(out\_flow) \times (\%CH4)_{std} \times (FID\_area)\right]}{(CH4\_area)_{std}}$$

time at 240 min;

$$Yield\_CH_4 = \frac{\left[(out\_flow) \times (\%CH_4)_{std} \times (CH_4 FID\_area)\right]}{(CH_4\_area)_{std}}$$

$$Yield\_CH_4 = \frac{\left[(0.0297) \times (0.0502)_{std} \times (280)\right]}{(62848.67)_{std}}$$

$$Yield\_CH_4 = 6.6486 \times 10^{-6}$$

$$Yield\_C_2H_4 = \frac{[(out\_flow) \times (\%CH_4)_{std} \times (C_2H_4 FID\_area)]}{(CH_4\_area)_{std}}$$

$$Yield\_C_2H_4 = \frac{[(0.0297) \times (0.0502)_{std} \times (421)]}{(62848.67)_{std}}$$

$$Yield\_CH_4 = 9.9967 \times 10^{-6}$$

$$Yield\_C_2H_6 = \frac{[(out\_flow) \times (\%CH_4)_{std} \times (C_2H_6 FID\_area)]}{(CH_4\_area)_{std}}$$

$$Yield\_C_2H_6 = \frac{[(0.0297) \times (0.0502)_{std} \times (49)]}{(62848.67)_{std}}$$

$$Yield\_C_2H_6 = 1.1635 \times 10^{-6}$$

$$Yield\_C_3H_6 = \frac{[(out\_flow) \times (\%CH_4)_{std} \times (C_3H_6 FID\_area)]}{(CH_4\_area)_{std}}$$

$$Yield\_C_3H_6 = \frac{[(0.0297) \times (0.0502)_{std} \times (412)]}{(62848.67)_{std}}$$

$$Yield\_C_3H_6 = 9.7829 \times 10^{-6}$$

$$Yield\_C_3H_8 = \frac{[(out\_flow) \times (\%CH_4)_{std} \times (C_3H_8 FID\_area)]}{(CH_4\_area)_{std}}$$

$$Yield\_C_3H_8 = \frac{[(0.0297) \times (0.0502)_{std} \times (51)]}{(62848.67)_{std}}$$

$$Yield\_C_3H_8 = 1.2109 \times 10^{-6}$$

$$Yield\_CH_3OH = \frac{[(out\_flow) \times (\%CH_4)_{std} \times (CH_3OHFID\_area)]}{(CH_4\_area)_{std}} \times FID\_factor$$

$$Yield\_CH_3OH = \frac{[(0.0297) \times (0.0502)_{std} \times (2912)]}{(62848.67)_{std}} \times 1.4681$$

$$Yield\_CH_3OH = 4.7098 \times 10^{-5}$$

$$Yield\_DME = \frac{[(out\_flow) \times (\%CH_4)_{std} \times (DMEFID\_area)]}{(CH_4\_area)_{std}} \times FID\_factor$$

$$Yield\_DME = \frac{[(0.0297) \times (0.0502)_{std} \times (5560)]}{(62848.67)_{std}} \times 2.0958$$

$$Yield\_DME = 6.2993 \times 10^{-5}$$

Therefore;

$$\%Selectivity\_CH_4 = \frac{6.6486 \times 10^{-6}}{1.3889 \times 10^{-4}} \times 100$$

$$\%Selectivity\_CH_4 = 4.78$$

$$\%Selectivity\_C_2H_4 = \frac{9.9967 \times 10^{-6}}{1.3889 \times 10^{-4}} \times 100$$

$$\% \, Selectivity \_ C_2H_4 = 7.20$$

$$\% \, Selectivity \_ C_2H_6 = \frac{1.1635 \times 10^{-6}}{1.3889 \times 10^{-4}} \times 100$$

$$\% \, Selectivity \_ C_2H_6 = 0.84$$

$$\% \, Selectivity \_ C_3H_6 = \frac{9.7829 \times 10^{-6}}{1.3889 \times 10^{-4}} \times 100$$

$$\% \, Selectivity \_ C_3H_6 = 7.04$$

$$\% \, Selectivity \_ C_3H_8 = \frac{1.2109 \times 10^{-6}}{1.3889 \times 10^{-4}} \times 100$$

$$\% \, Selectivity \_ C_3H_8 = 0.87$$

$$\% \, Selectivity \_ CH_3OH = \frac{4.7098 \times 10^{-5}}{1.3889 \times 10^{-4}} \times 100$$

$$\% \, Selectivity \_ CH_3OH = 33.91$$

$$\% \, Selectivity \_ DME = \frac{6.2993 \times 10^{-5}}{1.3889 \times 10^{-4}} \times 100$$
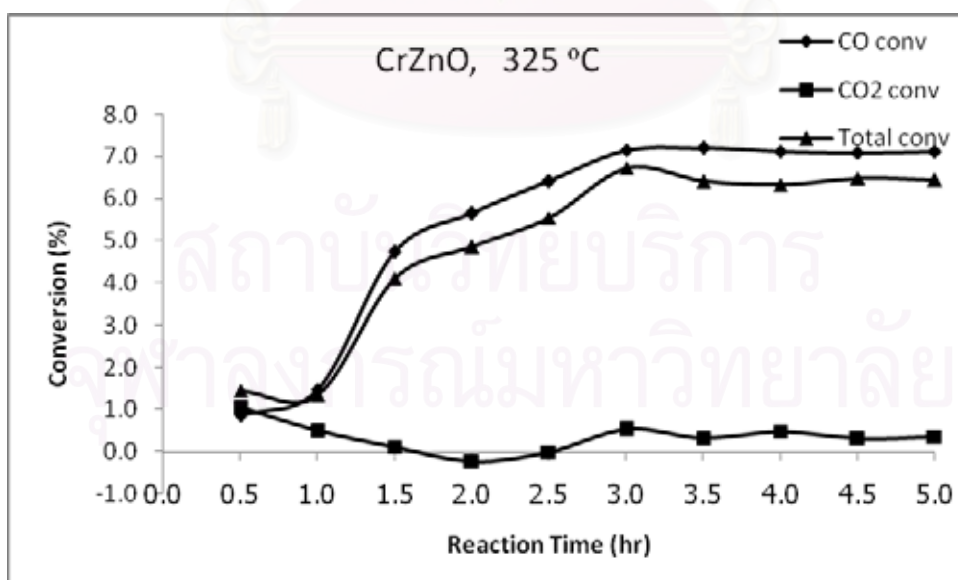
$$\% \, Selectivity \_ DME = 45.35$$
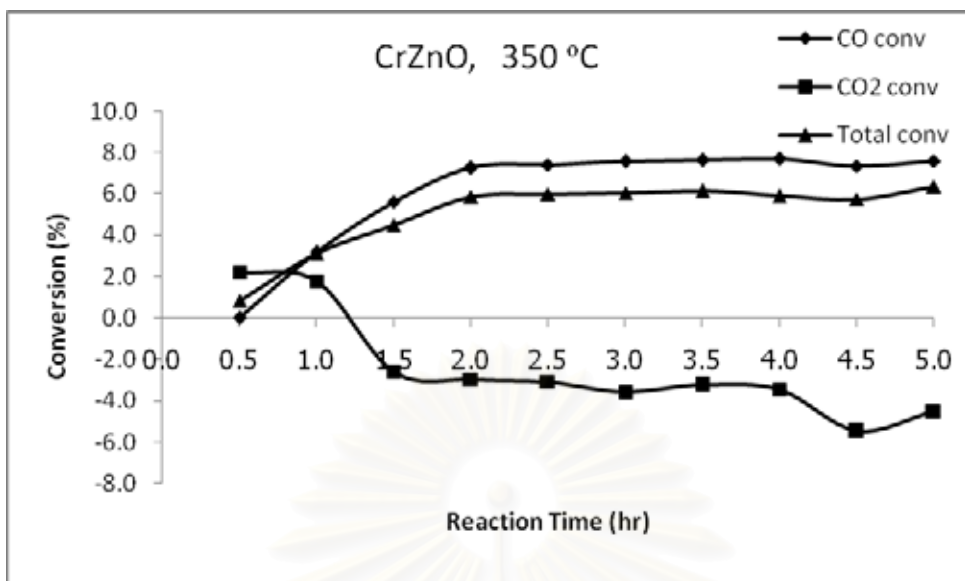
APPENDIX C

CO, CO_2 and total conversion as a function of a reaction time over CrZnO, CrZnO-S-Z
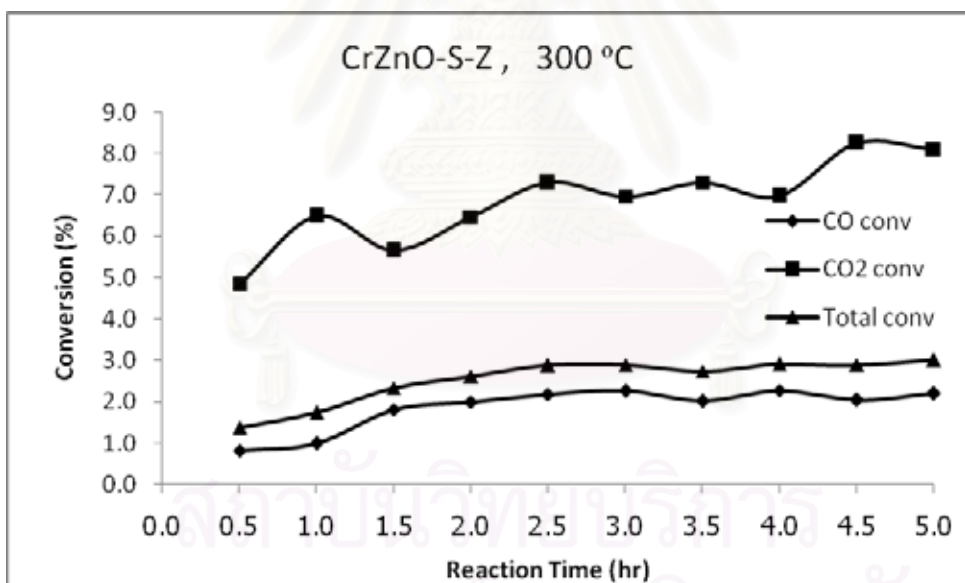and CrZnO-Z-M (In a fixed-bed reactor)
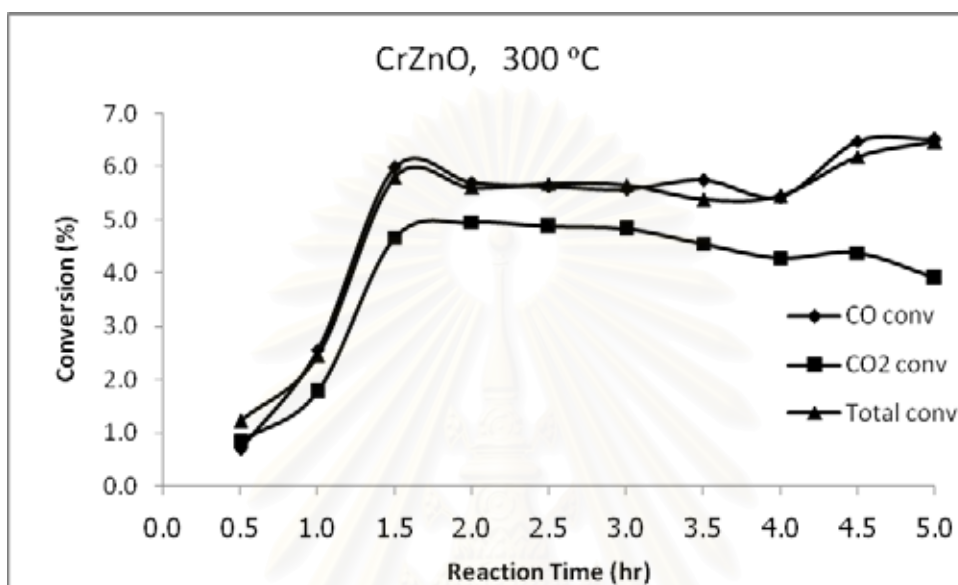
C1. Variation of CO, CO_2 and total conversion as a function of a reaction time over
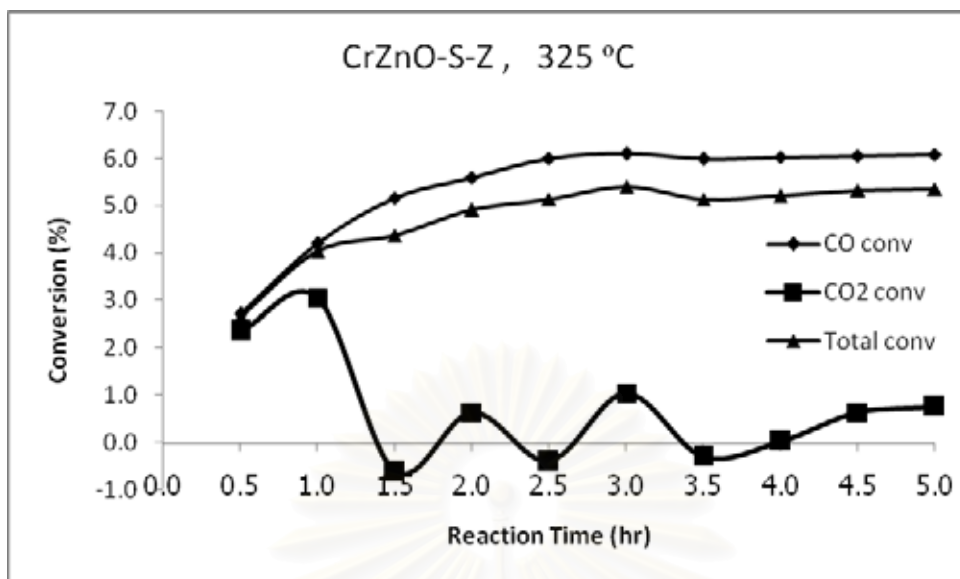
CrZnO at temperature of 300 $^{\circ}$C

C2. Variation of CO, CO_2 and total conversion as a function of a reaction time over
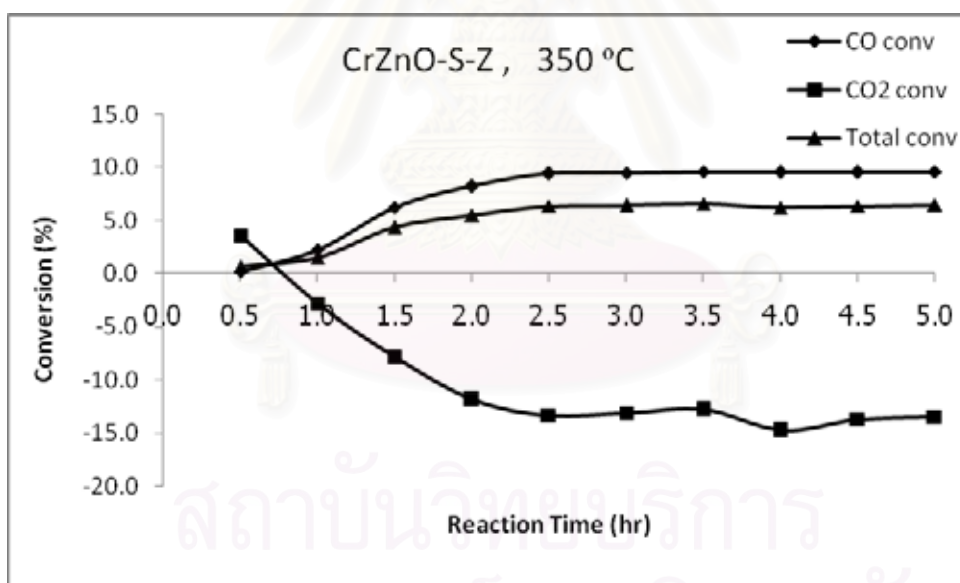
CrZnO at temperature of 325 $^{\circ}$C

C3. Variation of CO, CO_2 and total conversion as a function of a reaction time over
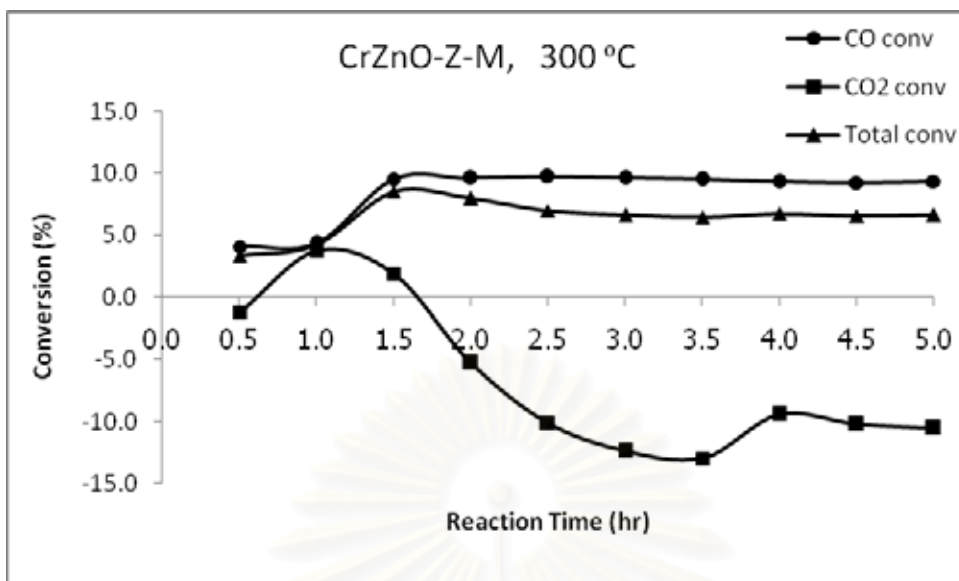
CrZnO at temperature of 350 $^{\circ}$C

C4. Variation of CO, CO_2 and total conversion as a function of a reaction time over

CrZnO-S-Z at temperature of 300 $^{\circ}$C

C5. Variation of CO, CO_2 and total conversion as a function of a reaction time over

   CrZnO-S-Z at temperature of 325 $^{\circ}$C

C6. Variation of CO, CO_2 and total conversion as a function of a reaction time over

   CrZnO-S-Z at temperature of 350 $^{\circ}$C

C7. Variation of CO, CO_2 and total conversion as a function of a reaction time over
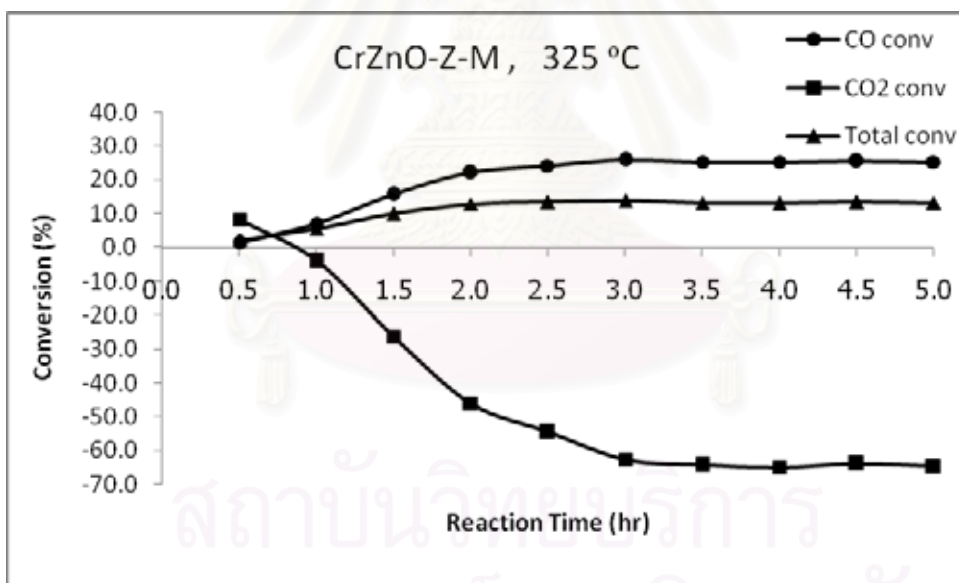
CrZnO-Z-M at temperature of 300 ^{o}C

C8. Variation of CO, CO_2 and total conversion as a function of a reaction time over
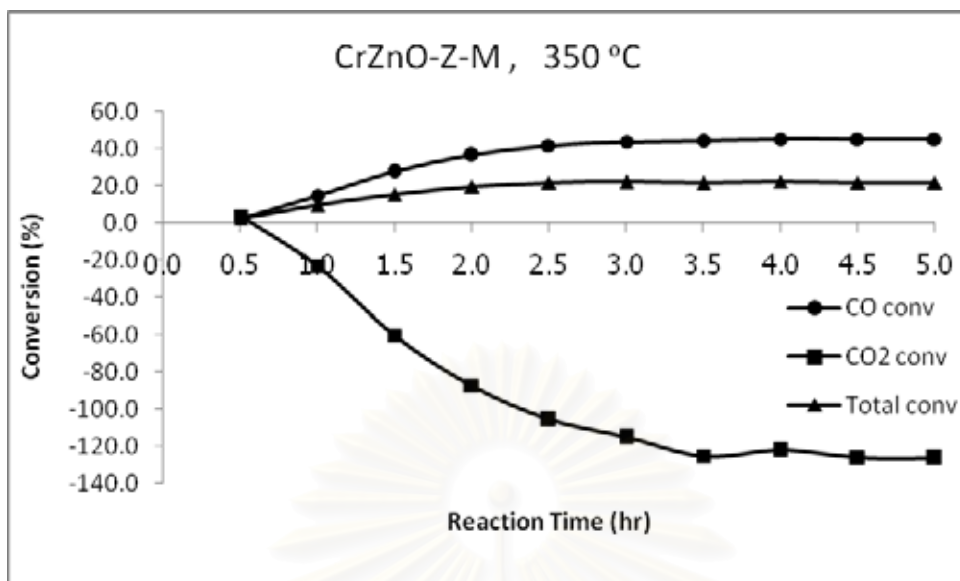
CrZnO-Z-M at temperature of 325 ^{o}C

C9. Variation of CO, CO_2 and total conversion as a function of a reaction time over

CrZnO-Z-M at temperature of 350 $^\circ$C

APPENDIX D

Data of experiment from gas chromatography (TCD and FID detector)

Analysis Date & Time	: 2/9/2551 18:46:26
User Name	: Admin
Vial#	: 0
Sample Name	:
Sample ID	:
Sample Type	: Unknown
Injection Volume	: 1.00
ISTD Amount	:
Data Name	: D:\PhD\JACKPHD\CrZnO+HZ(2-09-51)\4.gcd
Method Name	: D:\PhD\JACKPHD\DME rxn.gcm
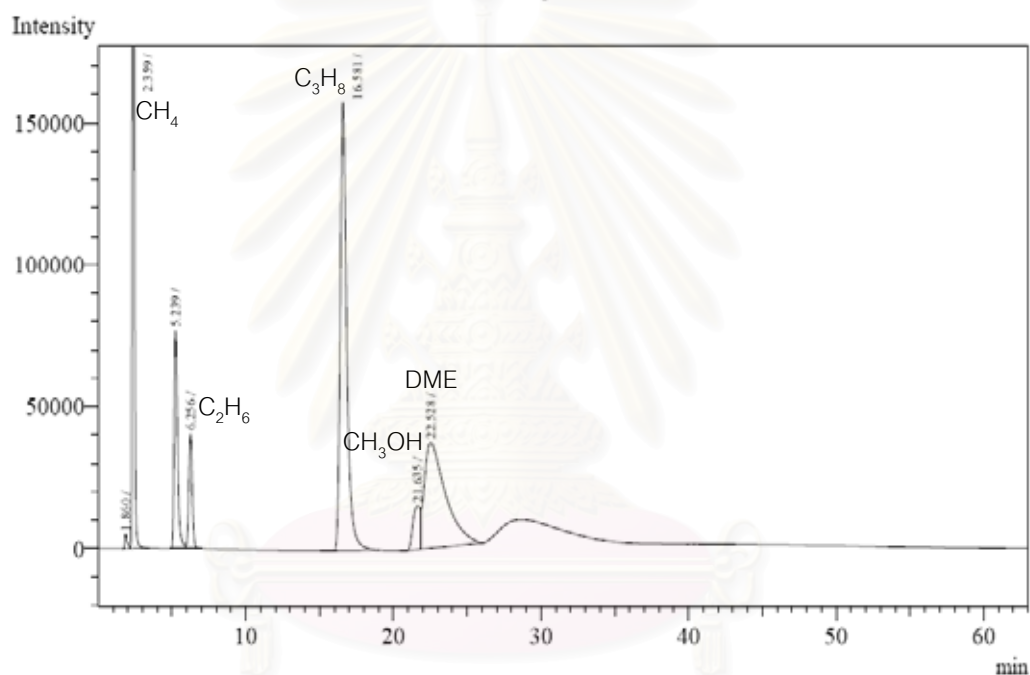
Peak#	Ret.Time	Area	Height	Conc.	Unit Mark	ID#	Cmpd Name
1	1.860	61123	5305	0.000			
2	2.359	4711751	591842	0.000	V		
3	5.239	1228039	76776	0.000			
4	6.256	658795	40371	0.000	V		
5	16.581	4864560	157953	0.000			
6	21.635	517882	15236	0.000			
7	22.528	3723882	37197	0.000	V		
Total		15766032	924680				

D1. Data of gas chromatography(FID) for physically mixing catalyst(CrZnO-Z-M)

Analysis Date & Time : 17/2/2552 11:55:01
User Name : Admin
Vial# : 0
Sample Name :
Sample ID :
Sample Type : Unknown
Injection Volume : 1.00
ISTD Amount :

Data Name : D:\PhD\JACKPHD\CrZnO(16Feb09)\20.gcd
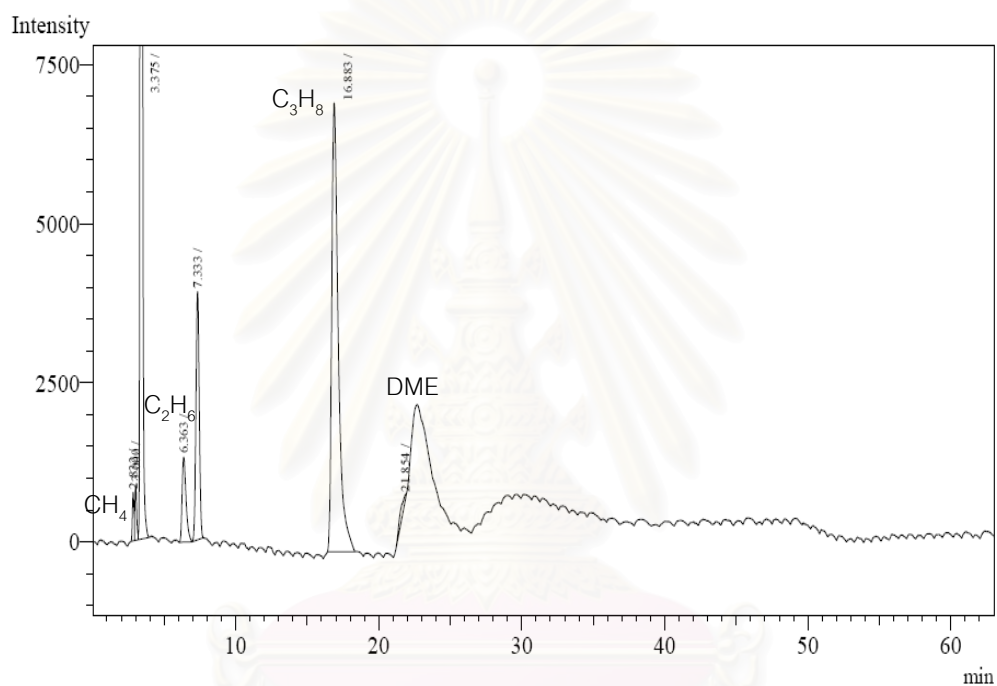Method Name : D:\PhD\JACKPHD\DME rxn.gcm

Intensity

Peak#	Ret.Time	Area	Height	Conc.	Unit Mark	ID#	Cmpd Name
1	2.832	5838	760	0.000			
2	3.000	7470	872	0.000	V		
3	3.375	492675	61180	0.000	V		
4	6.363	25605	1335	0.000			
5	7.333	63078	3901	0.000			
6	16.883	226158	7049	0.000			
7	21.854	5911	88	0.000			
Total		826735	75185				

D2. Data of gas chromatography(FID) for the conventional FTS catalyst (CrZnO)

Analysis Date & Time : 2/9/2551 18:38:08
User Name   : Admin
Vial#   : 0
Sample Name   :
Sample ID   :
Sample Type   : Unknown
Injection Volume   : 1.00
ISTD Amount   :

Data Name   : C:\GCsolution\Data\Jack\CrZnO+HZ(02-09-08)\4.gcd
Method Name   : C:\GCsolution\Data\Jack\H2 Ar CO CH4 CO2.gcm
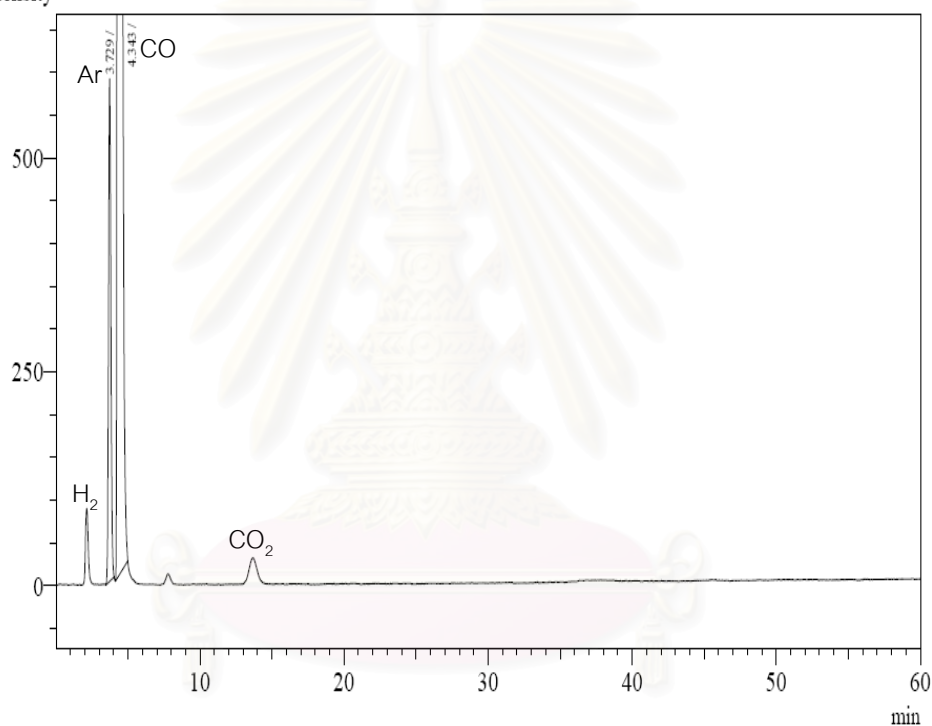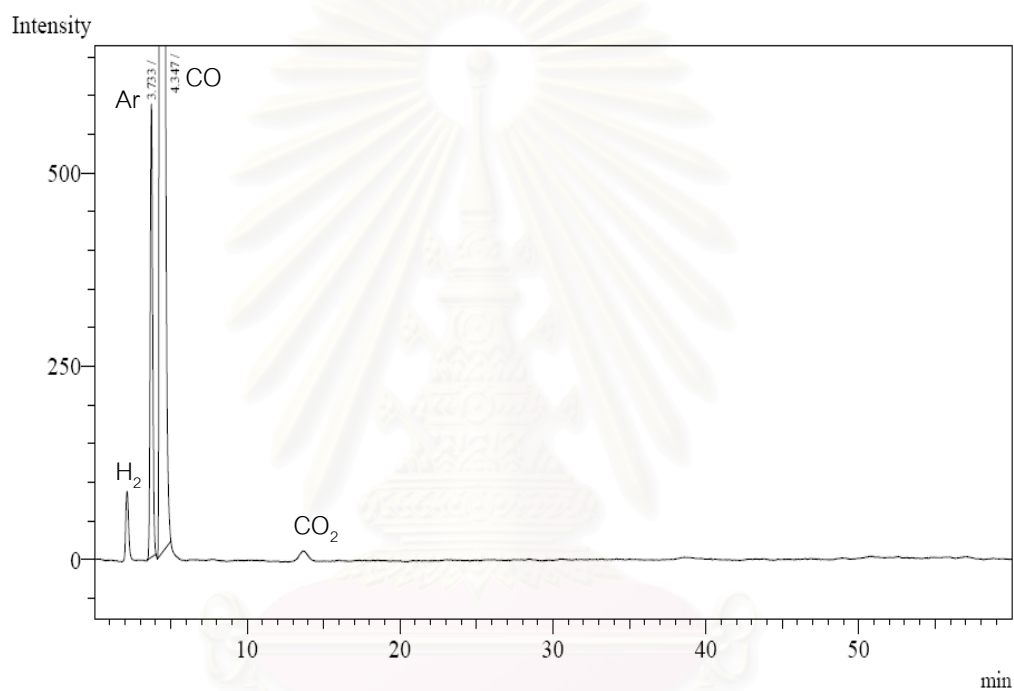

Peak#	Ret.Time	Area	Height	Conc.	Unit Mark	ID#	Cmpd Name
1	3.729	6592	585	0.000			
2	4.343	76635	4761	0.000			
Total		83227	5346				

D3. Data of gas chromatography(TCD) for physically mixing catalyst(CrZnO-Z-M)

Analysis Date & Time : 22/8/2551 7:50:30
User Name : Admin
Vial# : 0
Sample Name :
Sample ID :
Sample Type : Unknown
Injection Volume : 1.00
ISTD Amount :

Data Name : C:\GCsolution\Data\Jack\1%PdCrZn\14.gcd
Method Name : C:\GCsolution\Data\Jack\H2 Ar CO CH4 CO2.gcm

Peak#	Ret.Time	Area	Height	Conc.	Unit Mark	ID#	Cmpd Name
1	3.733	6549	582	0.000			
2	4.347	77516	4792	0.000			
Total		84065	5374				

D4. Data of gas chromatography(TCD) for the conventional FTS catalyst (CrZnO)

AUTHOR BIOGRAPHY

Mr.Montree Thongkam

Major: Chemical Technology & Engineering

Office location: Room 501 Building Chulaporn 1

Tel: 0-2326-4339-52 ext 342

Fax: (662) 3264415

Email address : ktmontre@kmitl.ac.th

Education

B.Sc (Industrial Chemistry) 1997, RMUTK, Thailand

M.Sc (Chemical Technology) 1999, Chulalongkorn University, Thailand

Research Interests

1. Reaction and Catalyst Engineering
2. FTS and DME synthesis
3. Kinetics and modeling of catalysts
4. New energy research

Honor Grants:

1. JASSO Short-Term Student Exchange Promotion Program Scholarship from University
   of Toyama, Japan in 2007-2008.
2. Teaching assistant funding from Chemical Technology, Chulalongkorn University in
   2006-2007.